

CASE FILE  
COPY

NACA TN 2924

NATIONAL ADVISORY COMMITTEE  
FOR AERONAUTICS

TECHNICAL NOTE 2924

COMBINED-STRESS FATIGUE STRENGTH OF 76S-T61 ALUMINUM  
ALLOY WITH SUPERIMPOSED MEAN STRESSES AND  
CORRECTIONS FOR YIELDING

By William N. Findley

University of Illinois

PROPERTY FAIRCHILD  
ENGINEERING LIBRARY



Washington

May 1953

MAY 29 1953



NATIONAL ADVISORY COMMITTEE FOR AERONAUTICS

---

TECHNICAL NOTE 2924

---

COMBINED-STRESS FATIGUE STRENGTH OF 76S-T61 ALUMINUM  
ALLOY WITH SUPERIMPOSED MEAN STRESSES AND  
CORRECTIONS FOR YIELDING

By William N. Findley

SUMMARY

Fatigue data for 76S-T61 aluminum alloy are presented for several combinations of bending and torsion with both alternating and mean stresses. Special fatigue equipment for these tests is described. Correction for yielding was applied to the mean stresses in the bending and in the torsion fatigue tests.

The literature on the effect of combined stress and of mean stress in fatigue is reviewed and the results of the present series are compared with those of various theories. A new notation for state of stress and a new criterion for combined stress fatigue are discussed. A new mode of presentation of combined stress results is described.

A correction for possible anisotropy is proposed and its effect on the selection of a theory for combined stress is discussed. Energy theories of fatigue under combined stress are critically examined and a test proposed.

The observed mode of fracturing is described and a qualitative theory of the mechanism of formation and propagation of fatigue cracks is proposed. Some of the observed facts are interpreted by means of this theory.

INTRODUCTION

The problem of fatigue failure of materials under different states of combined stress is of immediate importance in the design of many components of all types of machinery and transportation equipment. It has perhaps even greater importance as a key problem, the solution of which would contribute greatly to a better understanding of the phenomenon of fatigue failure and how to control it. That is, fatigue tests under combined stress provide data by which various theories of fatigue failure may be evaluated.

## Status of Problem

Combined stress.- The effect of different states of stress on the fatigue strength of metals has been studied sporadically since 1916. The problem has been difficult and very time consuming because of the large number of tests involved, the difficulty of designing suitable testing machines, the difficulty of devising and maintaining testing techniques which do not influence the results, and the inherent scatter in results of fatigue tests.

Most of the fatigue tests under combined stress which have been reported involved tests in axial load, bending, torsion, and various combinations of two of these three (references 1 to 18). The most extensive of these were reported between 1935 and 1949 by Gough for tests of steels and cast irons (references 8, 9, 10, and 18). A few fatigue tests of tubes under combined axial load and internal pressure have been reported for cast iron (reference 19), carbon steel (references 19 to 22), and aluminum alloy (references 23 and 24). Other tests of steels have been analyzed in which combined stresses were produced by axial or diametral loads on disks (reference 25), by circumferential notches on solid and hollow shafts (reference 25), and by bending or torsion of engine crankshafts and connecting rods (reference 26). Some investigators have described machines for fatigue tests under combined stresses without presenting new data (references 27 to 29) and others have presented analyses which they correlated with existing data (references 30 to 39).

Various conclusions have been reached by the different investigators concerning the applicability of the well-known theories of failure to the results of fatigue tests under combined stress. Gough found for high-strength cast iron that the results of tests under combined bending and torsion agreed with the theory of a limiting principal stress but that tests of other steels and cast irons were in approximate agreement with various theories (reference 8). He finally concluded that none of the rational theories of failure either did or could explain fatigue failure since the relationship between the fatigue strength in bending and that in torsion was not the same for all materials as required by the rational theories. Hence Gough proposed two empirical elliptical equations, the ellipse quadrant for ductile metals and the ellipse arc for cast irons. These equations avoided the difficulty by including as arbitrary constants the values of the fatigue strengths in bending and in torsion.

Other investigators of combined-bending-and-torsion fatigue have reported the following conclusions: Narmore found that the data from a hard SAE 4634 steel fitted the ellipse-quadrant equation and were nearest to the theory of a limiting total strain energy (reference 11). Nisihara and Kawamoto by testing an annealed 0.34-percent-carbon steel concluded

that the criterion of a limiting energy of distortion best represented their data and that the direction of the surface of fracture was perpendicular to the greatest principal stress (reference 13). Sauer in tests of 14S-T aluminum alloy concluded that his data were closest to the theory of a limiting principal shearing stress (reference 16).

Maier's tests of tubes of steel, cast iron, and brass under fluctuating internal pressure were inconclusive but indicated that a theory of a limiting principal stress might apply (reference 19). Morikawa and Griffis concluded from tests of tubes of mild steel under fluctuating internal pressure and axial load (reference 21) that the results did not seem to permit the verification or establishment of a theory of fatigue failure under combined stress which was appreciably different from the maximum-stress theory for the ductile metal tested. Majors, Mills, and MacGregor concluded from tests of tubes of mild steel under pulsating internal pressure and axial load that the distortion-energy theory was the best fit to their data (reference 22). Marin and Shelson reported so much anisotropy in the 24S-T aluminum-alloy tubes they tested under internal pressure and axial load that comparisons with existing theories were not possible (reference 23).

Sawert, testing disks and notched bars of mild steel and heat-treated chrome-vanadium steel (reference 25), concluded that the test results most closely approximated those predicted by the theory of a limiting energy of distortion.

An examination of most of the reports on fatigue tests under combined bending and torsion (references 8 to 11, 13, and 16 to 18) indicates that the effect of possible anisotropy in the material was not considered. In a discussion of Gough's most recent paper on this subject the present writer suggested that anisotropy may be the reason that the ratio of fatigue strength in bending to that in torsion was not the same for all materials (reference 40). A procedure was also suggested for correcting for anisotropy. When this correction was applied to the theory of a limiting principal shearing stress the resulting expression was found to be identical with the empirical equation proposed by Gough. This problem is discussed in greater detail in a later section.

Examination of the data presented by Morikawa and Griffis (reference 21) indicates for the combinations of stress employed that the principal-stress and shearing-stress theories are identical. Similarly one finds that the data of Majors, Mills, and MacGregor (reference 22) are not conclusive. Their comparison between the several theories and their data was based on the tacit assumption that the fatigue strength in bending was precisely determined and that all uncertainty or scatter in the data lay in the results obtained under other states of stress. If one removes this restriction it is found that the theory of a limiting

principal shearing stress fits the data better than the other theories considered by the authors as shown in figure 1(a). In figure 1 curve b' is the shearing-stress theory relocated to give the same weight to the data for all states of stress tested.

Examination of the data reported by Sawert (reference 25) indicates that he has also assumed that the fatigue strength under uniaxial stressing was exact and that all scatter must be in the data from the remaining states of stress. Again if all the data are considered equally they are found to fit the theory of a limiting principal shearing stress (curve b') as well as, if not better than, the theory of a limiting distortion energy reported by Sawert as the best fit to the data. (See figs. 1(b) and 1(c)). The significance, if any, of the fact that the data for a uniaxial state of stress are to the left of curve b' for all three investigations shown in figure 1 has not been determined.

It should be noted that the several errors and omissions in the diagrams appearing in Sawert's original paper have been corrected in figures 1(b) and 1(c). Also the duplicate plotting of each test result which Sawert accomplished by interchanging coordinates has been eliminated. While Sawert determined that orientation of the grain could cause a change of 15 percent in the fatigue strength, anisotropy was apparently not considered in the analysis of his combined-stress data.

Gadd, Zmuda, and Ochiltree concluded from their tests of engine components (reference 26) that the results are best predicted by what they call an equivalent shear-energy stress (proportional to the octahedral shearing stress). However, their analysis appears to be based on the maximum spread of the data.

If statistical measures of dispersion are applied to the seven test values reported by Gadd, Zmuda, and Ochiltree it is found that the standard deviation expressed as a percentage of the mean of the values is slightly in favor of the equivalent shear-energy stress while the average deviation from the mean expressed as a percentage of the mean is slightly in the favor of the principal-shear-stress theory. Also if the value having the greatest deviation from the mean is eliminated both measures of dispersion in the remaining six values show about 1 percent dispersion for the principal shear stress compared with 2 to 3 percent for the equivalent shear-energy stress.

The above analysis suggests that none of the available test data disagree with the theory of a limiting principal shearing stress.

Mean stress.- The effect of mean stress (often referred to as the effect of range of stress) has been investigated and discussed by many. The problem was reviewed by Peterson in 1937 (reference 41) and existing data interpreted by Smith in 1942 (reference 42). Some of the subsequent investigations (references 43 to 52) were reviewed and Smith's interpretation for tensile mean stresses was brought up to date by Schwartz in 1948 (reference 53).

Various empirical relations have been proposed to describe the observed effect of mean stresses in fatigue. Among these are the modified Goodman law (reference 54), the Gerber parabola (references 54 and 55), the Soderberg linear relation (references 30 to 32), Smith's equation for brittle metals (reference 42), and Seliger's parameter (reference 56).

The most widely used of these expressions for tension or bending are of the form

$$\frac{\sigma_a}{\sigma_r} + \frac{\sigma_m}{\sigma_{cr}} = 1 \quad (1)$$

where  $\sigma_a$  is the fatigue strength expressed as the alternating stress for a given mean stress,  $\sigma_m$  is the mean stress,  $\sigma_r$  is the fatigue strength for completely reversed stresses, and  $\sigma_{cr}$  is either the ultimate strength or the yield strength. Equation (1) has been modified by some by introducing a constant before either the first or second term.

For torsion fatigue Smith observed that the fatigue strength was nearly independent of the mean stress (reference 42).

#### Scope and Purpose of Investigation

The present investigation was undertaken to determine: (a) The effect of the different states of stress produced by different combinations of bending and torsion on the fatigue strength of an aluminum alloy (76S-T61) which was used for aircraft propellers and (b) the effect of different values of mean stress on the fatigue strength of the same alloy under the same states of stress.

At the time these tests were started in August 1942 fatigue tests of aluminum alloys under combined bending and torsion were unknown to the writer (although it is now known that tests by Nisihara and Kawamoto (reference 14) had just been published in Japan) and no tests had been reported for combined-stress fatigue tests with different values of mean stress superimposed on the alternating stresses. Recently Gough published results of such tests on steels (reference 18), but as far as is known the tests reported herein are the first to be reported for an aluminum alloy under combined bending and torsion with superimposed mean stresses.

#### Acknowledgments

The present investigation was conducted as a part of the work of the Engineering Experiment Station in the Department of Theoretical and Applied Mechanics, University of Illinois. The project was completed

under the sponsorship and with the financial assistance of the National Advisory Committee for Aeronautics. The author is also grateful to the Engineering Experiment Station and to Hamilton Standard Division, United Aircraft Corp., for additional financial support during the early portions of this program.

The following, to whom the author is greatly indebted, performed various phases of the project: Testing, Messrs. S. Yurenka, W. J. Worley, O. M. Sidebottom, and W. I. Mitchell; analysis, Messrs. F. Mergen, M. Peterson, B. A. Century, A. H. Rosenberg, and D. D. Strohbeck; and drafting, Messrs. C. K. Liu, J. H. Dabbert, and H. W. Peithman.

#### TERMINOLOGY AND SYMBOLS

For a discussion of terms not given here and an introduction to fatigue testing see reference 57.

#### State of Stress

The state of stress at a point in a stressed body may be described in terms of nine components of stress acting on three planes passing through the point so long as the planes do not all intersect in the same line. Each of these stress components must be described in terms of its magnitude, sense, and direction. Thus 27 quantities are required for the general description of the state of stress. The complexity of the description may be reduced by selecting orthogonal planes and further reduced by selecting the planes of reference so that the stresses are principal stresses.

Since for purposes of analysis it is highly desirable to be able to express the concept of the state of stress by a single quantity it is proposed that a quantity to be called the state-of-stress vector be employed. The state-of-stress vector is the vector sum of the three principal stresses  $\sigma_1 > \sigma_2 > \sigma_3$  at a point. (See fig. 2.) The relation between the state-of-stress vector  $\bar{S}$  and the principal stresses may be described by the magnitude of the state-of-stress vector  $S$ , where

$$S = \sqrt{\sigma_1^2 + \sigma_2^2 + \sigma_3^2} \quad (2)$$

and the direction cosines  $l$ ,  $m$ , and  $n$  of the angles  $\alpha$ ,  $\beta$ , and  $\gamma$  between the state-of-stress vector and the three principal stress axes (see fig. 2) are

$$\left. \begin{aligned} l &= \cos \alpha = \frac{\sigma_1}{S} \\ m &= \cos \beta = \frac{\sigma_2}{S} \\ n &= \cos \gamma = \frac{\sigma_3}{S} \end{aligned} \right\} \quad (3)$$

The limitations imposed by the requirements that a tensile principal stress is a positive vector, a compressive principal stress is a negative vector, and the three principal stresses are related to each other by  $\sigma_1 > \sigma_2 > \sigma_3$  cause all possible state-of-stress vectors to be confined within the semi-infinite wedge shown in figure 3. The edge of this wedge is along the line  $\sigma_1 = \sigma_2 = \sigma_3$  and its planes are defined by the edge line and the positive  $\sigma_1$ -axis on the back side of the wedge and by the edge line and the negative  $\sigma_3$ -axis on the front side.

Combined-bending-and-torsion tests permit state-of-stress vectors lying in an area within the wedge illustrated in figure 4(a), and combined axial load and internal pressure in tubes permit state-of-stress vectors lying within the areas illustrated in figure 4(b). If the axial stress is tension, the state-of-stress vector lies in the horizontal area, if compression, in the vertical area, of figure 4(b).

### Fatigue Strength

The fatigue strength is defined in this report as the largest alternating stress amplitude for which the specimen would withstand a given number of stress cycles at a given mean stress without fracture.

A cycle of stress in a fatigue test is illustrated in figure 5 together with the meaning of the terms alternating stress amplitude, mean stress, maximum stress, and minimum stress.

## Symbols

$\sigma$	bending stress at point of highest stress in specimens
$\sigma_r$	fatigue strength for completely reversed stresses
$\sigma_{cr}$	ultimate or yield strength
$\sigma_e$	stress at proportional limit
$\sigma_1 > \sigma_2 > \sigma_3$	principal stresses
$\bar{S}$	state-of-stress vector
$S$	magnitude of state-of-stress vector (see equation (2))
$\alpha, \beta, \gamma$	angles between state-of-stress vector and three principal stress axes
$l, m, n$	direction cosines of $\alpha$ , $\beta$ , and $\gamma$ , respectively
$\theta$	angle between axis of specimen and line joining point of loading on moment arm and midpoint of specimen; see description of testing machine ( $\theta = 0$ for bending only; $\theta = 90^\circ$ for twisting only)
$\tau$	shear stress at point of highest stress in specimens
$\tau_o$	octahedral shear stress
$b$	fatigue strength in bending
$t$	fatigue strength in torsion
$M$	applied bending moment
$M_e$	bending moment when maximum strain is at proportional limit
$s$	slope of dimensionless stress-strain curve above proportional limit for material in which stress-strain diagram above proportional limit is another straight line
$\epsilon$	normal strain

$\epsilon_e$	normal strain at proportional limit
T	torque
W	total strain energy
$W_D$	strain energy of distortion
$\mu$	Poisson's ratio
E	Young's modulus

## Subscripts

l	principal or particular value of quantity
a	alternating component
m	mean component

## FATIGUE MACHINE FOR COMBINED BENDING AND TORSION

One of the five Krouse fatigue machines of the constant-amplitude-of-deflection type used in this program is shown in figure 6(a). A special fixture was designed to permit this machine to be used for bending or torsion or a combination of bending and torsion. The apparatus was a revision of that previously constructed for tests of plastics (reference 45). It consisted of a plate A which was fastened in the grip of the testing machine. One end of the specimen B was fastened to this plate in the desired position by means of tapped holes in the plate. The position of attachment depended upon whether the specimen was to be subjected to bending, torsion, or some combination of the two.

The other end of the specimen was fastened by a single bolt to a lever C, the other end of which was deflected up and down by a connecting rod D driven by an adjustable crank E. Adjustment of the crank provided means for varying the amplitude of the stress. The grip was adjustable vertically in a slide F to permit selection of any desired mean stress. A dial G was mounted on a stiff arm attached to slide F so as to indicate the deflection of the lever C. A switch H was provided to stop the machine when the specimen fractured into two pieces and a counter was provided to indicate the number of cycles.

The arrangement for loading the specimen and the bending- and twisting-moment arms are illustrated diagrammatically in figure 6(b).

When the angle  $\theta$  was at  $90^\circ$  the midpoint of the specimen was subjected to a twisting couple, no bending moment, and a small vertical shear force (the stresses produced by the latter are negligible for the dimensions employed). On either side of the midpoint there is a bending moment which increases linearly from zero.

When the angle  $\theta$  was zero the midpoint of the specimen had a bending moment, no twisting moment, and a negligible vertical shear force. At other values of  $\theta$  combinations of bending and twisting moments were produced.

## TEST PROCEDURE

### Fatigue Tests

After the specimen had been mounted in the machine with the correct angle  $\theta$  small loads were applied in increments at the wrist pin (with the connecting rod detached). The resulting deflection was noted on dial G (fig. 6(a)) and a diagram of the load against deflection was plotted. These loads were kept within the elastic limit of the material to avoid yielding.

From the slope of the load-deflection line the deflection required to produce the desired maximum and minimum stress of the fatigue cycle was determined. If the desired maximum stress was above the proportional limit the resulting maximum stress, minimum stress, and corresponding loads would all be different from the nominal values calculated and used in obtaining the S-N diagrams. The correction of stresses for the effect of yielding is discussed in the appendix.

In adjusting the testing machine the desired amplitude was first provided while the mean stress was zero. Then the slide F was raised with the crank in the upper position until the desired minimum stress was reached. The machine was then started from this position so that yielding, if it occurred, always took place under as high a rate of straining as possible.

### Static Tests

Static tension tests were performed by Dolan on specimens  $1/2$  inch in diameter with an Amsler testing machine as described in reference 44. Compression tests were performed on specimens  $1/2$  inch in diameter and 2 inches long on a beam-weighing testing machine using the same apparatus and technique described in other papers by the present author on

tests of plastics (references 45 and 49). Torsion tests of specimens having a 1-inch gage length and a diameter approximately the same as that of the fatigue specimens were made by means of apparatus and technique described in references 45 and 49.

Tests were also performed (on specimens of the shape used for fatigue tests) in which static twisting moments were applied well beyond the proportional limit to the greatest moment used in the fatigue tests. Then the specimen was gradually unloaded and loaded in the reverse direction. In these tests the specimen was fastened in a fatigue machine, a dial was arranged to measure the deflection, a spring dynamometer was used to weigh the load, and the specimen was deflected by means of a screw. Readings of load and deflection were recorded.

#### MATERIAL TESTED

The material tested was originally designated M68 but now carries the numbers 76S-T61 from the Aluminum Co. of America. The material, which is used primarily for forging airplane propellers, was supplied by the Hamilton Standard Division of United Aircraft Corp. in swaged bars 1 inch in diameter by 12 inches long. Additional information on this material is contained in reports by Dolan (references 44 and 46). The material tested in this program is of the same heat and lot of alloy as that tested by Dolan. In fact, many of the specimens were prepared from the remaining portion of the long fatigue specimens employed by him.

#### SPECIMENS

Specimens for the tension, compression, torsion, and fatigue tests were machined from round bars to the dimensions shown in figure 7. A procedure was used for the fatigue specimens which minimized vibratory stresses resulting from the machining. The large radius was formed by swinging the compound of the lathe.

Polishing the critical section of the specimens was accomplished by mounting them between centers and rotating them about 700 rpm while polishing the surface with polishing paper wrapped around a 3/4-inch bar driven through a flexible shaft at 1750 rpm. Behr-Manning polishing papers of the following grits were used in succession: 1/0, 2/0, and 3/0. Oil was used in all the polishing and the angle of the polishing bar was altered between grades of paper. Polishing with each grade continued until scratches from the previous operation were removed.

## PRECISION OF TESTS

Each specimen was calibrated as its own dynamometer to determine the deflections required for the desired stresses. While the same dial was used for both calibration and adjustment, the accuracy of the dials probably was no greater than  $\pm 2$  percent for some tests.

An attempt was made to maintain a uniform testing procedure. However, the fact that five operators conducted the tests over a 3-year period precluded the attainment of complete uniformity. All calculations have been double-checked by different people and all results which deviated from the general trend have received special attention.

## RESULTS

## Fatigue Data

In figures 8 to 13 are shown the S-N diagrams for bending, four combinations of bending and torsion, and torsion. S-N diagrams are shown for several values of mean stress in bending (fig. 8), in torsion (fig. 13), and in one of the combinations of bending and torsion (fig. 10). These diagrams have logarithmic coordinates and a vertical scale modulus six times the horizontal for all diagrams.

The curves for all diagrams were drawn on separate sheets by inspection before being combined as shown in figures 8, 10, and 13. The curves shown represent the average relationship between the logarithm of the alternating stress and the logarithm of the number of cycles.

The ordinates in figures 9 to 12 represent only one of the two components of stress (flexural and torsional) applied to the specimens. The other component may be obtained by multiplying or dividing the given component by the constant given in the caption since the proportion of bending to torsion was the same in all tests of a series. That is, the state of stress was constant for all tests of a series and also constant at all points in the stress cycle for a given series of tests.

It will be observed that as the mean stress increased the S-N diagrams showed a greater tendency toward an endurance limit like that of ferrous metals and some plastics. This trend was observed in tests in bending (fig. 8) and combined bending and torsion (fig. 10) but was not apparent in torsion (fig. 13).

It also appeared that there was greater scatter in the results of the torsion tests (fig. 13) than in those of the other states of stress.

In figure 8 are also plotted data reported earlier by Dolan from bending tests of the same material using a specimen with a larger radius (reference 44). The agreement is satisfactory.

Fatigue tests in torsion are shown in figure 13 for two different types of machines: The H. F. Moore torsion machine and the machine described above. Initially it was planned to use the Moore machine for all torsion tests, but the plan was changed because of the scatter of data and because it was observed that unpredictable static bending stresses could not be avoided in clamping the specimen in the Moore machine. However, the results show that the amount of scatter from the two machines was comparable and the results are in reasonable agreement, as shown in figure 13. The results obtained from the Moore machine were not considered in drawing the curves in figure 13 nor in the analysis which follows in the next section.

#### Fatigue Fractures

Fractures of fatigue specimens representing various loading conditions are illustrated in figure 14. The entire group of fractured specimens was assembled in an orderly sequence according to stress amplitude, mean stress, and state of stress for examination. It was observed that there were from one to three long cracks lengthwise of the specimen in the torsion specimens having highest stress amplitudes. Some of these cracks were as deep as the center of the specimen. The final fractures, however, occurred as transverse cracks. As the stress amplitude decreased the extent of the longitudinal cracking decreased and at the lower stress amplitudes the final fractures changed to a spiral or stairstep pattern.

Examination of torsion specimens having mean stresses greater than zero showed that the transition from a final fracture of the transverse type to the spiral type occurred at higher stresses (from 17,000 to 25,000 psi) and smaller numbers of cycles (from  $23 \times 10^6$  to  $77 \times 10^3$ ) as the mean stress increased from 0 to 45,000 psi.

After cracks had formed in the fatigue tests, a black powder exuded from the cracks (especially in torsion). The fractured specimens also showed that fractured surfaces on which shear stresses had acted were blackened, except in some of the torsion specimens in which the transverse planes had been considerably gouged as a result of the large relative movements during the final stages of the test.

In the tests having a state of stress such that  $\tau = 1.207\sigma$  the two highest-stressed specimens had long longitudinal cracks which were at angles of  $3^\circ$ ,  $8^\circ$ , and  $12^\circ$  to the axes of the specimens. These angles

are in approximate agreement with the angle ( $11.3^\circ$ ) of the plane of maximum shearing stress. At lower stresses the general fracture is of the spiral type.

The specimens fractured in bending showed that all fractures were essentially transverse with small areas of black markings. The extent of the black markings decreased with increase in alternating stress and with increase in mean stress. At the highest amplitudes of stress, cracks appeared to form at several points. At zero mean stress and high amplitude, cracks formed on both top and bottom surfaces.

Microscopic examination of the fractures indicated that blackened areas were surfaces which would have been subjected to shear stress. It was also observed that the point of initiation of the fatigue cracks contained surfaces of fracture which were shear planes either at an angle to the axis and to the surface of the specimen or at an angle to the axis and perpendicular to the surface of the specimen.

The fractures under other combinations of bending and twisting were helical or diagonal fractures with some black markings as in the bending fatigue specimens. The angle of the helix or diagonal plane was roughly that of the plane of maximum principal stress, except that this angle decreased (tended to become a transverse plane) as the mean stress was increased in the tests for a state of stress such that  $\tau = 0.5\sigma$ .

#### Static Tests

Representative stress-strain curves for tension and compression tests are shown in figure 15. The curves for the tension tests are taken from the report by Dolan (reference 44). Figure 16 presents the nominal shearing stress against the shearing strain from a representative torsion test of the alloy. These data are plotted to two different scales in figure 16. Representative time-against-strain curves are also shown in figures 15 and 16. Several static properties measured from such curves are given in table I.

Because of the shortage of material for these tests supplementary static tests were made on specimens cut lengthwise from the root section of a propeller blade forged of the same alloy. The data obtained from these tests are also listed in table I.

The effect of the diameter on the nominal yield strength in a torsion test is illustrated by the test results at two different diameters given in table I.

The values of stress in the torsion test on an original bar of the alloy have been corrected as described in the appendix for the nonlinear stress distribution resulting from yielding. The corrected stress-strain diagram is also given in figure 16. Corrected values of yield strength and proportional limit are given in table I together with the true stress of fracture in tension and in torsion. The latter was calculated on the assumption that the stress on the cross section of the test bar was constant along any diameter at the ultimate torque. This calculation yields the result that the corrected ultimate strength is equal to three-fourths the nominal value regardless of the diameter.

For purposes of comparison the yield strengths in tension and compression tests have been calculated in terms of shearing stresses at the given values of offset corresponding to shearing strain, based on a Poisson's ratio of 0.3 in a tension test. That is, for the same value of shearing strain (or offset) in both tension and torsion the normal strain in the tension test would equal the shearing strain in the torsion test divided by  $1 + \mu$ , where  $\mu$  is Poisson's ratio.

It was observed that the shearing stress from the tension tests was nearly equal that from the torsion tests at the proportional limit, yield strength, and fracture stress.

Static tests beyond the proportional limit are illustrated in figure 17 for torsion of a specimen of the same shape as the fatigue specimens. For the first loading of the virgin specimen deflections were applied in increments until the maximum deflection encountered in the fatigue tests was reached. Then the specimen was unloaded until a substantial negative load was reached, which was less than the corresponding minimum load in a fatigue test. Above the proportional limit a decided curvature in the diagram was observed. However, on unloading a nearly linear relation was obtained at the same slope as the initial tangent. Subsequent loading and unloading between these two deflections produced curves which followed the first unloading line rather closely but showed a small hysteresis loop.

On the fourth, fifth, and sixth loadings the maximum deflection was increased somewhat with the results shown in figure 17. The curve showing the increase in deflection followed approximately the trend of the original plastic-flow curve. The maximum strain was increased again for the seventh and eighth loadings with similar results. A slight Bauschinger effect was observed in the last four unloadings.

The presence of a Bauschinger effect is shown much more clearly in figure 18 in which are plotted data from a second static torsion test of a specimen shaped like the fatigue specimens. The two complete cycles of loading and unloading illustrated were obtained by loading the specimen to the maximum deflection, unloading, applying reverse loading until the reverse-loading curve intersected the negative extension of the initial tangent line, and then removing the reverse load. The second loading duplicated the first loading almost exactly. However, the

remainder of the second cycle did not repeat exactly, possibly because the maximum deflection was somewhat greater.

Since the maximum variation in shearing stress (twice the alternating stress) in the torsion fatigue tests was 60,000 psi, it is evident from figures 17 and 18 that the minimum stress was never low enough for the Bauschinger effect to be significant even at the highest mean stress, where the Bauschinger effect would be most pronounced.

Since the unloading curves and subsequent reloading curves were linear as long as the unloading proceeded no further than was required in the fatigue tests (as shown by fig. 5, specimen A) changes in load within this linear region produce changes in stress which are elastic and can be calculated by ordinary formulas. Thus the nominal values of the alternating stresses calculated on the assumption of elastic behavior and reported in figures 1 to 3 are the correct values and were not influenced by yielding.

## ANALYSIS AND DISCUSSION

### Correction of Mean Stress for Effect of Yielding

The fatigue strength was measured from all S-N diagrams at  $3 \times 10^4$ ,  $10^5$ ,  $10^6$ ,  $10^7$ , and  $10^8$  cycles. The values obtained are given in table II. All subsequent calculations and diagrams are based on these values.

The methods of testing used together with the characteristics of the material were such that the alternating stress values reported are correct values within the limits of precision of the test in spite of any residual stresses or yielding that might occur. This results from the fact that the alternating stress was calculated on the assumption that the deflections observed resulted from elastic stresses and the further fact that following the initial plastic loading the subsequent unloading and reloading were nearly elastic as shown in figures 17 and 18.

In instances in which the maximum stress of the cycle was above the proportional limit the actual maximum stress was less than the nominal stress calculated from the deflection of the specimen. Thus the mean stress was also lower by an equal amount since the mean stress was equal to the maximum stress minus the alternating stress and the latter was not influenced by yielding.

Inasmuch as one of the objects of this investigation was to determine the effect of the mean stress, it seemed necessary to extend the range of mean stresses to as large values as possible and then to correct the nominal mean stresses for yielding. The tests at zero mean stress and at some of the lower values of mean stress did not require

correction. Also no correction has been attempted for yielding under combined bending and torsion. Plasticity theory and experiment have not yet been developed to a point where the problem of yielding under combined bending and torsion of a material having a curved stress-strain diagram is readily solved.

Corrections were made where needed for all tests in bending and in torsion. The procedure used for correcting the bending tests was based in part on the semigraphical procedure developed by Morkovin and Sidebottom from the equation of Herbert (reference 58), whereas the corrections in torsion were based in part on the procedure described by Nadai (reference 59). The application of these procedures to the present data is described in the appendix. The resulting corrected values of mean stress are given in table II.

The corrections for yielding are not exact, as discussed in the appendix, nor is it likely that the maximum stress remains entirely constant during the test. Residual stresses which may have been present in the specimens in spite of the care used in their preparation may also have affected the maximum stress.

#### Theories of Failure under Combined Stress

Many theories have been proposed as governing yielding or fracture under a single application of combined stress. Several of the same theories have been proposed for fatigue failure, but none has received universal acceptance. Possibly the nature of fatigue, commencing as it does on a small scale at the atomic or crystal level, may in the final analysis make it impossible to define the conditions of failure in terms of the usual concept of stress or strain. However, at present there is no choice but to express these conditions in terms of stress or strain.

All theories which have seemed to hold any promise have been investigated in the present analysis. The list of theories considered is given in table III together with the corresponding equation expressed in terms of the principal stresses and the equation as simplified for the case of combined bending and torsion. The latter equation is expressed in terms of the flexural stress  $\sigma$  and torsional stress  $\tau$ .

In addition to the well-known theories the empirical equations proposed by Gough (the ellipse arc and ellipse quadrant) have been tried, together with a theory not previously considered. This theory is that fatigue failure may occur when a limiting magnitude of the state-of-stress vector is reached. No physical significance is attached to the latter theory as it is not much more than an empirical equation.

## Effect of State of Stress

By use of (1) the equations given in table III, (2) the relation between  $\sigma$  and  $\tau$  for the different states of stress, (3) the fatigue strengths, and (4) the corrected mean stresses, the values of the quantity corresponding to the fatigue strength and to the mean stress were computed for each of the theories.

In making the computations the value of the modulus of elasticity employed was  $9.69 \times 10^6$  psi as reported by Dolan from tension tests (reference 44). A larger value would have been justified by the compression-test data subsequently obtained. A value of 0.3 was used for Poisson's ratio. No direct measurements of Poisson's ratio are available for 76S-T61 aluminum alloy.

Poisson's ratio calculated from the average of the tension and compression modulus determinations and from the shearing modulus from the torsion test gives values of 0.31 for the original bar stock and 0.39 for the propeller blade. Available data on 75S-T6 aluminum alloy (reference 60) indicate a value of 0.33. Poisson's ratio during yielding probably has a still higher value as shown by Stang, Greenspan, and Newman (reference 61). However, on unloading and reloading after yielding it seems probable that Poisson's ratio would be similar to that of virgin material.

The values of  $b$  and  $t$  used in making the computations for Guest's law, the ellipse quadrant, and the ellipse arc were the values of the fatigue strength in bending and in torsion, respectively, at the number of cycles considered.

The value of the theory based on the alternating stress at zero mean stress was then plotted as a function of the state of stress for each of the theories, as illustrated in figure 19 for the theory of a limiting principal shear stress. The measure used for the state of stress was the least direction cosine of the state-of-stress vector

$$n = \sigma_3/S \quad (4)$$

For the range of states of stress employed in this investigation only one direction cosine is necessary to identify the state of stress, since all the state-of-stress vectors lie in one plane. The direction cosine  $n$  was chosen because it spaced the test values of state of stress more evenly than the first direction cosine. The values of  $n$  employed are given in table II.

The greatest principal shear stress corresponding to the fatigue strength at five different numbers of cycles to failure is shown in

figure 19. On this type of diagram exact agreement with the theory would be represented by straight horizontal lines. The sloping lines shown in figure 19 indicate that fatigue failure of this material under combined bending and torsion is not predicted accurately by the theory of a limiting principal shear stress.

A logarithmic ordinate was used in all of these diagrams because the percent change in a quantity is represented by the same linear distance on a logarithmic scale regardless of the magnitude of the quantity. Thus logarithmic diagrams permit direct comparison (between the various curves) of the relative deviation of the test values from the theory. A scale is inset in figure 19 by which the percent deviation from the theory may be measured. An examination of these diagrams for all theories indicated the following order of merit (as indicated by the present data) for the several theories and empirical equations where the first theory represents the test data the closest:

- (1) Guest's law (complete)
- (2) Ellipse quadrant
- (3) Magnitude of state-of-stress vector
- (4) Ellipse arc
- (5) Total strain energy
- (6) Octahedral shear stress
- (7) Largest principal strain
- (8) Energy of distortion
- (9) Largest principal shear stress
- (10) Largest principal shear strain
- (11) Largest principal stress

There is no difference between the predictions of items (9) and (10) above as the corresponding equations in table III show.

Since a complete statistical analysis of the data for these theories did not seem practical, the above order of merit was determined by drawing the straight lines which best represented the data in diagrams such as figure 19 and using the slopes of these lines and the maximum deviations from the lines as guides in arriving at an opinion.

#### Effect of Mean Stress

On the basis of these results several of the more-promising theories were selected for a complete study at all values of mean stress. As reported by Gough (reference 18) and discussed by the writer (reference 40) the ellipse arc is related to the complete Guest law and in a way which makes the ellipse arc too general. Hence, in the complete analysis the ellipse arc has not been considered. Similarly the ellipse quadrant was not considered since, as described in the discussion in reference 40 and in a later section, the ellipse quadrant is identical to a squared form of the equation for the greatest principal shear stress, when corrected for anisotropy in the manner to be described.

The following quantities were computed from the alternating stresses and from the mean (corrected wherever possible) stresses at each value of fatigue strength considered:

- (1) Guest's law (complete)
- (2) Magnitude of state-of-stress vector
- (3) Total strain energy

The value of each of the three quantities based on the alternating stress was plotted as a function of the corresponding value of the quantity based on the mean stress as shown in figures 20 to 28. In addition to the data obtained under dynamic conditions the value of each quantity computed from the yield strength at 0.05-percent offset is represented by the diagonal line in the figures for bending fatigue and for torsion fatigue.

It is of interest to note from table I that the yield strength at 0.05-percent offset based on shearing stress and shearing strain<sup>1</sup> was nearly identical between the results of tension, compression, and torsion tests when the stresses in the torsion test were corrected for the distribution of stress resulting from yielding as described in the appendix.

The values of  $b$  and  $t$  used in calculating Guest's law were the same for all mean values at a given number of cycles and equal to the bending and twisting fatigue strengths, respectively, at zero mean stress and the given number of cycles.

The following observations were made from figures 20 to 28:

(1) For all theories, at any number of cycles to failure, the value of the theory based on the alternating stress decreased with increase in the value of the theory based on the mean stress.

(2) In bending and in combined bending and torsion the effect which an increase in the value of the theory based on the mean stress had on the value of the theory based on the alternating stress was less at large numbers of cycles to failure than at small numbers of cycles to failure. This suggests that the material may have an endurance limit which for some states of stress and for high mean stresses may be reached at about  $10^6$  cycles but for lower mean stresses may not be reached until perhaps  $10^{12}$  cycles. (See also figures 8 and 10.)

(3) There is poor agreement between the test data and common empirical formulas such as the modified Goodman or Soderberg linear equations or the Gerber parabola, although the latter is the best representation. This is true whether the ordinary stress is plotted or the

---

<sup>1</sup>The normal strain corresponding to 0.05-percent offset of shearing strain is less than 0.05-percent offset of normal strain.

quantities corresponding to the theories are plotted. The slopes of the curves in figures 20 to 22, for example, are not steep enough, the curves for torsion (fig. 22), for example, do not converge with increasing mean stress, and the lower four curves for bending (fig. 20), for example, curve in the wrong sense for the Gerber parabola. The empirical formulas are not shown in the figures to avoid confusion.

(4) In all except the energy theory there is only a slight decrease in fatigue strength with increasing mean stress for maximum stresses below the proportional limit. As the maximum stresses began to cause yielding, the fatigue strength decreased more rapidly in the torsion tests and in the bending tests at high alternating stresses than in tests at other combinations of stresses. This may be the effect on the fatigue strength of changes in microstructure resulting first from a nominally elastic static stress and second from the plastic deformation at yielding.

(5) Examination of the curves in these figures reveals poor correlation between (a) the values of maximum stress beyond which the fatigue strength decreases markedly and (b) the yield strength from static tests. A marked decrease in fatigue strength is apparent in the torsion tests as shown in figure 22, for example. For bending, however, the top curve of figure 20 suggests only that a marked decrease in fatigue strength may be impending at higher values of maximum stress. Little can be said about combined-bending-and-torsion tests (fig. 21, for example) since corrections for yielding have not been made. The indications are that no marked decrease occurred within the range of the tests shown in figure 21.

#### Effect of State of Stress at Different Mean Stresses

The values of the ordinate at several values of the mean stress, or mean energy, and so forth, were read from each of the curves in figures 20 to 28. These values were plotted as a function of the state of stress as represented by the direction cosine  $n$  in figures 29 to 31. These figures are of the same type as figure 19 except that values of the quantity corresponding to several mean stresses are also presented. It should be noted that the values for combined bending and torsion are not corrected for yielding.

Appraisal of the data for all mean values presented in figures 29 to 31 indicates the following order of merit of the several theories: Complete Guest's law, magnitude of state-of-stress vector, and total energy. There is, however, not much choice between the first two.

## CORRECTIONS FOR ANISOTROPY OF MATERIAL IN FATIGUE

## TESTS UNDER COMBINED BENDING AND TORSION

## Discussion of Anisotropy in Fatigue

The possible contribution of anisotropy to the results of fatigue tests under combined stress has been recognized by some of the investigators although it has not been acknowledged in the literature on fatigue tests under combined bending and torsion. However, it has been recognized that the ratio of the fatigue strength in bending to that in torsion was not the same for different materials as required by the rational theories of failure of elastic action. To avoid this difficulty Gough (reference 18) proposed two empirical expressions, the ellipse quadrant for ductile metals and the ellipse arc for cast irons, which include as constants the values of the fatigue strength in bending  $b$  and in torsion  $t$ .

From the present knowledge of the structure of metals, it is difficult to account for variations in the ratio  $b/t$  between different isotropic metals composed of polycrystalline aggregates. One possible interpretation is that fatigue failure is governed by one of the theories for which  $b/t$  is a function of Poisson's ratio (see table III) and that variations in Poisson's ratio account for the observed variations in  $b/t$ . For these theories the possible variations in  $b/t$  resulting from a change in Poisson's ratio from 0 to  $1/2$  are as follows: Principal-strain theory, 1 to 1.5, and theory of total energy of deformation,  $\sqrt{2}$  to  $\sqrt{3}$ . The last is the only one whose values are in the right range, but the limits are not broad enough to cover all the observed values for ductile metals. Also only relatively small variations in Poisson's ratio have been observed for ductile metals.

Hence, it seems appropriate to consider whether lack of isotropy may be the cause of the observed variations. A striking example of the effect of anisotropy on this ratio is to be found in the recent work of Gough (reference 18) in which are reported results of combined-bending-and-torsion fatigue of a splined shaft. The value of  $b/t$  for the splined shaft was 3.04 as compared with a value of 1.62 for smooth specimens of the same steel. In this case the anisotropy is predominantly caused by external shape and not by structure of the material. However, it seems possible that rolled metal bars may have internal shape characteristics caused by slag or other inclusions which may produce an effect similar to the anisotropic stress concentration of the splined shaft.

Similar examples of anisotropy are to be found in results reported by the author (references 49 and 62) from fatigue tests of specimens cut

from sheets of laminated plastics in such a way that the laminations were parallel to the axis of the specimen. Ratios of  $b/t$  computed from these tests varied from 1.61 for a grade C canvas laminate to 8.5 for a Mitscherlich paper laminate in which there was evidence of poor bond between laminations.

The concept of an anisotropic stress concentration may be illustrated by considering the effect of machining a set of parallel grooves on the surface of a flat plate of isotropic material. The grooves would have almost no effect on the stress resulting from bending couples in the planes containing the grooves, but the peak stresses produced by the same bending couples in planes normal to the grooves would be increased. Thus the grooves produce an anisotropic stress concentration, that is, a stress concentration whose properties depend on the direction of stressing.

#### Data on Isotropy in Fatigue of Metals

Unfortunately, the isotropy under fatigue conditions of the present material and of the materials tested by other investigators in fatigue under combined bending and torsion is unknown, although preparations are under way to determine the isotropy of the present aluminum alloy.

However, some data are available (references 22 and 25) on the isotropy of metals as indicated by the comparative fatigue strength of specimens in which the greatest principal stress is in one case parallel and in the other case transverse to the grain direction of the stock. Cazaud also lists the results of several investigations (reference 63). The results differ among themselves but indicate for wrought materials that the transverse fatigue strength is about 15 percent lower than the longitudinal fatigue strength.

Templin, Howell, and Hartman report the results of a thousand fatigue tests of both longitudinal and transverse specimens of aluminum alloys (reference 64). They observed a relatively small effect of orientation which they considered to be insignificant. It is difficult to evaluate this effect quantitatively from the diagrams presented but the data seem to admit the possibility that the magnitude of the effect may be comparable with that reported by previous investigators.

#### Corrections for Anisotropy

If it is assumed, pending further evidence of isotropy, that variations in  $b/t$  are the result of anisotropy, then none of the rational theories of failure can be discarded because of the variations in  $b/t$  among materials. Instead, one may attempt to correct for anisotropy.

The equation proposed by Guest (see table III) may be considered to be an equation corrected for anisotropy since it includes the values of  $b$  and  $t$  as constants. These are introduced in the equation in such a way that the resulting expression is satisfied by the test data for pure bending or pure torsion regardless of the ratio  $b/t$ . This is also true of the equations for the ellipse arc and ellipse quadrant.

It seems reasonable to assume, as a first approximation, that anisotropy in the strength of a material may be similar to the effect of a straight groove in that it may raise the local stress above that predicted by the formulas used for isotropic materials for stresses normal to the direction of the groove but not parallel to it. Then in specimens cut lengthwise from bar stock and tested so that the plane of bending and axis of twisting are always parallel to the lengthwise direction of the stock one may expect that: Anisotropy of the material will raise (or lower) the nominal stress computed from the twisting moment more than (or less than) the stress computed from the bending moment; the resulting bending or twisting stresses caused by anisotropy will be linear functions of the nominal bending or twisting stresses, respectively; and the resulting bending and twisting stresses will be the same functions of the nominal stresses regardless of the combination of bending and twisting employed.

Under these conditions one can then reexamine all of the rational theories of inelastic action (which require specific values of the ratio  $b/t$ ) by multiplying the nominal twisting stress  $\tau$  by a correction constant for each material such that the resulting equation satisfies the conditions for pure bending and pure twisting. A correction constant could have been applied to the bending stress instead of to the twisting stress or to both stresses; the result would have been the same.

For example, the theory of a limiting principal shearing stress may be written for combined bending and torsion as follows:

$$\frac{1}{2} \sqrt{\sigma^2 + 4\tau^2} = \text{Constant such as } t \quad (5)$$

This equation requires that  $b/t = 2$ , as is shown by solving the equation for the cases of pure bending and pure torsion. Therefore in accordance with the above suggestions one can correct for anisotropy by multiplying every value of  $\tau$  introduced in equation (5) by  $b_1/2t_1$  where  $b_1$  and  $t_1$  are the measured values of the fatigue strength in

bending and in torsion, respectively. The number of cycles for which  $b_1$  and  $t_1$  are determined are the same as the number which are expected to produce failure under the given values of  $\sigma$  and  $\tau$ . If the adjusted value  $\tau_1 = b_1\tau/2t_1$  is substituted in equation (5) the following equation results:

$$\frac{1}{2} \sqrt{\sigma^2 + \left(\frac{b_1}{t_1}\right)^2 \tau^2} = t \quad (6)$$

This equation may be rationalized and rewritten as

$$\left(\frac{\sigma}{b_1}\right)^2 + \left(\frac{\tau}{t_1}\right)^2 = 4\left(\frac{t}{b_1}\right)^2 \quad (7)$$

which is identical with the ellipse-quadrant equation (see table III) since for pure twisting

$$t = \frac{b_1}{2t_1} t_1$$

from which

$$4\left(\frac{t}{b_1}\right)^2 = 1$$

Thus the ellipse quadrant may be considered to be a rationalized equation for the limiting principal shearing stress with a correction for anisotropy applicable for the special type of testing and orientation of specimens considered. Of course, proof of the effect of anisotropy must be sought before the validity of the above explanation may be demonstrated.

In a similar way this correction may be applied to the other rational theories of failure. The values of  $b/t$  required by these theories and the resulting equations are given in table III. It is significant to note that the equations for six of these theories, when rationalized, are identical to the empirical equation proposed by Gough - the ellipse-quadrant equation. The six theories are:

- (1) Principal shear stress
- (2) Principal shear strain
- (3) Energy of distortion
- (4) Octahedral shear stress

- (5) Total energy of deformation
- (6) Magnitude of state-of-stress vector

The theories whose rationalized equations (with correction for anisotropy) differ from the ellipse quadrant are:

- (1) Principal stress
- (2) Principal strain

## EFFECT OF MEAN STRESS AND STATE OF STRESS CONSIDERING ANISOTROPY

### Mean Stress

Since six of the theories are identical in form (within the states of stress covered by combined bending and torsion) when corrected for anisotropy the curves for only one of the six need to be plotted. The theory of a limiting principal shear stress was selected because of its possibilities as shown by the review of the literature and because of the considerations discussed in the next section.

The effect of mean stress is shown in figures 32 to 34 for the principal-shear-stress theory with correction for anisotropy. The values of  $b$  and  $t$  used in correcting for both alternating and mean stresses were the values of the bending and twisting fatigue strengths, respectively, at zero mean stress and the given number of cycles.

There is no reason to think that the values of  $b$  and  $t$  are any more accurate than the fatigue strength at any combination of bending and twisting. Thus a certain latitude commensurate with the scatter of the data might be allowed in the value of  $b/t$  used in correcting for anisotropy if indicated by the trend of data for combined bending and torsion.

The disagreement which exists in figures 32 and 34 between the yield strength and the maximum stress beyond which the fatigue strength decreases markedly may be the result of correcting both the fatigue-strength and mean-stress values for anisotropy.

An excellent correlation was observed between the yield strengths from static tests and results predicted by the principal-shear theory as mentioned earlier. This suggests that the original material may have been nearly isotropic as far as general yielding is concerned and that the material may have been anisotropic only at the level of the localized action which initiates fatigue failure.

If this is the case then the correction for anisotropy should have been applied only to the alternating components of the stress. This revision does not affect the diagram for bending, figure 32, but does affect figures 33 and 34. The revised diagram for torsion is shown in

figure 35. The apparent effect of yielding on the fatigue strength resulting from a high mean stress is in better agreement with static yielding in figure 35.

The same reasoning when applied to the Guest theory had a similar result although the agreement was not so favorable.

The magnitude of the correction for yielding and its effect on the diagram of amplitude of stress against mean stress are illustrated in figures 32 and 34 in which both corrected and uncorrected values are plotted.

#### State of Stress at Different Mean Stresses

From ordinates at four values of mean stress in diagrams such as figure 35 and from the data at other states of stress for zero mean stress, diagrams showing the effect of state of stress were constructed as shown in figure 36 for the theory of a limiting value of principal shear stress (with a correction for anisotropy applied to the alternating stress). An examination of figure 36 revealed that this theory is a closer representation of the test data than any other considered, with the possible exception of Guest's law. It should be recalled, however, that the alternating values are the same, except for a constant factor, for six of the theories - not just the shear-stress theory. The diagrams for mean stresses above zero are, however, dependent on the shear-stress theory (or shear-strain theory, which is identical) since the mean stress does not contain a correction for anisotropy.

The principal-stress theory and principal-strain theory with correction for anisotropy were also considered for zero mean stress. The agreement with the test data was not nearly so good as for the principal-shear-stress theory corrected for anisotropy.

The effect of the correction for yielding is indicated in figure 36 by showing the ordinates to both the corrected and uncorrected curves of alternating against mean stress.

When the corrections for anisotropy and the data for all states of combined stress, all values of mean stress, and all cycles to failure were considered, the theories of fatigue failure were found to have the following order of merit (where the first theory represents the test data the closest):

- (1) Principal shear stress (principal shear strain, etc.) corrected for anisotropy
- (2) Complete Guest law
- (3) Principal strain corrected for anisotropy
- (4) Magnitude of state-of-stress vector
- (5) Total strain energy

## ENERGY AND OTHER CONSIDERATIONS

Of the six theories whose equations for bending and torsion become identical when corrected for anisotropy two are based on an energy concept. Also, even without correction for anisotropy, energy theories rank high in the order of the rational theories (see section entitled "Effect of State of Stress").

## Energy as a Scalar

There are a number of observations which seem incompatible with energy concepts. Energy is a scalar quantity so that the characteristics of strain energy are independent of orientation of the principal stresses relative to the material. Thus anisotropy in the material should not affect the results of fatigue tests of specimens having different orientations if energy is the criterion of fatigue failure. However, data referred to in the section entitled "Data on Isotropy in Fatigue of Metals" indicate that orientation probably affects the results of fatigue tests.

Microscopic studies have indicated that slip bands are present in the vicinity of fatigue cracks and that they probably precede actual fatigue cracks. This being the case, the orientation of stress (or forces) would seem to be an important factor in the origin of fatigue cracking. Thus one might question whether a scalar quantity such as energy could be a controlling factor.

It has been suggested by Fowler (in a private discussion) that energy theories might be tested if one could devise a means of maintaining the state and intensity of stress constant in a specimen (no fluctuation in stress) and fluctuate the orientation of the principal stress axes with respect to the specimen. Fatigue fracture might or might not occur at high stresses, according to whether orientation of stressing is or is not a factor in the fatigue phenomena. It seems to the writer that fatigue would very probably occur.

Such a test might be accomplished by using a disk as a specimen. The disk should have a heavy rim and be dished on both sides so that when loaded diametrically there would be a section of uniform high stress in the center whose state of stress was biaxial (an unequal tension and compression). If the disk is loaded through rollers and rotated under load the strain energy in the high-stress portion of the disk would remain constant but the principal stress directions would rotate with respect to the disk.

In such a test if either the state of stress or the material is isotropic nothing should happen, but if both are anisotropic it should be possible to produce fatigue fracture. This should be true even though the material is statistically isotropic since fatigue fracture originates from phenomena occurring in individual grains, whose properties are known to be anisotropic.

In view of the above it would seem that correction of an isotropic theory such as an energy theory for anisotropy is meaningless. This leads one to suspect that energy theories are not applicable to this problem, or that the concept of energy as a scalar must be modified.

### Strain Energy and Mean Stress

Another difficulty arises in trying to apply the energy theory to the problem when the mean stress is not zero. The variation of strain energy with time when calculated from stresses must be based on the variation of the total stress, not on the variation of components such as alternating and mean stress. Residual stresses must also be added to the applied stresses before calculating the energy. If this is not done large errors in energy will result since stresses are squared in computing the strain energy. Thus diagrams such as figures 26 to 28 in which the alternating and mean total energies are computed directly from the alternating and mean stresses, respectively, do not present the correct relation between the components of energy.

An attempt to present a more accurate picture of the energy relation discloses the following difficulties:

(1) When the minimum stress of the cycle is of the same sign as the maximum stress there is no difficulty other than that the energy cycle is not sinusoidal as the stress cycle was. The maximum energy is calculated from the maximum stress and the minimum energy from the minimum stress. The alternating and mean energies are calculated as half the difference and half the sum of these maximums and minimums.

(2) Since energy is a scalar and always positive a completely reversed sinusoidal cycle of stress will produce not a completely reversed cycle of strain energy but a cycle of energy varying from zero (at zero stress) to a maximum (at both maximum and minimum stress) which is not sinusoidal and has a frequency twice the frequency of the stress cycle. Thus the total number of energy cycles sustained before fracture is twice the total number of stress cycles sustained. These facts have not been discussed (as far as is known) in previous studies of energy theories of failure applied to fatigue.

(3) When the stress during the cycle is partly of one sign but mostly of the opposite sign, the energy cycle consists of two alternate pulses of the same sign but different magnitude. The frequency of the larger pulse is the same as that of the stress cycle.

When the above factors are taken into account a new diagram representing the actual alternating energy against actual mean energy may be constructed as shown in figure 37. This is accomplished by (a) computing the alternating and mean energies as described in item (1) above,

(b) accounting for the change in frequency noted in item (2), and (c) neglecting the smaller pulse described in item (3). A zero value of mean energy is not possible. Figure 37 shows that the alternating energy for fatigue failure increases equally with increase in mean energy until the minimum energy of the cycle becomes greater than zero. This behavior does not seem reasonable as a theory of fatigue failure under combined stress. The stress and corresponding energy cycles are illustrated in figure 37 for typical values of mean stress. While the relation shown in figure 37 is for total energy, a similar relation would obtain for distortion energy.

Another possible way of handling the strain-energy relationship that avoids the difficulties enumerated above is to give energy an arbitrary sign the same as the sign of the corresponding stress. If this is done the alternating energy decreases and then increases markedly with increase in mean stress.

The least unreasonable of these methods of handling energy is that shown in figures 26 to 28. But the most reasonable explanation for this interpretation seems to require that fatigue failure is associated with the dynamic (fluctuating) strain energy independent of the mean strain energy and that the mean energy, whether from externally applied mean stress, residual macrostress, or residual microstress, merely acts in a manner similar to a change in the internal structure of the alloy. Such a change in structure may or may not greatly affect the fatigue strength of the alloy. Of course, it may be that the change in structure is caused by some factor other than mean energy such as mean shearing stress while the alternating energy controls the initiation of fatigue fracture.

The above explanation of the relation between strain energy (either total or distortional) and fatigue failure at different values of mean stress would seem rather plausible if it were not for the other difficulties with an energy theory which were discussed in this section.

#### Theories of Octahedral Shear and State-of-Stress Vector

The octahedral shear stress has been proposed as a limiting condition for yielding. It has been examined here as a possible theory for fatigue. However, it is difficult to understand why a shear stress (such as octahedral shear stress) which is less than the maximum shear stress could be the controlling factor either in initiation of yielding or more especially in fatigue. The greatest merits of the octahedral shear stress seem to be that its equation includes the intermediate principal stress like the distortion-energy theory but that it is a vector quantity.

Of course the magnitude of the state-of-stress vector has no more significance as a fundamental theory of fatigue failure under combined stress than the octahedral shear stress since it has no physical significance in terms of mechanisms of failure.

## MODE OF FRACTURING

## Origin of Fatigue Cracks

The observations on the fractured specimens and other factors suggest the following as the possible sequence in formation of fatigue cracks. Under the action of repeated stressing slip occurs in crystal grains which are favorably oriented for slip along planes in or near the orientation of planes of maximum shear stress and which have grain boundaries, that is, relationships with neighboring grains (such as a free surface on one side), which permit slip under the applied stress.

The reversal or pulsation of stress causes repeated and reversed slip in some grains which may result first in a breakdown of the ordered atomic array in the crystal along the planes of slip and finally in the formation of a crack. Under further reversals of load the removal of restraint resulting from the initial crack permits slip to occur more readily in adjacent crystals so that the crack tends to spread roughly in the plane of maximum shearing stress.

## Propagation of Fatigue Cracks

As the crack becomes larger the shearing displacement between the two faces of the crack increases with a consequent mechanical interference between the irregularities left in the wake of the crack. This interference results in abrasion of the walls of the crack and the formation of fine black particles of crystalline aluminum alloy<sup>2</sup> which exude from the crack as the black dust observed coming from cracks and deposited on surfaces of shear planes. It may be that the fineness of the particles, the fact that the particles are formed from disordered material and that the temperature (resulting from friction) at which they form is probably high all contribute to the black color of the aluminum. (A full account of aluminum black is found in a paper by Milligan and Focke (reference 65).)

As long as (a) the alternating principal shear stress and (b) the ratio of the alternating principal shear stress to the maximum principal stress are larger than a certain value the cracks continue to propagate rapidly as shear cracks. But, as either of these values becomes less than a certain limit, the propagation of the crack appears to change to a tensile fracture on planes of greatest principal stress. However, the

---

<sup>2</sup>The identity of the black particles was established by an X-ray analysis conducted for the author by Messrs. G. L. Clark and E. P. Bertin.

initiation of fracture appears still to be on shear planes. Thus the number of cycles to failure, as determined in the ordinary fatigue test, depends on the influence of both modes of propagation of cracks. This conclusion is in disagreement with that of Almen who says that "fatigue failures are tensile failures" (reference 66).

#### Effect of Alternating Stress, Mean Stress, and State of Stress

It would appear from the effect of mean stress on the transition from shear propagation of cracks to tensile propagation of cracks that the initiation and propagation of shear cracks are dependent on the alternating component of shear stress (which must cause repeated and reversing slip). On the other hand the propagation of cracks by tension would appear to depend on the repeated application of the maximum (alternating plus mean) principal tension stress. Hence as the mean stress increases propagation of cracks by tension tends to predominate.

The effect of changing the state of stress from that produced by torsion through combined bending and torsion to bending is to decrease the relative magnitude of the principal shear stress compared with that of the largest principal stress. This has the effect of causing an earlier transition from shear to tensile propagation of cracks, as observed.

The fact that as the amplitude of stress decreases in tests at zero mean stress the propagation of the cracks changes from shear to tension even though the ratio of tension to shear remains constant suggests that the conditions controlling the propagation of cracks (or perhaps the rate of propagation of cracks) by the two mechanisms are not both linear functions of the magnitude of stress. Propagation of cracks by shear must be proportional to a higher power of the applied stress than the rate of propagation of cracks by tension.

#### Relation to Theories and Observations

The observation that the results of fatigue tests under combined stress of metals composed of reasonably continuous polycrystalline aggregates have never been predicted by the theory of a limiting principal stress but have been more nearly predicted by a theory of a limiting shear stress is in agreement with the observation that the initiation of fatigue fractures is on shear planes. The observed deviations from the shear theory may be due in part to the differences in rate of crack propagation by shear and by tension.

On the other hand the observation that fatigue of cast irons under combined stresses is most nearly predicted by the theory of a limiting

principal stress may result from the fact that the cast irons contain large inclusions of soft graphite flakes. It seems entirely possible that these inclusions act as cracks in the metal from which, under many states of stress, the fatigue cracks propagate directly as tension fractures without the preliminary stage of slip and shear cracking described above for metals which do not contain these internal cracks.

The principles described above may also explain the observation reported by Smith (reference 42) that the fatigue strength of metals (other than cast iron) in torsion is nearly independent of the mean stress (and hence the maximum stress) whereas cast iron in torsion and most metals in tension are strongly dependent on the mean stress (and hence the maximum stress). That is, in torsion the propagation of fatigue cracks is largely by shear cracks and hence controlled by the alternating shear stress except for cast iron where the presence of internal cracks permits propagation of fatigue cracks as a result of the repeated application of the maximum (alternating plus mean) principal stress. In bending the propagation of the cracks in cast iron is by the same mechanism as in torsion. In other metals in bending the cracks are initiated as shear cracks but propagate as tension cracks especially at higher mean stresses where the maximum (alternating plus mean) principal stress becomes predominant.

#### Relation to Surface Residual Stress

This theory of fatigue cracking may also explain the phenomenon of zones of compressive biaxial residual stresses blocking the propagation of fatigue cracks into the zones of compressive residual stress. This phenomenon has been widely used as a means of improving the fatigue strength of machine parts subjected to bending or torsion repeated stress.

All means of producing compressive residual stresses probably alter the structure of the material in the compressively stressed zone. This alteration in the material may improve the resistance of the material to fatigue, thus in part accounting for the observed fact. However, the arresting of crack propagation in zones of compressive residual stress may also be explained by the mechanisms of crack propagation described above. The alternating shear stresses which have been described as causing the initiation of fatigue failure are independent of the presence of residual stresses (or mean stresses) of any kind.

However, once the crack is initiated its propagation by a tension crack will not occur unless repeated tension stresses are applied. In regions of sufficiently high residual compression stresses tension stresses will not occur. Hence the only mechanism for crack propagation available is by shear.

It also seems probable that the presence of compressive stresses on the planes of maximum shear stresses such as would be the case in regions of compressive residual stresses would raise the shear stress required for slip and would retard the development and propagation of cracks from repeated slip. Thus even in torsion compressive biaxial residual stresses on the surface should be beneficial, as observed.

It should be acknowledged at this point that the above analysis of fatigue cracking is tentative, qualitative, and incomplete and hence leaves much to be desired.

#### EFFECT OF MAXIMUM STRESS ON FATIGUE STRENGTH

If, as seems to be the case, general yielding affects the fatigue strength, then it should perhaps be questioned whether the fatigue strength should be expressed in terms of the mean stress. Perhaps the maximum stress would be a more logical parameter. The alternating principal shear stress as corrected for anisotropy has been plotted as a function of the maximum value (occurring in a cycle of stress) of the principal shearing stress (corrected for yielding). This is shown in figure 38 for bending and figure 39 for torsion. The limit of proportionality, yield strength, ultimate strength, and fracture stress are also shown in figures 38 and/or 39.

It is evident that the region of these diagrams above the diagonal line is unavailable for testing, especially in torsion. In bending or at least for axial loading this region would be available if the material had a much higher yield strength in compression than in tension. Since this is not the case for ductile metals one can only speculate on the shape of curves in this region. Points on the vertical axis would represent the fatigue strength of virgin material unaffected by stresses which might cause yielding or other alterations of the material.

The reason for the difference in shape and slope of these curves for bending and for torsion may be found in the mode of fracturing in fatigue as discussed above in the light of the observed fractures. In the torsion test the fatigue cracks propagate mostly by repeated slip under cyclic shearing stress (or shearing strain) and the major effect of an increase in the maximum stress is to produce a change in the structure of the material especially when the maximum stress produces yielding.

In bending, however, there is the additional factor of tension stresses on the slip planes which tend to change the mechanism of crack propagation and perhaps to accelerate it. Since the magnitude of the tension stress increases with the maximum stress of the cycle whereas the alternating shear stress is independent of the maximum stress, the rate of crack propagation may be greater at higher maximum stresses for bending tests. Thus it seems entirely possible that both anisotropy and the factors controlling crack propagation may influence the results.

The curves in the unavailable region may be as shown by the dashed lines in figures 38 and 39. These considerations might account at least in part for the divergence observed between the test data and the uncorrected principal-shear-stress theory. The values of the alternating stress at zero mean stress (uncorrected) obtained from the torsion tests are shown plotted in figure 38 for bending tests as short dash lines on the vertical axis. This corresponds to an assumption that the principal-shear theory governs fatigue under these conditions and that the maximum stress has no effect on the fatigue strength within the unavailable region of the torsion diagram (fig. 39). It was observed that the values from the torsion tests are consistent with a possible shape of the dashed curves (fig. 38) for the bending tests.

While the maximum stress seems to be the most logical parameter from a theoretical standpoint, it is probable that from a design standpoint the mean stress is the more useful in describing the range of stress because of the unavailable region in the diagram of alternating stress against maximum stress.

#### CONCLUSIONS

The following conclusions are obtained from an investigation of the combined-stress fatigue strength of 76S-T61 aluminum alloy with superimposed mean stresses and corrections for yielding.

1. A review of the status of the problem shows that the available test data under types of combined loadings other than bending and torsion do not eliminate the limiting shear stress as a possible theory of fatigue failure under combined stress.
2. If anisotropy is considered as affecting the results then fatigue tests under combined bending and torsion are inadequate to differentiate between six of the theories. Tests at other states of stress are needed to separate these theories and to test the applicability of the theories over a wider range of states of stress.
3. A more thorough study of the influence of anisotropy on fatigue under combined stress is needed.
4. The proposed theories governing fatigue failure under combined stresses which best represented the test data are as follows in order of merit: (a) Principal shear stress (principal shear strain, etc.) corrected for anisotropy, (b) complete Guest law, (c) principal strain corrected for anisotropy, (d) magnitude of state-of-stress vector, and (e) total strain energy.

5. Several consequences of energy theories are discussed which seem to indicate that energy theories are inadequate to describe failure under combined-bending-and-torsion fatigue with superimposed static stresses. Additional tests of the adequacy of energy theories are desirable.

6. In view of the inconsistencies and limitations of several of the theories as discussed above the only ones of the theories which seem to hold much promise are as follows: (a) Principal shear stress (or strain) corrected for anisotropy, (b) complete Guest law, and (c) principal strain corrected for anisotropy.

7. The mean stress in the stress cycle was shown to have a small but important effect on the fatigue strength (measured in terms of stress) for the 76S-T61 aluminum alloy tested. If strain energy were used as a measure of fatigue strength the mean energy would have a very pronounced effect.

8. The data indicate that the initial fracture occurs as a shear crack.

9. The propagation of fatigue cracks occurs by either of two mechanisms, a shearing displacement or a tension separation, depending on the state of stress and the magnitude of the alternating and static stresses.

10. The analysis presented suggests that the effect of the mean stress (really the maximum stress) on the fatigue strength results from two phenomena distinct from the fatigue process: (a) The maximum stress may produce elastic or plastic structural changes in the material which affect its fatigue strength and (b) one of the modes of crack propagation (propagation by tension separation) is a function of the maximum (alternating plus mean) principal stress. Thus cracks once formed propagate more rapidly under high mean (i.e., maximum) stresses. The other mode of crack propagation is apparently dependent on the alternating principal shear stress and the magnitude and sign of the normal stress on the plane of the principal shear stress.

Department of Theoretical and Applied Mechanics  
University of Illinois  
Urbana, Ill., July 1, 1951

## APPENDIX

## CORRECTION OF STRESSES IN BENDING OR TORSION TESTS

## IN WHICH PROPORTIONAL LIMIT WAS EXCEEDED

The alternating nominal stress in these tests required no correction because: (1) The alternating deflection applied to the specimen was based on elastic behavior of the specimen and (2) the unloading curves following the initial loading and subsequent loading cycles were nearly elastic. (See figs. 17 and 18.) Thus the only correction required for bending or torsion was the determination of the actual maximum stress. From this the mean stress could be determined.

The correction of the maximum stress required a knowledge of the maximum load applied to the specimen. Since in these fatigue tests only the maximum and minimum deflection and the elastic stiffness were determined it was necessary to prepare a calibration curve of load against deflection for the shape of specimen and test conditions employed in the fatigue tests. Such curves were obtained for bending and for torsion. Allowance was made for slight deviations of individual test conditions.

## Corrections for Bending

The correction employed for bending was a semigraphical procedure based on an extension of the Herbert equation by Morkovin and Sidebottom (reference 58). The steps involved were as follows:

The stress-strain curve in tension was found to be nearly the same as that in compression for the range of strain employed in the fatigue tests. So the analysis was based on relationships applicable only when the stress-strain relation was the same in tension and compression.

From two static tension and two static compression tests an average stress-strain curve was constructed and the stress at the apparent proportional limit  $\sigma_e$  and the corresponding strain  $\epsilon_e$  were obtained. (See fig. 15.)

From this curve values of strains  $\epsilon$  and corresponding stresses  $\sigma$  were selected and divided by the respective values at the proportional limit in order to plot a dimensionless stress-strain curve such as curve 1 in figure 40. Point A is the proportional limit.

A dimensionless moment-strain curve was then constructed based on the equation from Morkovin and Sidebottom

$$\frac{M}{M_e} = \frac{1-s}{\pi} \left[ \frac{4}{3} \left( 1 - \frac{\epsilon_e^2}{\epsilon^2} \right)^{3/2} + 2 \left( 1 + \frac{\epsilon_e^2}{\epsilon^2} \right)^{1/2} + 2 \frac{\epsilon}{\epsilon_e} \arcsin \frac{\epsilon_e}{\epsilon} \right] + s \frac{\epsilon}{\epsilon_e} \quad (8)$$

where  $M$  is the applied bending moment,  $M_e$  is the bending moment when the maximum strain is at the proportional limit, and  $s$  is the slope of the dimensionless stress-strain curve above the proportional limit for a material in which the stress-strain diagram above the proportional limit is another straight line.

Since the plastic stress-strain diagram for this aluminum alloy was a curve above the proportional limit, a point-by-point procedure described by Sidebottom in an unpublished paper was employed to construct the  $M/M_e$  diagram. By this procedure the stress-strain diagram up to any given stress was approximated by two intersecting straight lines, the second of which terminated at the required stress  $\sigma_1/\sigma_e$  and strain  $\epsilon_1/\epsilon_e$ . (See fig. 40.) The point of intersection  $F$  (fig. 40) formed a new (apparent) proportional limit. In order for the simplified stress-strain diagram to produce the same resisting moment in a beam as the actual stress-strain diagram the moment of the area under the stress-strain diagram up to the given stress should have the same value about the vertical axis of the simplified diagram as that in the actual stress-strain diagram. This was approximated in the present calculations by making the area enclosed by the two stress-strain diagrams above the straight line equal the area enclosed below. The error involved was shown to be negligible.

The calculations were simplified by the observations that for  $s = 0$  equation (8) becomes

$$\frac{M}{M_e} \Big|_{s=0} = \frac{1}{\pi} \left[ \frac{4}{3} \left( 1 - \frac{\epsilon_e^2}{\epsilon^2} \right)^{3/2} + 2 \left( 1 - \frac{\epsilon_e^2}{\epsilon^2} \right)^{1/2} + 2 \frac{\epsilon}{\epsilon_e} \arcsin \frac{\epsilon_e}{\epsilon} \right] \quad (9)$$

so that equation (8) may be rewritten as

$$\left. \frac{M_i}{M_e} \right|_{s=s_i} \Bigg|_{i=1,2,3,\dots} = \left[ (1 - s_i) \left( \frac{M_i}{M_e} \Big|_{s=0} \right) + s_i \frac{\epsilon_i'}{\epsilon_e} \right] \Bigg|_{i=1,2,3,\dots} \quad (10)$$

where  $\left. \frac{M_i}{M_e} \right|_{s=s_i}$  is the bending moment for the stress  $\sigma_i$  considered,  $s_i$  is the slope of the corresponding straight line representing the plastic part of the stress-strain diagram,  $\left. \frac{M_i}{M_e} \right|_{s=0}$  is the bending moment corresponding to stress  $\sigma_i$  obtained from a plot of equation (8) (curve 2, fig. 40), and  $\epsilon_i'$  is the corresponding strain divided by the abscissa of point F in order to correct for the change in scale on the dimensionless diagram (fig. 40) resulting from the fact that point F does not coincide with point A.

The values of  $\left. \frac{M_i}{M_e} \right|_{s=s_i}$  must be multiplied by the ordinate to point F to correct for the change in scale previously noted. These values may then be plotted as curve 3 in figure 40.

The corrected maximum stress for any specimen can then be obtained from figure 40 by determining the dimensionless bending moment  $M/M_e$  for the specimen and locating the corresponding value of the dimensionless strain  $\epsilon/\epsilon_e$  from curve 3, figure 40. The dimensionless stress  $\sigma/\sigma_e$  corresponding to the maximum stress is then found from curve 1 at the same value of  $\epsilon/\epsilon_e$ . The dimensionless stress  $\sigma/\sigma_e$  multiplied by the stress at the proportional limit  $\sigma_e$  gives the desired corrected stress  $\sigma$ .

The mean stress  $\sigma_m$  then becomes

$$\sigma_m = \sigma - \sigma_a \quad (11)$$

where  $\sigma_a$  is the alternating stress.

It should be noted that this correction is probably not exact because of several simplifications from actual material behavior among which are: The yielding was probably not homogeneous or continuous and the specimen

shape confined yielding to a small region which may have further complicated the geometry of plastic straining; the rate of straining in the static tests was much slower than the rate of straining during the first load application in the fatigue tests.

#### Correction for Torsion

The shearing stress at the surface of a specimen with a circular cross section subjected to a torque  $T$  is given by the following equation (according to Nadai in reference 59) for stress above the proportional limit:

$$\tau = \frac{3T + \theta \frac{dT}{d\theta}}{2\pi a^3} \quad (12)$$

where  $\tau$  is the corrected shearing stress and  $\theta$  is the angle of twist per inch in a section of constant diameter  $a$ .

The graphical technique outlined by Nadai in reference 59 for use with this equation was employed. This technique required a curve of torque against angle of twist of a cylindrical specimen of circular cross section. The graphical procedure was applied to this curve to determine the corrected shearing stress at the extreme fiber caused by a torque  $T$ .

From the results of these calculations a corrected curve of shearing stress against shearing strain was constructed as shown in figure 16, and a curve of nominal shearing stress against corrected shearing stress was constructed. By means of the latter curve the maximum stress  $\tau$  in specimens tested in torsion above the proportional limit was determined. The corrected mean stress  $\tau_m$  for a given alternating stress  $\tau_a$  was then determined by the equation

$$\tau_m = \tau - \tau_a \quad (13)$$

It should be observed that the same limitations apply to this correction procedure as those that apply to the bending procedure.

## REFERENCES

1. Stanton, T. E., and Batson, R. G.: The Fatigue Resistance of Mild Steel under Various Conditions of Stress Distribution. British Assoc. Rep. (Newcastle), 1916, pp. 288-291.
2. Ono, A.: Fatigue of Steel under Combined Bending and Torsion. Memoirs Col. Eng. Kyushi Imperial Univ. (Japan), vol. 2, no. 2, 1921, pp. 117-142.
3. Lea, F. C., and Budgen, H. P.: Combined Torsional and Repeated Bending Stresses. Engineering, vol. CXXII, Aug. 20, 1926, pp. 242-245.
4. Nimhanmimie, S. K.: Static Torque Combined with Cyclic Bending. Master's Thesis, London Univ., July 1931.
5. Hohenemser, K., and Prager, W.: Zur Frage der Ermüdungsfestigkeit bei Mehrachsigen Spannungszuständen. Metallwirtschaft, Bd. 12, Heft 24, June 1933, pp. 342-343.
6. Huitt, W. J.: Static Torque Combined with Cyclic Bending. Master's Thesis, London Univ., July 1935.
7. Cox, H. L., and Glenshaw, W. J.: Behavior of Three Single Crystals of Aluminum in Fatigue under Complex Stresses. Proc. Roy. Soc. (London), ser. A, vol. 149, 1935, pp. 312-326.
8. Gough, H. J., and Pollard, H. V.: The Strength of Metals under Combined Alternating Stresses. Proc. Inst. Mech. Eng. (London), vol. 131, Nov. 1935, pp. 1-103.
9. Gough, H. J., and Pollard, H. V.: The Effect of Specimen Form on the Resistance of Metals to Combined Alternating Stresses. Proc. Inst. Mech. Eng. (London), vol. 132, Dec. 1936, pp. 549-573.
10. Gough, H. J., and Pollard, H. V.: Properties of Some Materials for Cast Crankshafts, with Special Reference to Combined Stresses. Proc. Inst. Automotive Eng. (London), vol. 31, March 1937, pp. 821-896.
11. Narmore, Phil Blasier: A Fatigue Study of Strong Steel under Combined Alternating Stresses. Ph.D. Thesis, Univ. of Mich., Nov. 1937.

12. Körber, F., and Hempel, M.: Zugdruck-, Biege-, und Verdrehwechselbeanspruchung an Stahlstäben mit Querbohrungen und Kerben. Mitt. Kaiser-Wilhelm Inst. Eisenforsch., Bd. 21, Heft 1, 1939, pp. 1-19.
13. Nisihara, T., and Kawamoto, M.: The Fatigue Test of Steel under Combined Bending and Torsion. Trans. Soc. Mech. Eng. (Japan), vol. 6, no. 24, Aug. 1940, pp. 1-8; English abstract, p. S-2. Also, English Translation No. 95, Caterpillar Tractor Co.
14. Nisihara, T., and Kawamoto, M.: Fatigue Testing of Duralumin under Combined Bending and Torsion. Trans. Inst. Metals (Japan), vol. 5, no. 3, 1941, pp. 110-115. Abstract, The Jour. Inst. Metals, vol. 8, 1941, pp. 238-239.
15. Nisihara, Tosio, and Kawamoto, Minoru: The Strength of Metals under Combined Alternating Bending and Torsion. Memoirs Col. Eng., Kyoto Imperial Univ., vol. 10, no. 6, 1941, pp. 177-201. Abstract, The Jour. Inst. Metals, vol. 10, April 1943, p. 124.
16. Sauer, J. A.: A Study of Fatigue Phenomena under Combined Stresses. Vol. 4. Proc. Seventh Int. Cong. Appl. Mech. (Sept. 1948, London), 1948, pp. 150-164.
17. Frith, P. H.: Fatigue Tests on Crankshaft Steels. Jour. Iron and Steel Inst., vol. 159, 1948, pp. 385-409.
18. Gough, H. J.: Engineering Steels under Combined Cyclic and Static Stresses. The Engineer (London), Oct. 28, 1949, pp. 497-500; Nov. 4, 1949, pp. 510-514; Nov. 11, 1949, pp. 540-543; Nov. 18, 1949, pp. 570-573. (See also: Proc. Inst. Mech. Eng., vol. 160, no. 4, pp. 417-440, and Jour. Appl. Mech., vol. 17, no. 2, June 1950, pp. 113-125.)
19. Maier, A. F.: Stress Reversal in Tubes under Internal Pressure. Stahl und Eisen, vol. 54, no. 50, Dec. 13, 1934, pp. 1289-1291.
20. Marin, Joseph: Strength of Steel Subjected to Biaxial Fatigue Stresses. The Welding Jour., vol. 21, Nov. 1942, pp. 554s-559s.
21. Morikawa, G. K., and Griffis, LeVan: The Biaxial Fatigue Strength of Low-Carbon Steels. The Welding Jour., vol. 24, March 1945, pp. 167s-174s.
22. Majors, H., Jr., Mills, B. D., Jr., and MacGregor, C. W.: Fatigue under Combined Pulsating Stresses. Jour. Appl. Mech., vol. 16, no. 3, Sept. 1949, pp. 269-276.

23. Marin, Joseph, and Shelson, William: Biaxial Fatigue Strength of 24S-T Aluminum Alloy. NACA TN 1889, 1949.
24. Marin, Joseph: Biaxial Tension - Tension Fatigue Strengths of Metals. Jour. Appl. Mech., vol. 16, no. 4, Dec. 1949, pp. 383-388.
25. Sawert, Walter: Verhalten der Baustähle bei wechselnder mehrachsiger Beanspruchung. Z.V.D.I., Bd. 87, Nr. 39/40, Oct. 2, 1943, pp. 609-615.
26. Gadd, Charles W., Zmuda, Andrew, and Ochiltree, N. A.: Correlation of Stress Concentration with Fatigue Strength of Engine Components. SAE Jour., vol. 53, no. 11, Nov. 1945, pp. 640-647.
27. Lehr, E., and Prager, W.: Fatigue Testing Machine for Superimposed Tension-Compression and Alternating Shear Loading. Forsch. Geb. Ing.-Wes., vol. 4, 1933, p. 209.
28. Bruder, E.: Maschine zur Erzeugung synchroner, kombinierten Biege-Verdreh-Dauerbeanspruchungen. Z.V.D.I., Bd. 87, Nr. 5/6, Feb. 6, 1943, p. 82.
29. Puchner, O.: The Production of Synchronous Superimposed Alternating Bending and Torsional Loads. Schweizer Archiv angewandte Wiss. und Tech., vol. 12, no. 9, Sept. 1946, pp. 289-293.
30. Soderberg, C. R.: Factors of Safety and Working Stresses. Trans. A.S.M.E., APM 52-2, vol. 52, no. 2, 1930, pp. 13-28.
31. Soderberg, C. R.: Working Stresses. Trans. A.S.M.E., APM 55-16, vol. 55, no. 16, 1933, pp. 131-144.
32. Soderberg, C. R.: Working Stresses. Trans. A.S.M.E., vol. 57, 1935, pp. A-106-A114.
33. Capper, P. L.: Fatigue under Combined Bending and Torsion. The Engineer (London), vol. CLXIV, Aug. 6, 1937, pp. 150-152.
34. Guest, J. J.: Recent Research on Combined Stress. Proc. Inst. Auto Eng., vol. 35, no. 3, Dec. 1940, p. 33.
35. Marin, Joseph: Interpretation of Experiments on Fatigue Strength of Metals Subjected to Combined Stresses. The Welding Jour., vol. 21, no. 5, May 1942, pp. 245s-248s.
36. McAdam, D. J., Jr.: The Influence of the Combination of Principal Stress in Fatigue of Metals. Proc. A.S.T.M., vol. 42, 1942, pp. 576-592.

37. Peterson, R. E.: Application of Stress Concentration Factors in Design. Exp. Stress Analysis, vol. 1, no. 1, 1943, pp. 118-127.
38. Fowler, F. H., Jr.: On Fatigue Failure under Triaxial Static and Fluctuating Stresses and a Statistical Explanation of Size Effect. Trans. A.S.M.E., vol. 67, no. 3, April 1945, pp. 213-215.
39. Johnston, George S.: Fatigue Strength under Combined Stress. Master's Thesis, Purdue Univ., Feb. 1950.
40. Findley, W. N.: Discussion of "Engineering Steels under Combined Cyclic and Static Stresses" by H. J. Gough. Jour. Appl. Mech., vol. 18, no. 2, June 1951, pp. 211-213.
41. Peterson, R. E.: Discussion on "Nomenclature on Range in Stress in Fatigue." Proc. A.S.T.M., vol. 37, pt. I, 1937, pp. 162-163.
42. Smith, James O.: The Effect of Range of Stress on the Fatigue Strength of Metals. Bull. No. 334, Eng. Exp. Station, Univ. of Ill., Feb. 1942.
43. Bollenrath, F., and Cornelius, H.: Zeit- und Dauerfestigkeit einfach gestalteter metallischer Bauteile. Z.V.D.I., Bd. 84, Nr. 24, June 15, 1940, pp. 407-412.
44. Dolan, Thomas J.: Effects of Range of Stress and of Special Notches on Fatigue Properties of Aluminum Alloys Suitable for Airplane Propellers. NACA TN 852, 1942.
45. Findley, William N.: Mechanical Tests of Macerated Phenolic Molding Material. NACA ARR 3F19, 1943.
46. Dolan, Thomas J.: Certain Mechanical Strength Properties of Aluminum Alloys 25S-T and X76S-T. NACA TN 914, 1943.
47. Brueggeman, W. C., Mayer, M., Jr., and Smith, W. H.: Axial Fatigue Tests at Zero Mean Stress of 24S-T Aluminum-Alloy Steel with and without a Circular Hole. NACA TN 955, 1944.
48. Jackson, L. R., and Grover, H. J.: The Application of Data on Strength under Repeated Stresses to the Design of Aircraft. NACA ARR 5H27, 1945.
49. Findley, W. N.: Fatigue Tests of a Laminated Mitscherlich-Paper Plastic. Proc. A.S.T.M., vol. 45, 1945, pp. 878-903.

50. Russell, H. W., Jackson, L. R., Grover, H. J., and Beaver, W. W.: Fatigue Strength and Related Characteristics of Aircraft Joints. II - Fatigue Characteristics of Sheet and Riveted Joints of 0.040-Inch 24S-T, 75S-T, and R303-T275 Aluminum Alloys. NACA TN 1485, 1948.
51. Grover, H. J., Bishop, S. M., and Jackson, L. R.: Fatigue Strengths of Aircraft Materials - Axial-Load Fatigue Tests on Unnotched Sheet Specimens of 24S-T3 and 75S-T6 Aluminum Alloys and of SAE 4130 Steel. NACA TN 2324, 1951.
52. Sauer, J. A., and Lemmon, D. C.: Effect of Steady Stress on Fatigue Behavior of Aluminum. Trans. Am. Soc. Metals, vol. 42, 1950, pp. 559-576.
53. Schwartz, R. T.: Correlation of Data on the Effect of Range of Stress on the Fatigue Strength of Metals for Tensile Mean Stresses. Master's Thesis, Ohio State Univ., 1948.
54. Moore, H. F., and Kommers, J. B.: The Fatigue of Metals. McGraw-Hill Book Co., Inc., 1927.
55. Gerber W.: Relation between the Superior and the Inferior Stresses of a Cycle of Limiting Stress. Vereins Zeit. Bayerischen Archiv. Ing., 1874.
56. Seliger, Victor: A Suggested New Parameter for Fatigue Strength Analysis. Bull. No. 132, A.S.T.M. Jan. 1945, pp. 29-32.
57. Committee E-9 on Fatigue: Manual on Fatigue Testing. Special Tech. Pub. No. 91, A.S.T.M., 1949.
58. Morkovin, D., and Sidebottom, O.: The Effect of Non-uniform Distribution of Stress on the Yield Strength of Steel. Bull. No. 372, Eng. Exp. Station, Univ. of Ill., Dec. 1947.
59. Nadai, Arpád: Theory of Flow and Fracture of Solids. Vol. 1. Second ed., McGraw-Hill Book Co., Inc., 1950, p. 349.
60. Templin, R. L., and Hartmann, E. C.: The Elastic Constants for Wrought Aluminum Alloys. NACA TN 966, 1945.
61. Stang, Ambrose H., Greenspan, Martin, and Newman, Sanford B.: Poisson's Ratio of Some Structural Alloys for Large Strains. Res. Paper RP 1742, Jour. Res., Nat. Bur. Standards, vol. 37, no. 4, Oct. 1946, pp. 211-221.

62. Findley, William N., and Worley, Will J.: Mechanical Properties of Five Laminated Plastics. NACA TN 1560, 1948.
63. Cazaud, R.: *La Fatigue des Métaux*. Third ed., Dunod (Paris), 1948, pp. 181-187.
64. Templin, R. L., Howell, F. M., and Hartmann, E. C.: Effect of Grain Direction on Fatigue Properties of Aluminum Alloys. *Product Engineering*, vol. 21, no. 7, July 1950, pp. 126-130.
65. Milligan, W. O., and Focke, A. B.: The Crystal Structure of Aluminum Black. *Jour. Phys. Chem.*, vol. 45, no. 1, Jan. 1941, pp. 107-108.
66. Almen, J. O.: Fatigue Failures are Tensile Failures. *Product Engineering*, vol. 22, no. 3, March 1951, pp. 102-124.

TABLE I  
STATIC TESTS

Description of data	Elastic modulus (psi)	Apparent proportional limit (psi)	Yield strength		Ultimate strength (psi)	True fracture stress, (psi)	Strain rate (in./in.) min
			0.05-percent offset (psi)	0.2-percent offset (psi)			
Tension tests							
Data as reported by Dolan (reference 44), average of six tests	$9.69 \times 10^6$	-----	64,200	67,200	72,500	-----	-----
Revised from Dolan's fig. 8, average of three tests							
Normal stress and strain	9.66	51,000	64,000	67,400	73,100	95,000	-----
Shearing stress and strain		25,500	31,500	33,500	36,500	47,500	-----
Specimens from propeller blade, average of two tests							
Normal stress and strain	10.2	47,000	65,000	69,900	75,200	-----	-----
Shearing stress and strain		23,500	31,900	34,500	37,600	-----	-----
Compression tests							
Specimens from original bars, average of two tests							
Normal stress and strain	$10.5 \times 10^6$	60,000	67,800	72,300	<sup>a</sup> 77,100	-----	0.00065
Shearing stress and strain		30,000	33,500	35,700	<sup>a</sup> 38,500	-----	-----
Specimen from propeller blade, one test							
Normal stress and strain	10.9	61,000	71,400	75,400	<sup>a</sup> 83,300	-----	.0005
Shearing stress and strain		30,500	35,200	37,300	<sup>a</sup> 41,600	-----	-----
Tension and compression tests							
Data from average curve of tension and compression, average of four tests							
Normal stress and strain	$10.1 \times 10^6$	54,000	65,500	69,800	-----	-----	-----
Shearing stress and strain		27,000	32,300	34,600	-----	-----	-----
Torsion tests, data based on shear stress and strain							
Data as reported by Dolan (reference 44), average of three tests							
Specimens 0.56-in. diam., nominal stress	$4.06 \times 10^6$	-----	59,500	-----	63,600	-----	-----
Specimen from original bars, 0.261-in. diam., one test							
Nominal values of stress	3.85	31,000	38,800	44,200	60,800	-----	0.0021
Stresses corrected for yielding		27,000	32,600	36,000	-----	45,600	-----
Specimens from propeller blade, average of two tests							
Specimen 0.261-in. diam., nominal stresses	3.73	31,000	35,500	40,100	59,000	-----	.0024

<sup>a</sup>Load was still increasing; specimen did not fracture.



TABLE II  
FATIGUE DATA

State of stress			Number of cycles	Flexural stresses, $\sigma$			Torsional stresses, $\tau$		
$\theta$ (deg)	$\tau/\sigma$	$n$		Nominal mean stress (psi)	Corrected mean stress (psi)	Fatigue strength (stress amplitude) (psi)	Nominal mean stress (psi)	Corrected mean stress (psi)	Fatigue strength (stress amplitude) (psi)
0	0	0	$3 \times 10^4$	0	0	47,700	0	0	0
			$10^5$	0	0	41,000	0	0	0
			$10^6$	0	0	31,600	0	0	0
			$10^7$	0	0	27,300	0	0	0
			$10^8$	0	0	24,700	0	0	0
0	0	0	$3 \times 10^4$	12,000	11,800	44,500	0	0	0
			$10^5$	12,000	12,000	36,500	0	0	0
			$10^6$	12,000	12,000	27,600	0	0	0
			$10^7$	12,000	12,000	24,700	0	0	0
			$10^8$	12,000	12,000	22,900	0	0	0
0	0	0	$3 \times 10^4$	30,000	26,200	39,000	0	0	0
			$10^5$	30,000	29,400	30,000	0	0	0
			$10^6$	30,000	30,000	20,800	0	0	0
			$10^7$	30,000	30,000	20,800	0	0	0
			$10^8$	30,000	30,000	20,800	0	0	0
0	0	0	$3 \times 10^4$	45,000	36,400	31,600	0	0	0
			$10^5$	45,000	40,300	25,000	0	0	0
			$10^6$	45,000	42,000	21,500	0	0	0
			$10^7$	45,000	42,300	20,700	0	0	0
			$10^8$	45,000	42,600	20,100	0	0	0
0	0	0	$3 \times 10^4$	65,000	38,000	33,400	0	0	0
			$10^5$	65,000	48,300	21,900	0	0	0
			$10^6$	65,000	50,200	19,700	0	0	0
			$10^7$	65,000	50,400	19,300	0	0	0
			$10^8$	65,000	50,600	19,000	0	0	0
$22\frac{1}{2}$	0.207	-0.0395	$3 \times 10^4$	0	0	45,000	0	0	9,320
			$10^5$	0	0	39,500	0	0	8,180
			$10^6$	0	0	31,300	0	0	6,480
			$10^7$	0	0	26,200	0	0	5,420
			$10^8$	0	0	<sup>a</sup> 23,400	0	0	<sup>a</sup> 4,840
45	0.500	-0.169	$3 \times 10^4$	0	0	37,800	0	0	18,900
			$10^5$	0	0	32,500	0	0	16,250
			$10^6$	0	0	24,800	0	0	12,400
			$10^7$	0	0	20,200	0	0	10,100
			$10^8$	0	0	18,100	0	0	9,050
45	0.500	-0.169	$3 \times 10^4$	12,000	(b)	<sup>a</sup> 35,000	6000	(b)	<sup>a</sup> 17,500
			$10^5$	12,000		27,000	6000		13,500
			$10^6$	12,000		22,200	6000		11,100
			$10^7$	12,000		19,800	6000		9,900
			$10^8$	12,000		18,000	6000		9,000

<sup>a</sup>Extrapolated from S-N curve.

<sup>b</sup>Corrected mean stress unobtainable for this group.



TABLE II.- Concluded  
FATIGUE DATA - Concluded

State of stress			Number of cycles	Flexural stresses, $\sigma$			Torsional stresses, $\tau$		
$\theta$ (deg)	$\tau/\sigma$	n		Nominal mean stress (psi)	Corrected mean stress (psi)	Fatigue strength (stress amplitude) (psi)	Nominal mean stress (psi)	Corrected mean stress (psi)	Fatigue strength (stress amplitude) (psi)
45	0.500	-0.169	$3 \times 10^4$	30,000	(b)	27,100	15,000	(b)	13,550
			$10^5$	30,000		21,300	15,000		10,650
			$10^6$	30,000		18,800	15,000		9,400
			$10^7$	30,000		17,700	15,000		8,850
			$10^8$	30,000		<sup>a</sup> 16,700	15,000		<sup>a</sup> 8,350
45	0.500	-0.169	$3 \times 10^4$	45,000	(b)	24,200	22,500	(b)	12,100
			$10^5$	45,000		17,500	22,500		8,750
			$10^6$	45,000		15,000	22,500		7,500
			$10^7$	45,000		15,000	22,500		7,500
			$10^8$	45,000		15,000	22,500		7,500
56 $\frac{3}{4}$	0.732	-0.268	$3 \times 10^4$	0	0	-----	0	0	-----
			$10^5$	0	0	28,100	0	0	20,550
			$10^6$	0	0	20,200	0	0	14,780
			$10^7$	0	0	17,100	0	0	12,500
			$10^8$	0	0	14,900	0	0	10,900
67 $\frac{1}{2}$	1.207	-0.408	$3 \times 10^4$	0	0	22,800	0	0	27,500
			$10^5$	0	0	19,700	0	0	23,800
			$10^6$	0	0	15,150	0	0	18,300
			$10^7$	0	0	12,580	0	0	15,100
			$10^8$	0	0	<sup>a</sup> 11,510	0	0	<sup>a</sup> 13,900
90	$\infty$	-0.707	$3 \times 10^4$	0	0	0	0	0	29,500
			$10^5$	0	0	0	0	0	26,000
			$10^6$	0	0	0	0	0	20,800
			$10^7$	0	0	0	0	0	17,300
			$10^8$	0	0	0	0	0	15,900
90	$\infty$	-0.707	$3 \times 10^4$	0	0	0	15,000	8,600	28,200
			$10^5$	0	0	0	15,000	11,800	23,500
			$10^6$	0	0	0	15,000	14,000	17,600
			$10^7$	0	0	0	15,000	14,600	15,000
			$10^8$	0	0	0	15,000	14,700	14,300
90	$\infty$	-0.707	$3 \times 10^4$	0	0	0	30,000	11,400	27,400
			$10^5$	0	0	0	30,000	15,900	22,200
			$10^6$	0	0	0	30,000	21,500	15,700
			$10^7$	0	0	0	30,000	23,800	12,800
			$10^8$	0	0	0	30,000	24,400	<sup>a</sup> 12,000
90	$\infty$	-0.707	$3 \times 10^4$	0	0	0	45,000	11,000	29,000
			$10^5$	0	0	0	45,000	18,700	20,700
			$10^6$	0	0	0	45,000	26,600	12,200
			$10^7$	0	0	0	45,000	29,500	9,000
			$10^8$	0	0	0	45,000	30,300	8,000

<sup>a</sup>Extrapolated from S-N curve.

<sup>b</sup>Corrected mean stress unobtainable for this group.

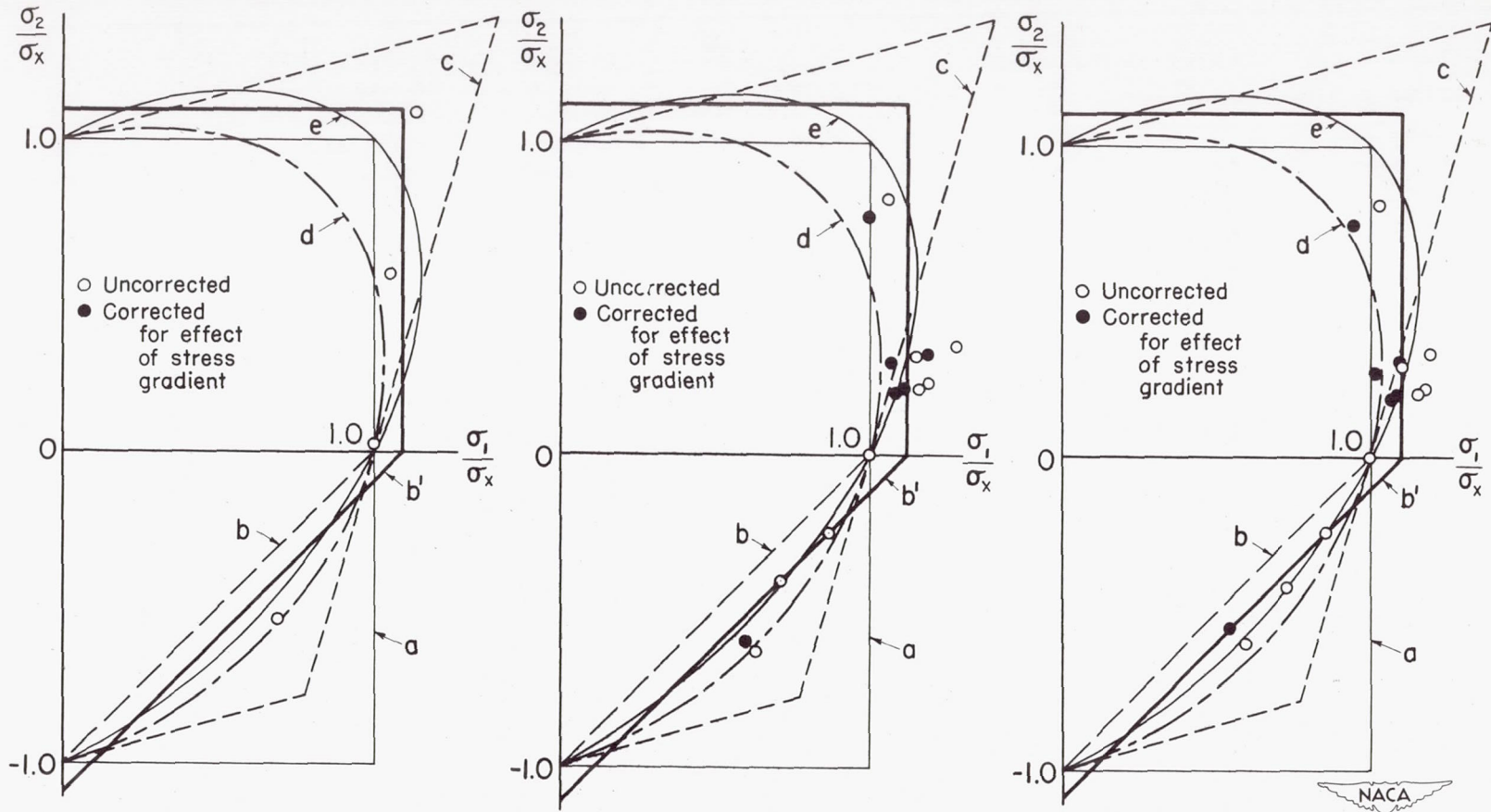


TABLE III  
THEORIES OF FAILURE

Theory	Equation of limiting value in terms of principal stresses $\sigma_1 > \sigma_2 > \sigma_3$	Equation for combined bending $\sigma$ and twisting $\tau$	Required ratio b/t	Equation corrected for anisotropy in terms of bending $\sigma$ , twisting $\tau$ , and b/t
Principal stress	$\sigma_1$	$\sigma_1 = \frac{1}{2}(\sqrt{\sigma^2 + 4\tau^2} + \sigma)$	$a_1$	$\sigma_1 = \frac{1}{2}\left[\sqrt{\sigma^2 + 4\left(\frac{b}{t}\right)^2\tau^2} + \sigma\right]$
Principal shear stress	$\tau_1 = \frac{\sigma_1 - \sigma_3}{2}$	$\tau_1 = \frac{1}{2}\sqrt{\sigma^2 + 4\tau^2}$	2	$\tau_1 = \frac{1}{2}\sqrt{\sigma^2 + \left(\frac{b}{t}\right)^2\tau^2}$
Principal strain	$\epsilon_1 = \frac{1}{E}[\sigma_1 - \mu(\sigma_2 + \sigma_3)]$	$\epsilon_1 = \frac{1+\mu}{2E}\left(\sqrt{\sigma^2 + 4\tau^2} + \frac{1-\mu}{1+\mu}\sigma\right)$	$1 + \mu^a$	$\epsilon_1 = \frac{1+\mu}{2E}\left\{\sqrt{\sigma^2 + \left[\frac{2b}{t(1+\mu)}\right]^2\tau^2} + \frac{1-\mu}{1+\mu}\sigma\right\}$
Principal shear strain	$\gamma_1 = \frac{1+\mu}{E}(\sigma_1 - \sigma_3)$	$\gamma_1 = \frac{1+\mu}{E}\sqrt{\sigma^2 + 4\tau^2}$	2	$\gamma_1 = \frac{1+\mu}{E}\sqrt{\sigma^2 + \left(\frac{b}{t}\right)^2\tau^2}$
Energy of distortion	$W_D = \frac{1+\mu}{6E}[(\sigma_1 - \sigma_2)^2 + (\sigma_2 - \sigma_3)^2 + (\sigma_3 - \sigma_1)^2]$	$W_D = \frac{1+\mu}{3E}(\sigma^2 + 3\tau^2)$	$\sqrt{3}$	$W_D = \frac{1+\mu}{3E}\left[\sigma^2 + \left(\frac{b}{t}\right)^2\tau^2\right]$
Octahedral shear stress	$\tau_o = \frac{1}{3}\sqrt{(\sigma_1 - \sigma_2)^2 + (\sigma_2 - \sigma_3)^2 + (\sigma_3 - \sigma_1)^2}$	$\tau_o = \frac{\sqrt{2}}{3}\sqrt{\sigma^2 + 3\tau^2}$	$\sqrt{3}$	$\tau_o = \frac{\sqrt{2}}{3}\sqrt{\sigma^2 + \left(\frac{b}{t}\right)^2\tau^2}$
Total energy of deformation	$W = \frac{1}{2E}[\sigma_1^2 + \sigma_2^2 + \sigma_3^2 - 2\mu(\sigma_1\sigma_2 + \sigma_2\sigma_3 + \sigma_3\sigma_1)]$	$W = \frac{1}{2E}[\sigma^2 + 2(1+\mu)\tau^2]$	$\sqrt{2(1+\mu)}$	$W = \frac{1}{2E}\left[\sigma^2 + \left(\frac{b}{t}\right)^2\tau^2\right]$
Magnitude of state-of-stress vector	$S = \sqrt{\sigma_1^2 + \sigma_2^2 + \sigma_3^2}$	$S = \sqrt{\sigma^2 + 2\tau^2}$	$a\sqrt{2}$	$S = \sqrt{\sigma^2 + \left(\frac{b}{t}\right)^2\tau^2}$
Complete Guest's law	$t = \frac{1}{2}\left[\sigma_1 - \sigma_3 + \left(\frac{2t}{b} - 1\right)(\sigma_1 + \sigma_3)\right]$	$t = \frac{1}{2}\left[\sqrt{\sigma^2 + 4\tau^2} + \left(\frac{2t}{b} - 1\right)\sigma\right]$	Any	No correction needed
Ellipse quadrant	-----	$1 = \left(\frac{\tau}{t}\right)^2 + \left(\frac{\sigma}{b}\right)^2$	Any	No correction needed
Ellipse arc	-----	$1 = \left(\frac{\tau}{t}\right)^2 + \left(\frac{b}{t} - 1\right)\left(\frac{\sigma}{b}\right)^2 + \left(2 - \frac{b}{t}\right)\frac{\sigma}{b}$	Any	No correction needed

<sup>a</sup>Required b/t less than actual value (1.55).





(a) Tests of tubes of SAE 1020 steel by Majors, Mills, and MacGregor (reference 22).

(b) Tests of various shapes of 14-percent-carbon steel by Sawert (reference 25).

(c) Tests of various shapes of chrome vanadium steel by Sawert (reference 25).

Figure 1.- Results of biaxial fatigue tests of steels. a, Principal-stress theory; b, b', principal-shearing-stress theory; c, principal-strain theory; d, total-strain-energy theory; e, distortion-energy theory;  $\sigma_1$ ,  $\sigma_2$ , principal stresses; and  $\sigma_x$ , uniaxial fatigue strength.

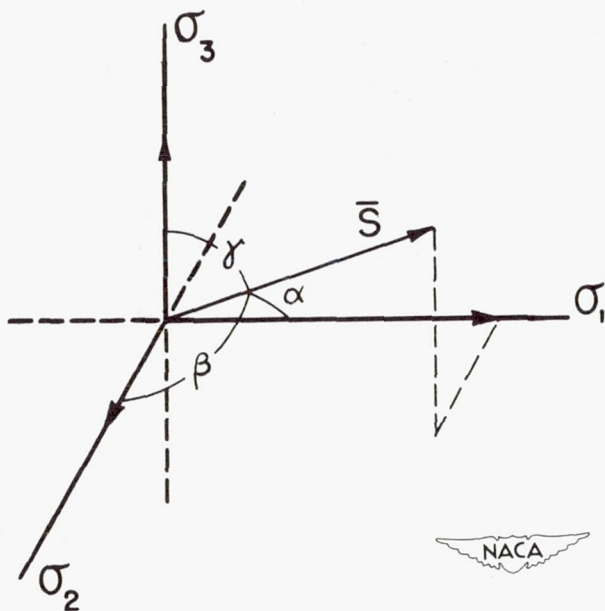


Figure 2.- State-of-stress vector for three principal stresses of unequal tension.

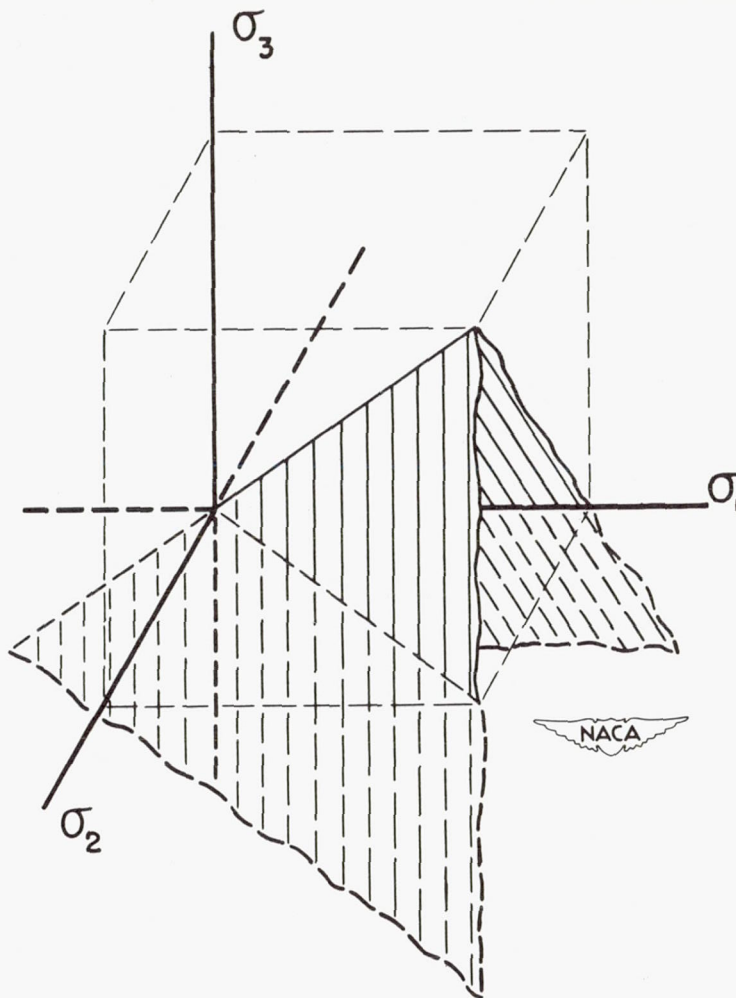
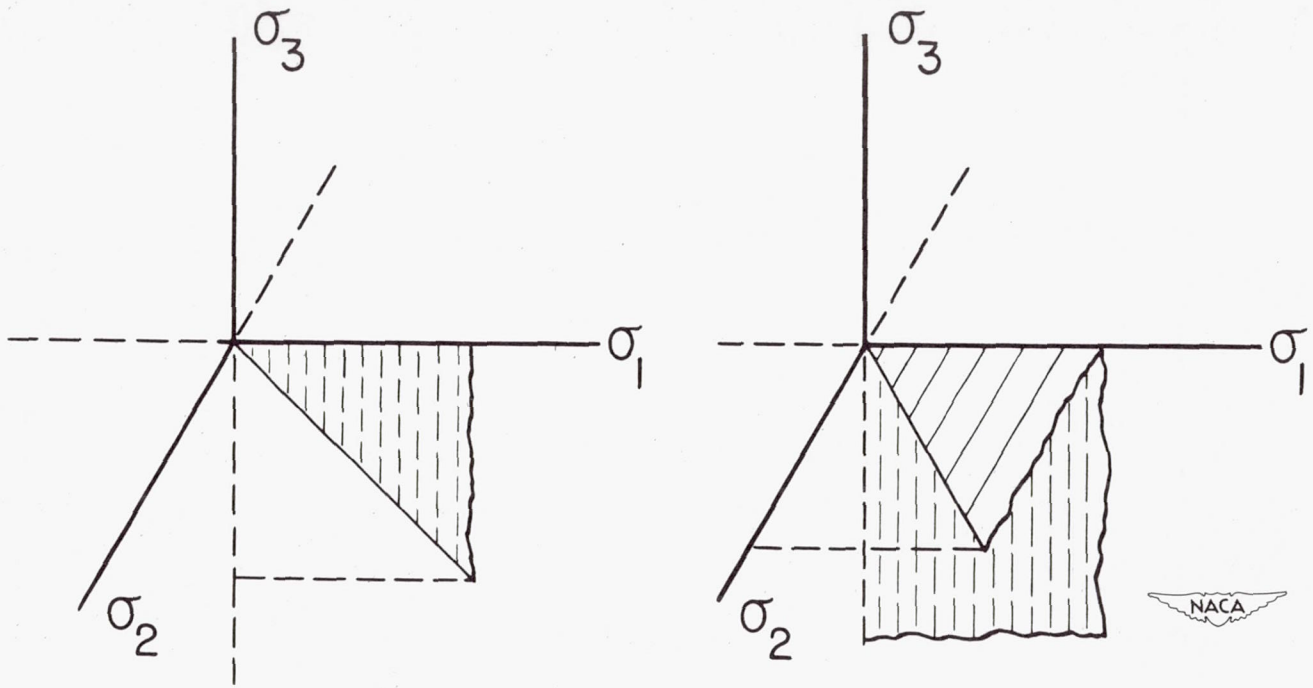


Figure 3.- Semi-infinite wedge of possible state-of-stress vectors.



(a) Combined bending and torsion.

(b) Combined axial load and internal pressure in thin tubes.

Figure 4.- State-of-stress vectors which can be produced by combined bending and torsion and combined axial load and internal pressure in thin tubes.

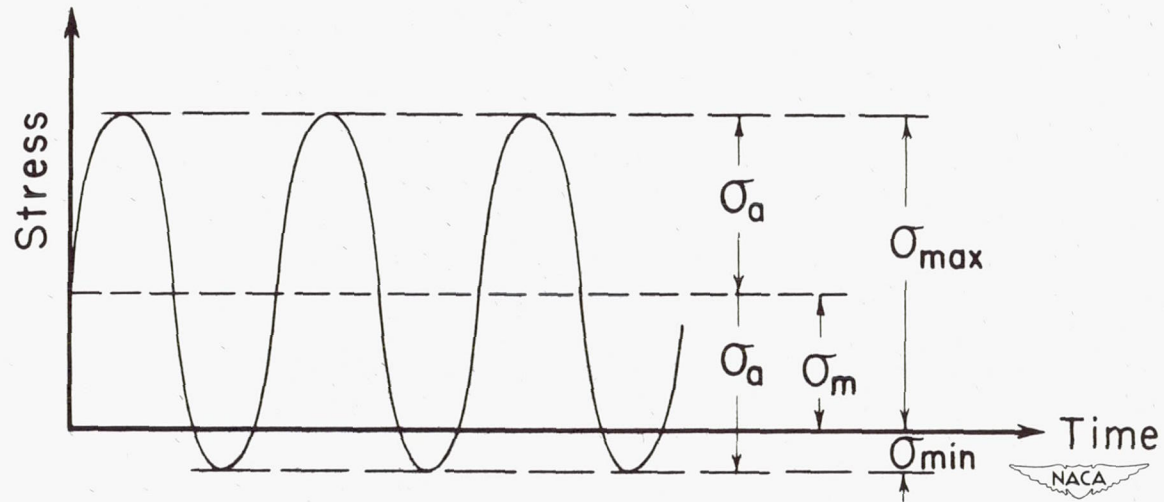
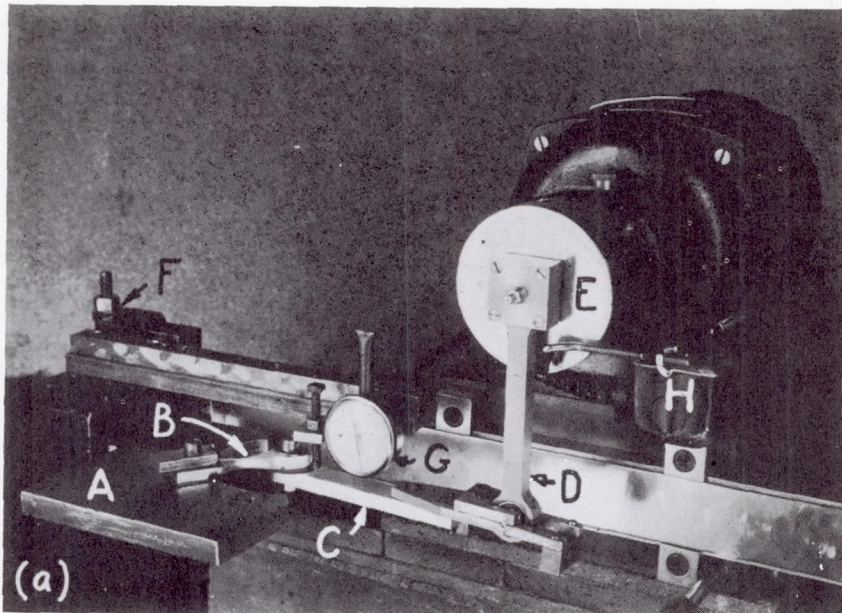
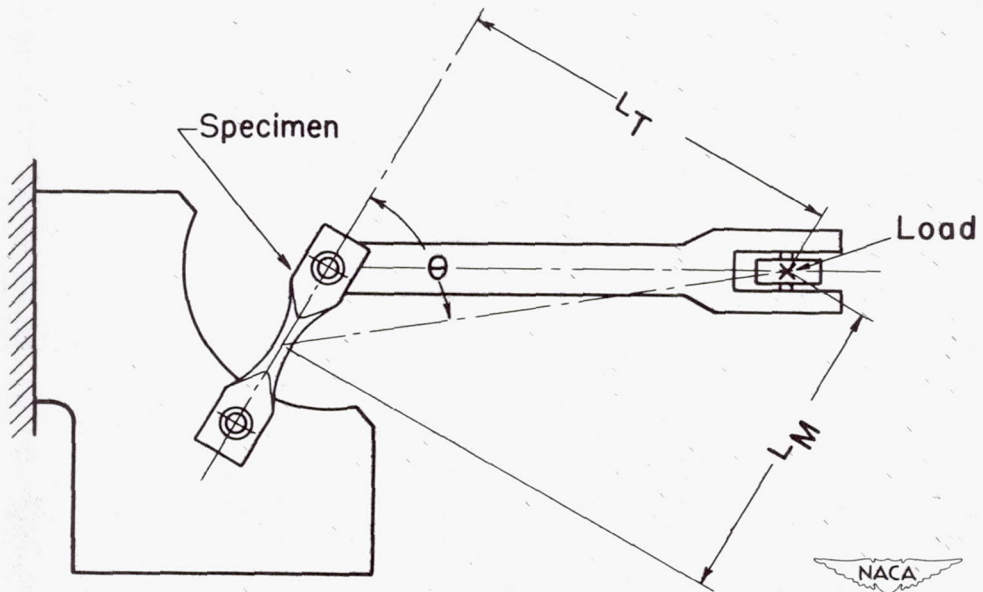


Figure 5.- Terminology of stress cycle:  $\sigma_a$ , alternating stress amplitude;  $\sigma_m$ , mean stress;  $\sigma_{max}$ , maximum stress; and  $\sigma_{min}$ , minimum stress.

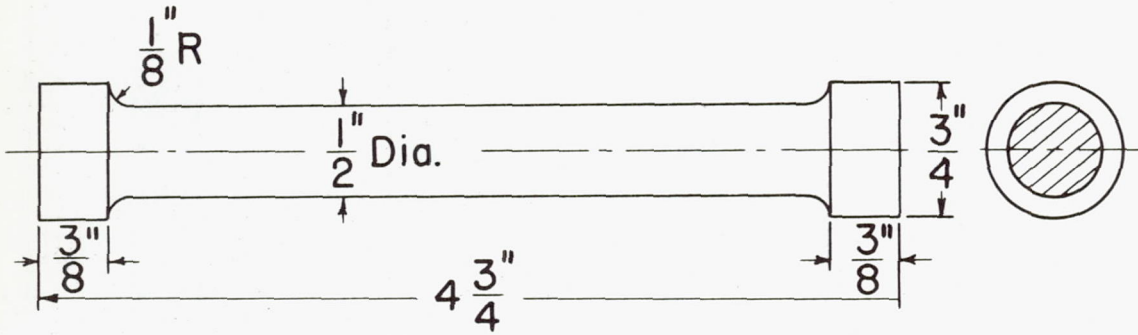


(a) Fatigue machine used in investigation. A, plate fastened in grip of testing machine; B, specimen; C, lever; D, connecting rod; E, adjustable crank; F, slide; G, dial; and H, switch.

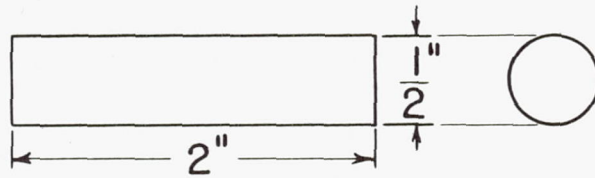


(b) Sketch of arrangement for loading specimen.  $L_M$ , bending-moment arm;  $L_T$ , twisting-moment arm.

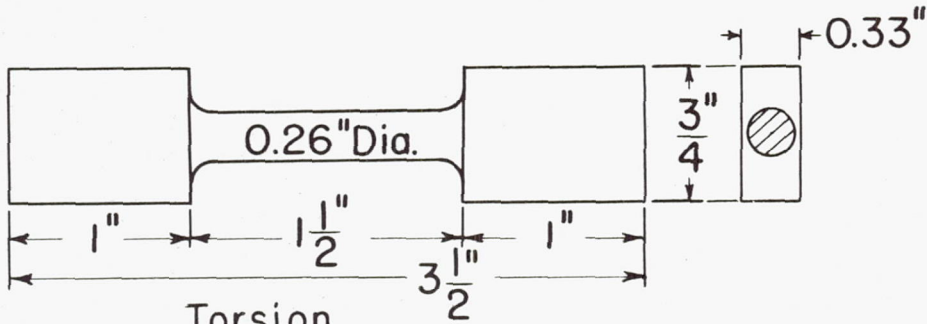
Figure 6.- Fatigue machine and arrangement for loading specimen for combined-bending-and-torsion tests.



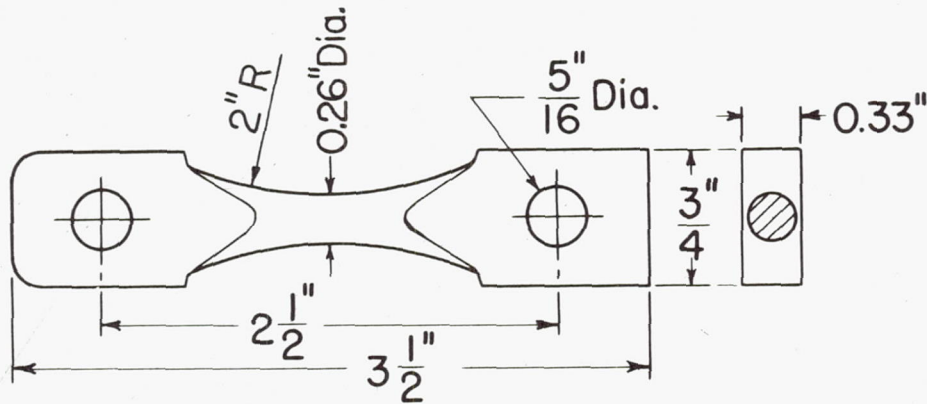
Tension



Compression



Torsion



Fatigue



Figure 7.- Test specimens.

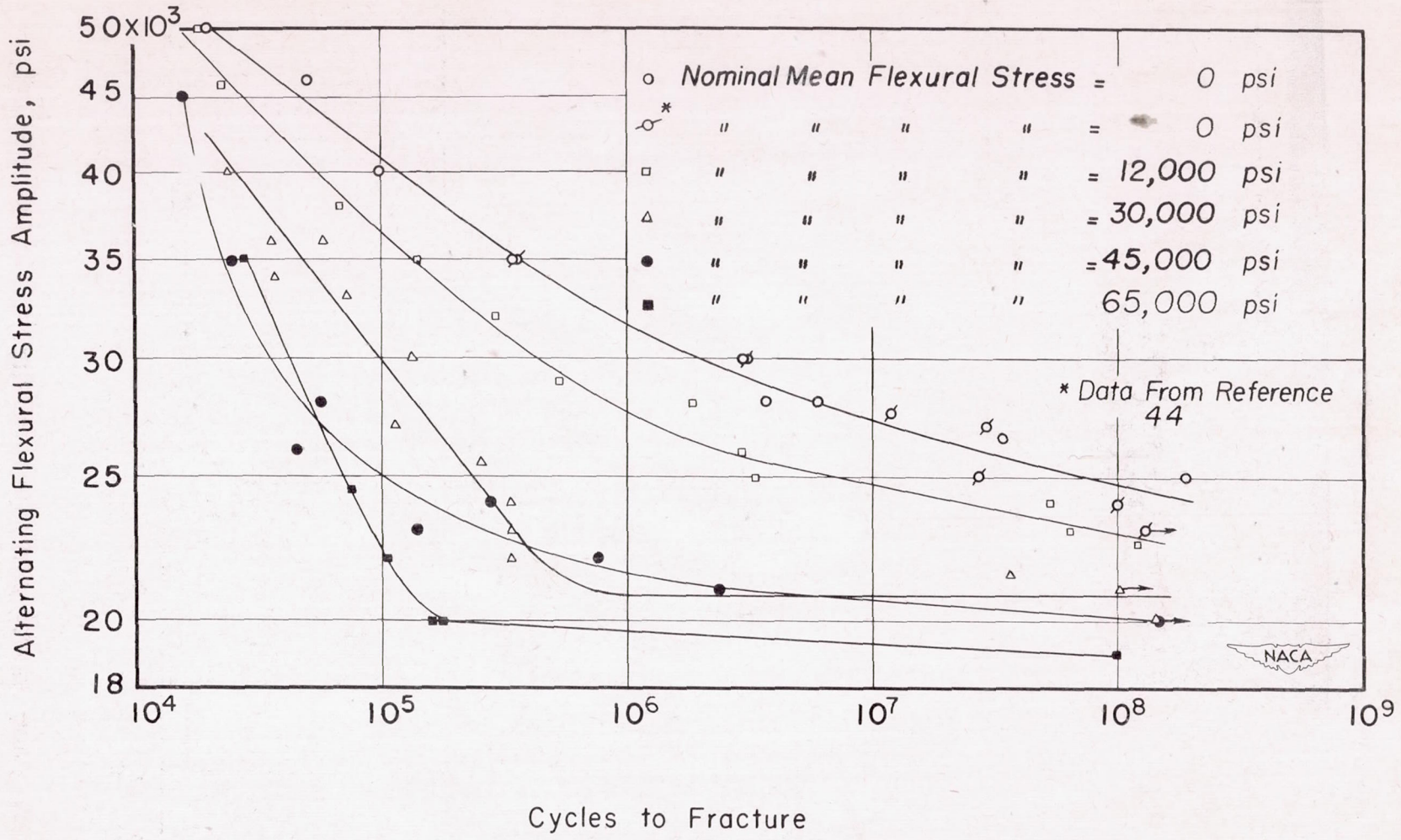


Figure 8.- S-N diagrams for bending fatigue.

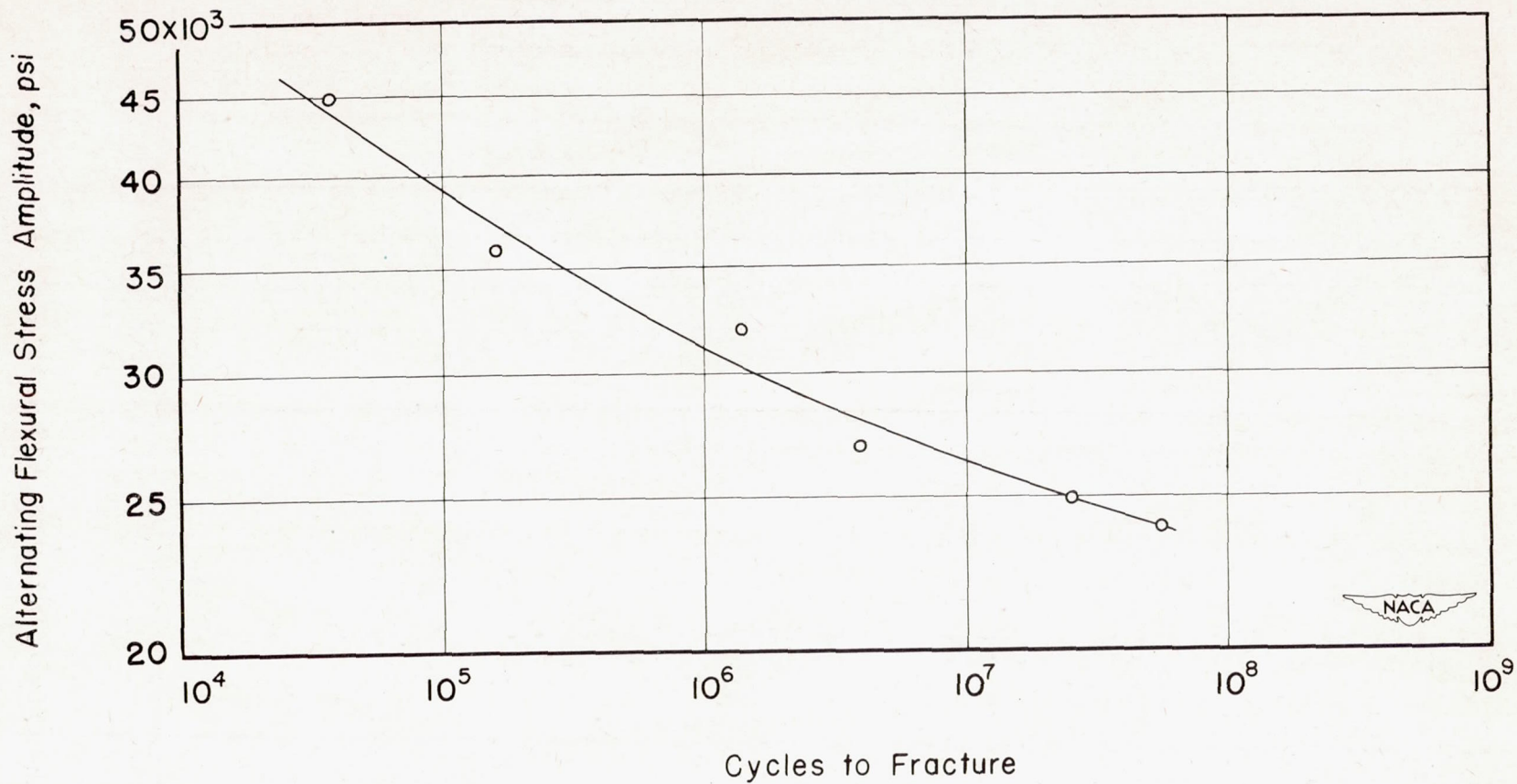


Figure 9.- S-N diagram for combined bending and torsion fatigue; mean stress zero. Alternating torsional stress amplitudes and mean torsional stresses are equal to 0.207 times corresponding flexural stresses.

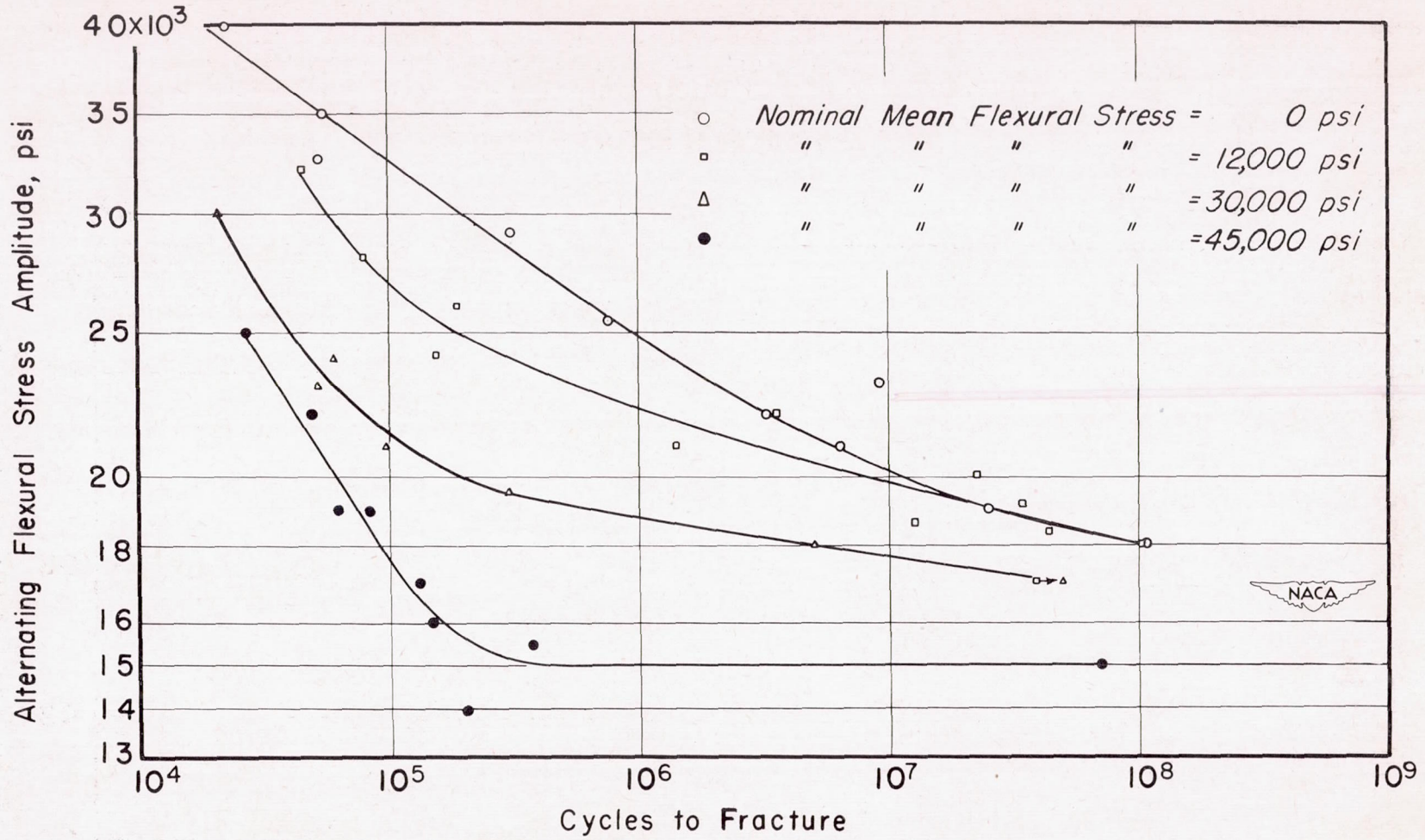


Figure 10.- S-N diagrams for combined bending and torsion fatigue.  
Alternating stress amplitudes and mean torsional stresses are equal to 0.500 times corresponding flexural stresses.

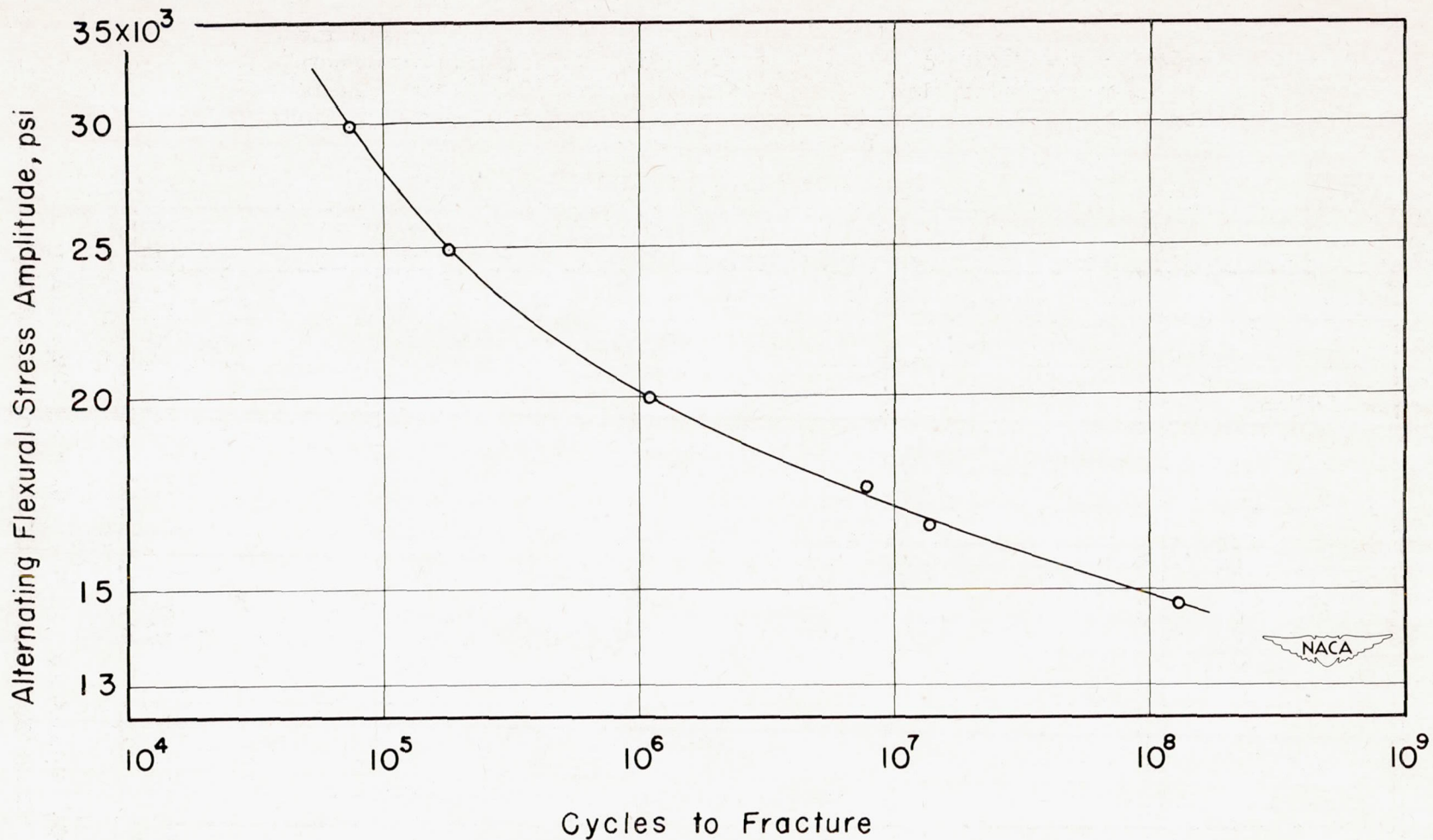


Figure 11.- S-N diagram for combined bending and torsion fatigue; mean stress zero. Alternating torsional stress amplitudes and mean torsional stresses are equal to 0.732 times corresponding flexural stresses.

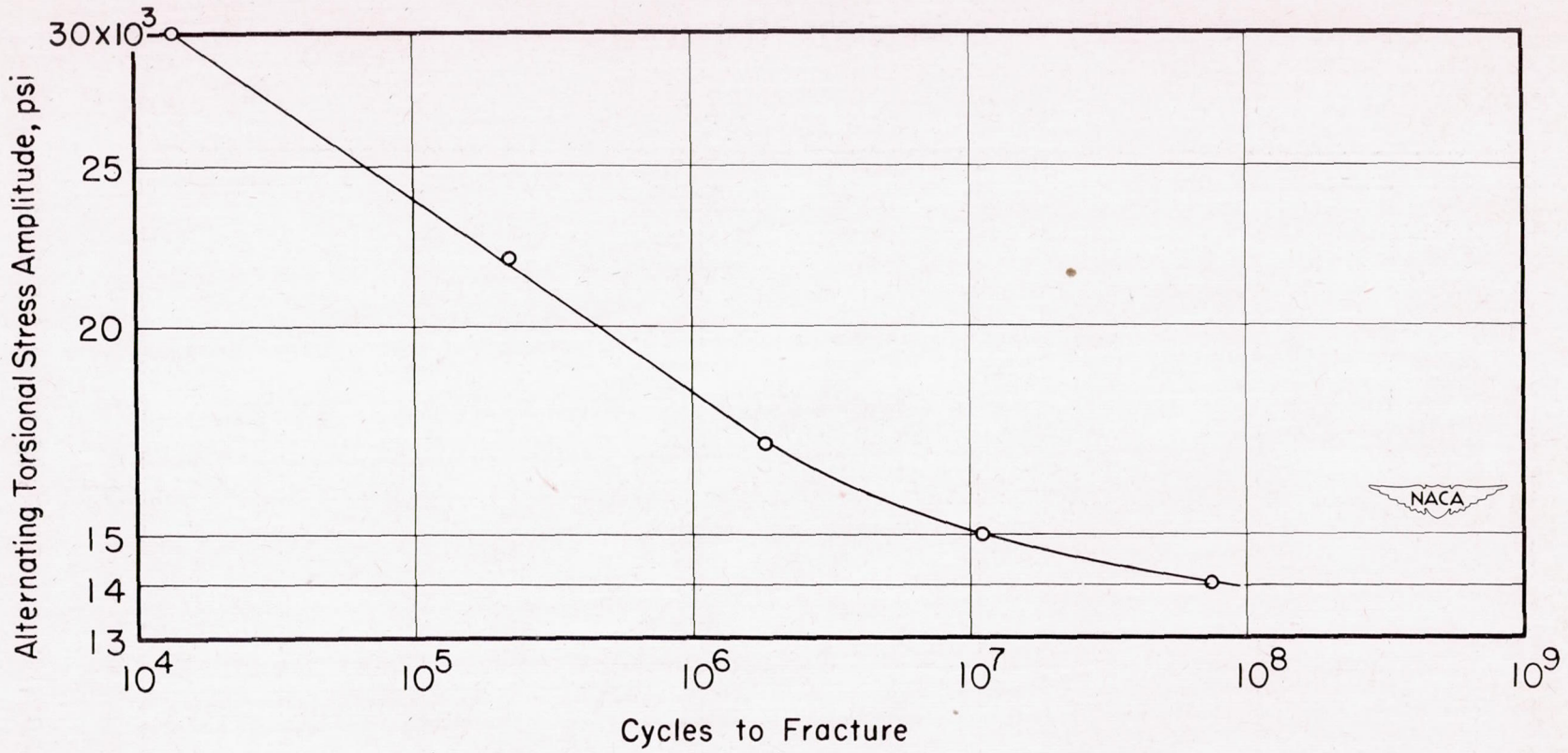


Figure 12.- S-N diagram for combined bending and torsion fatigue; mean stress zero. Alternating torsional stress amplitudes and mean torsional stresses are equal to 1.207 times corresponding flexural stresses.

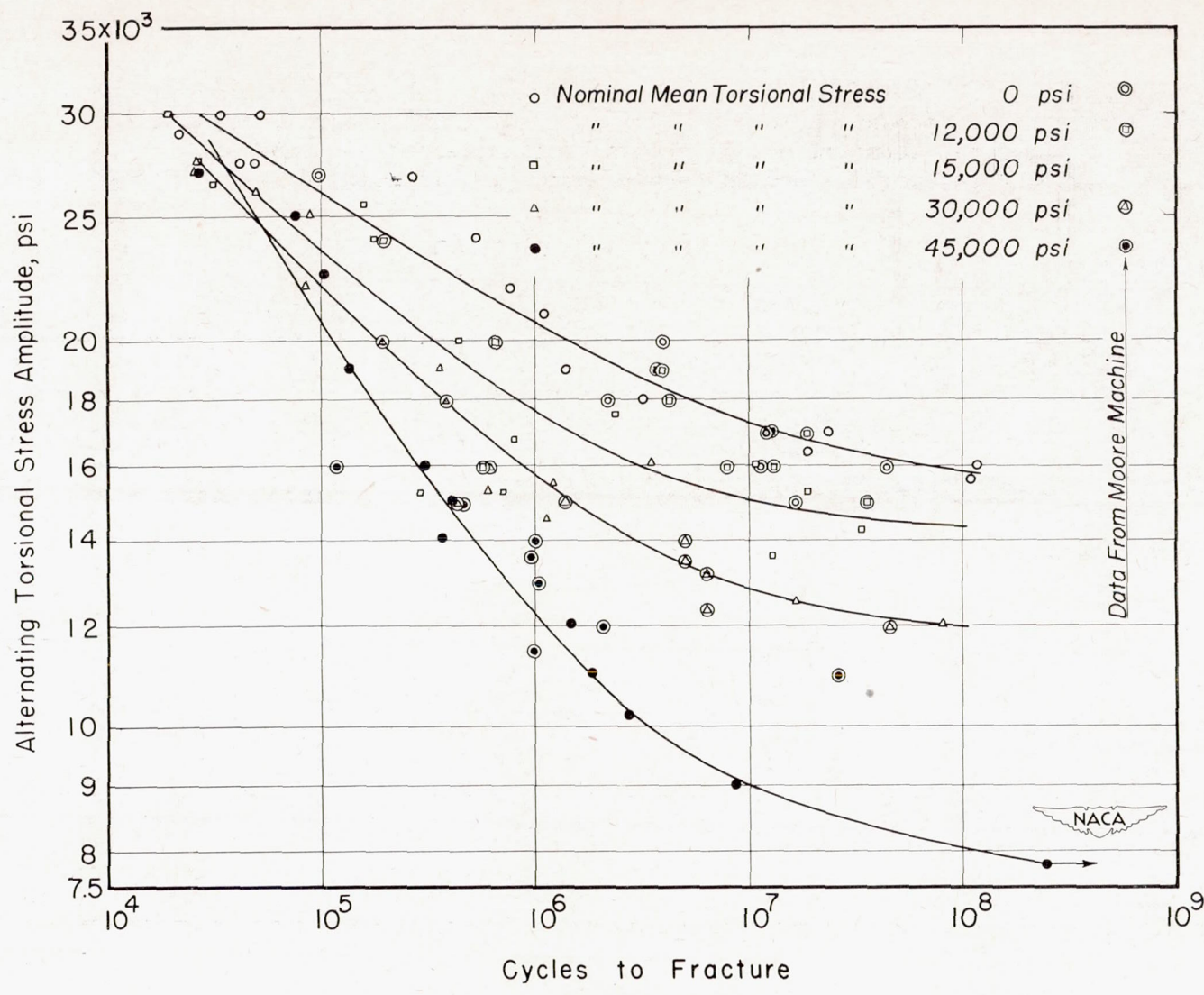
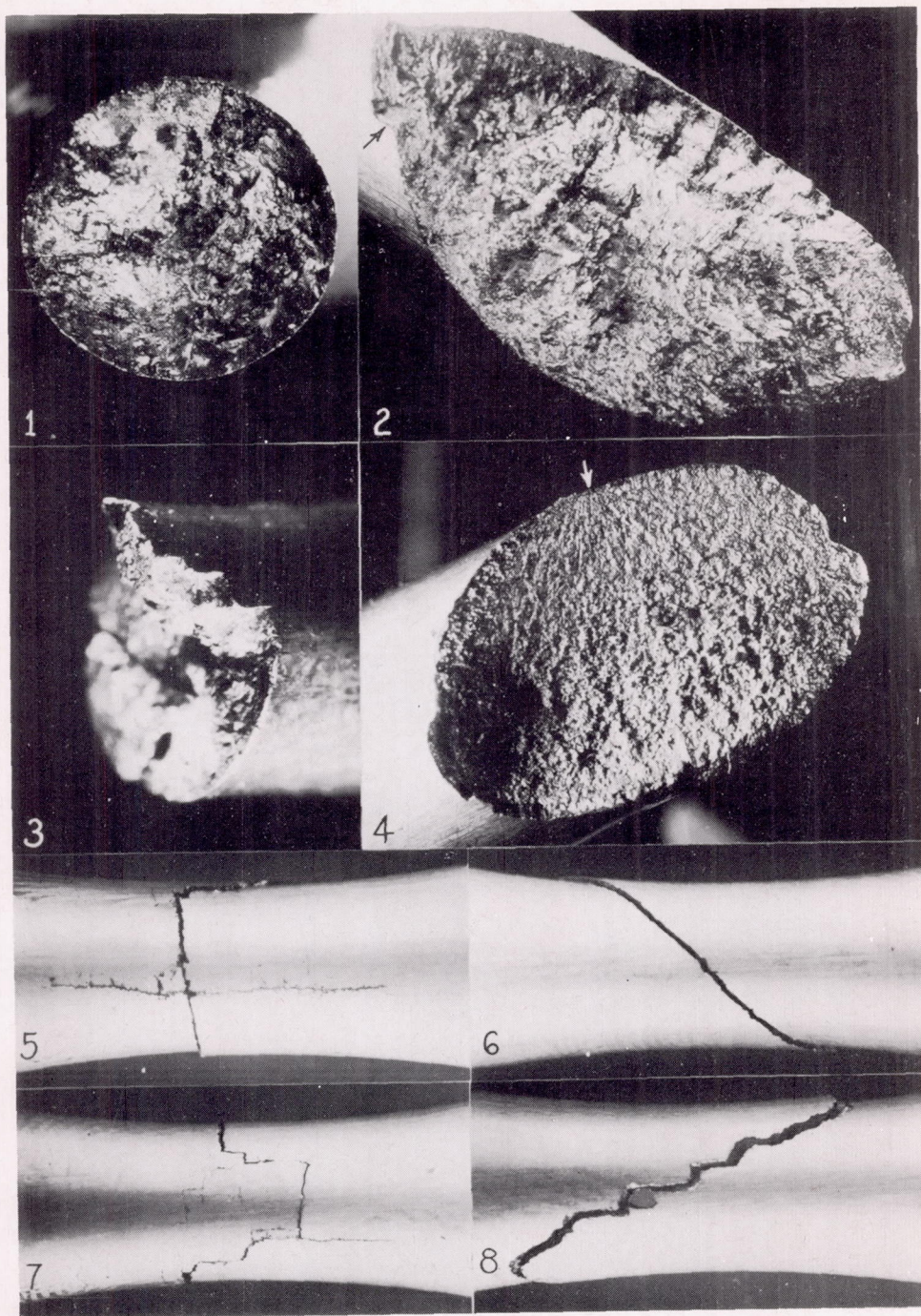


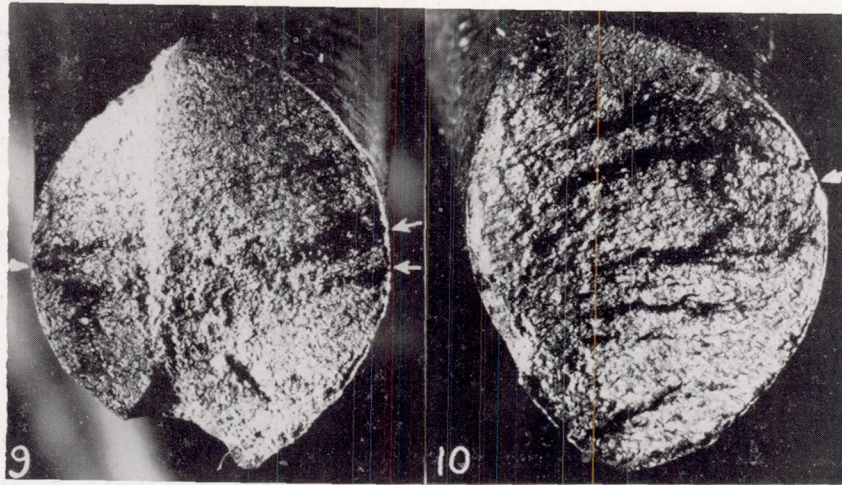
Figure 13.- S-N diagrams for torsion fatigue.



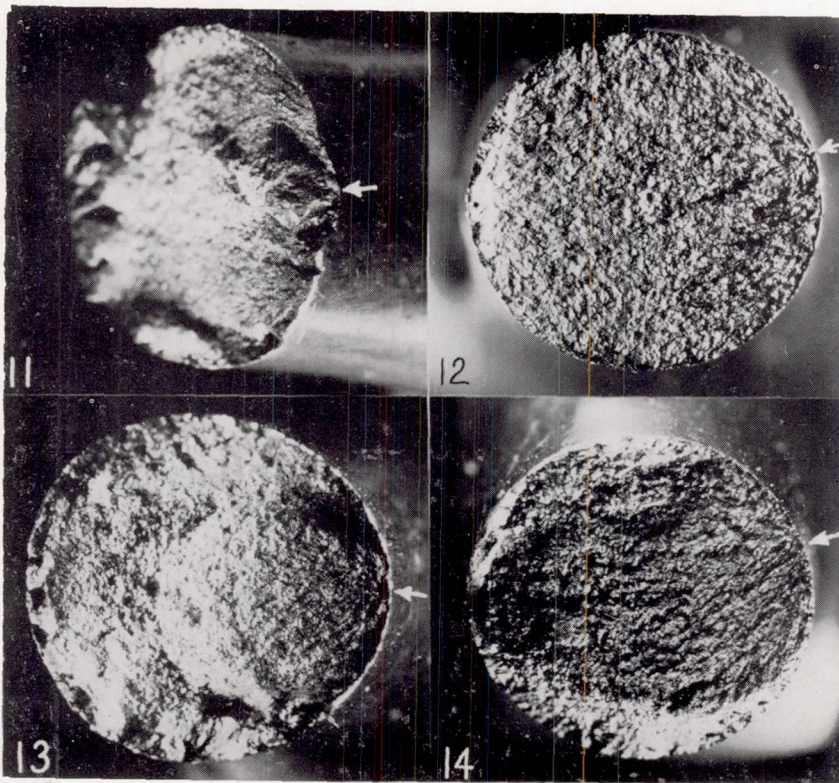
(a) Fractures from torsion fatigue. High alternating stresses are on the left and low, on the right. Zero mean stress: 1, 2, 6, and 8. High mean stress: 3, 4, 5, and 7. Two views of the same specimen: 5 and 7, and 6 and 8.



Figure 14.- Fractures of fatigue specimens representing various loading conditions. Arrows show origin of fractures.



(b) Fractures from combined-bending-and-torsion fatigue at zero mean stress. High alternating stress, 9; low alternating stress, 10.



(c) Fractures from bending fatigue. High alternating stresses are on the left and low, on the right. Zero mean stress: 11 and 12. High mean stress: 13 and 14.



Figure 14.- Concluded.

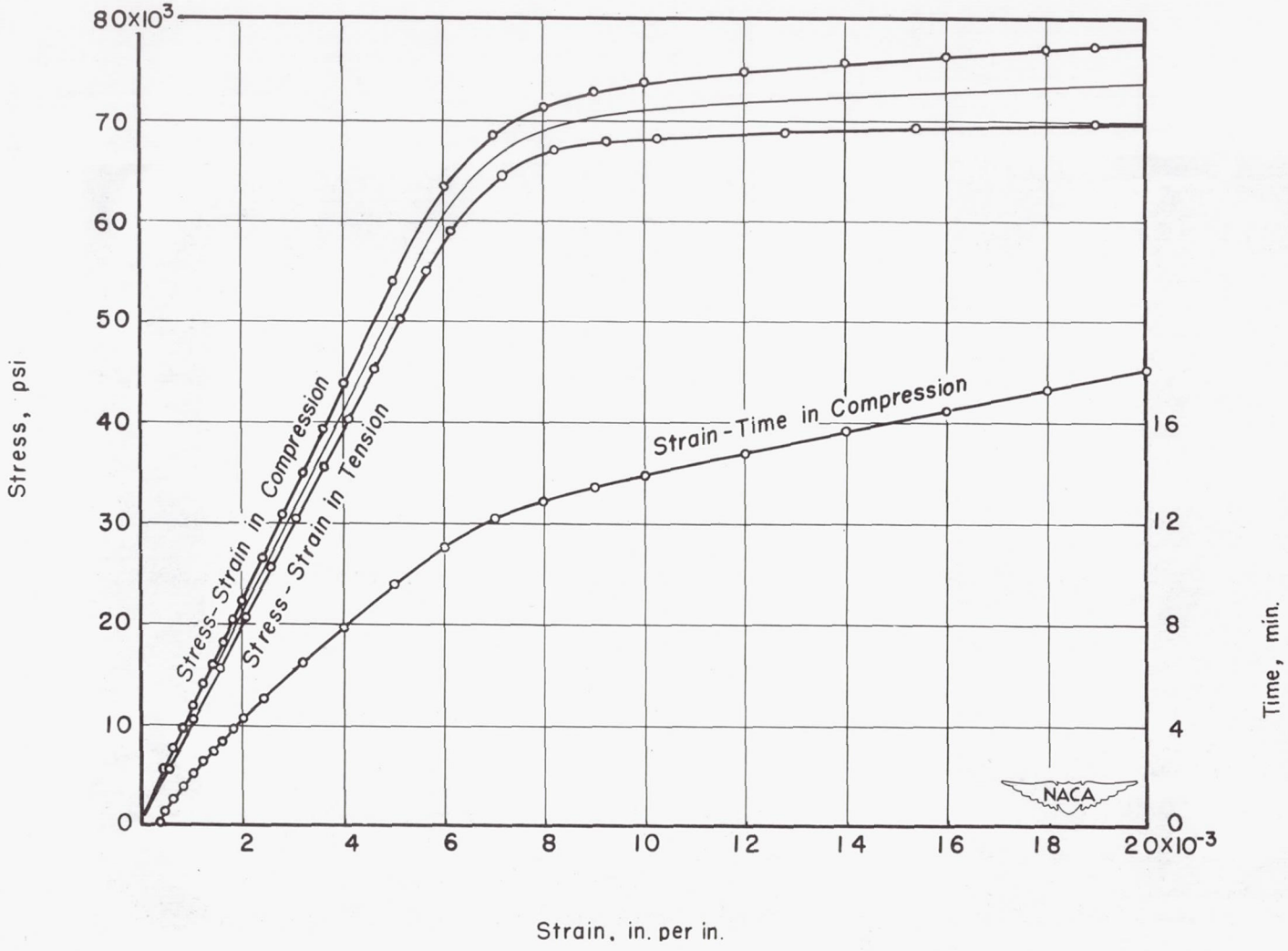


Figure 15.- Stress-strain curves for tension and compression. Curves for tension tests are taken from reference 44.

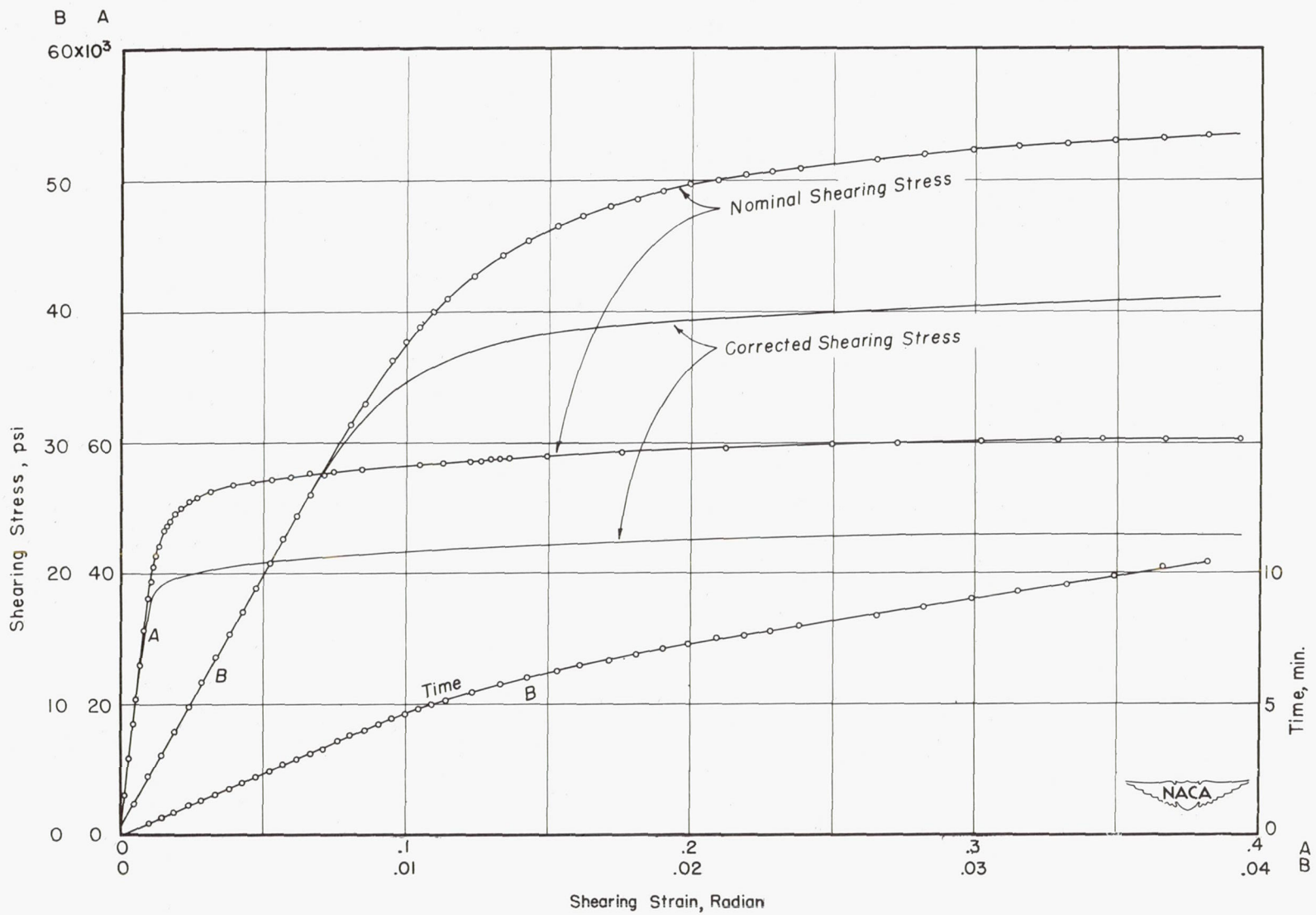


Figure 16.- Static torsion test (diam. of specimen, 0.261 in.).

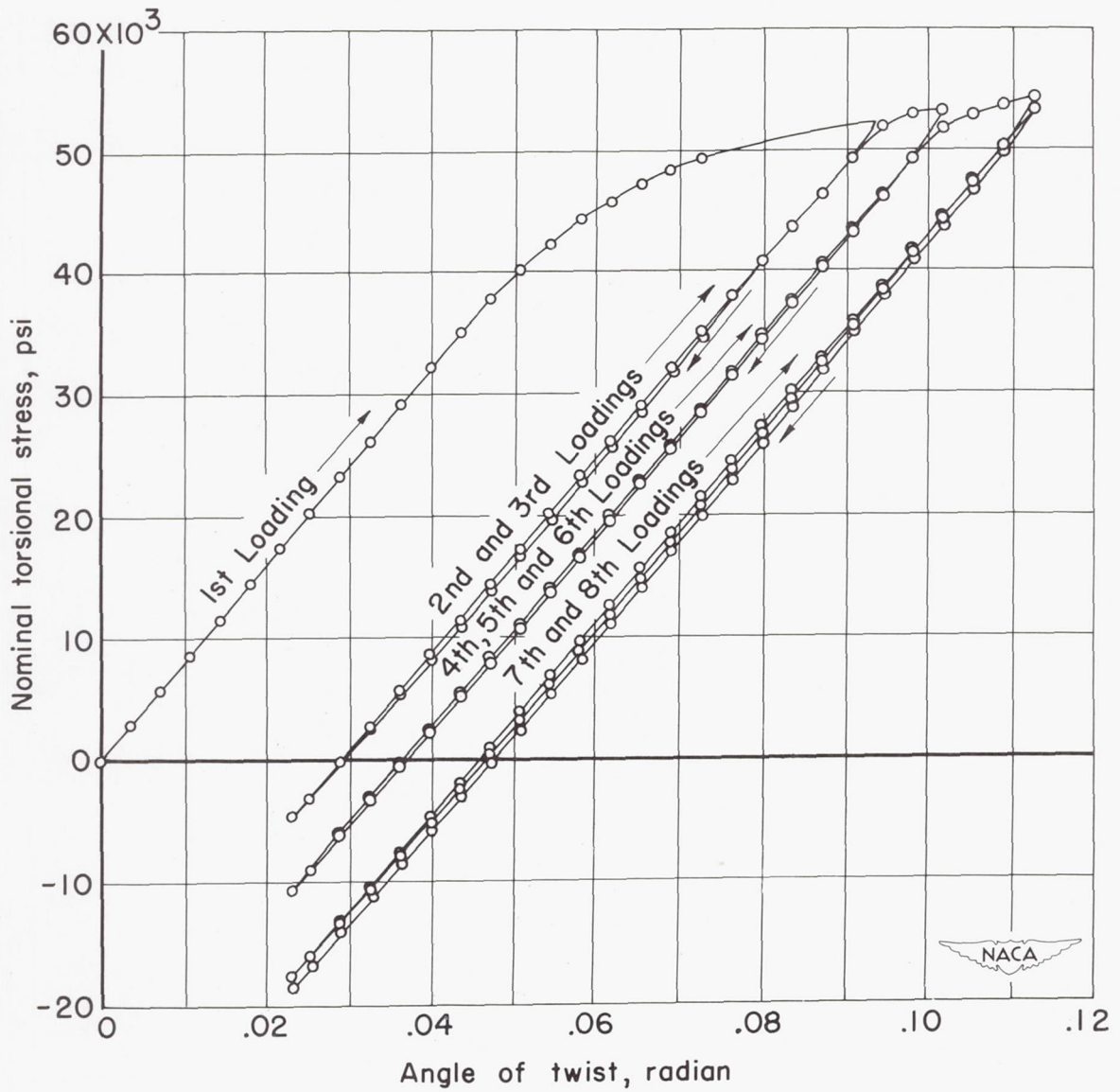


Figure 17.- Load-deflection test of fatigue specimen in torsion.

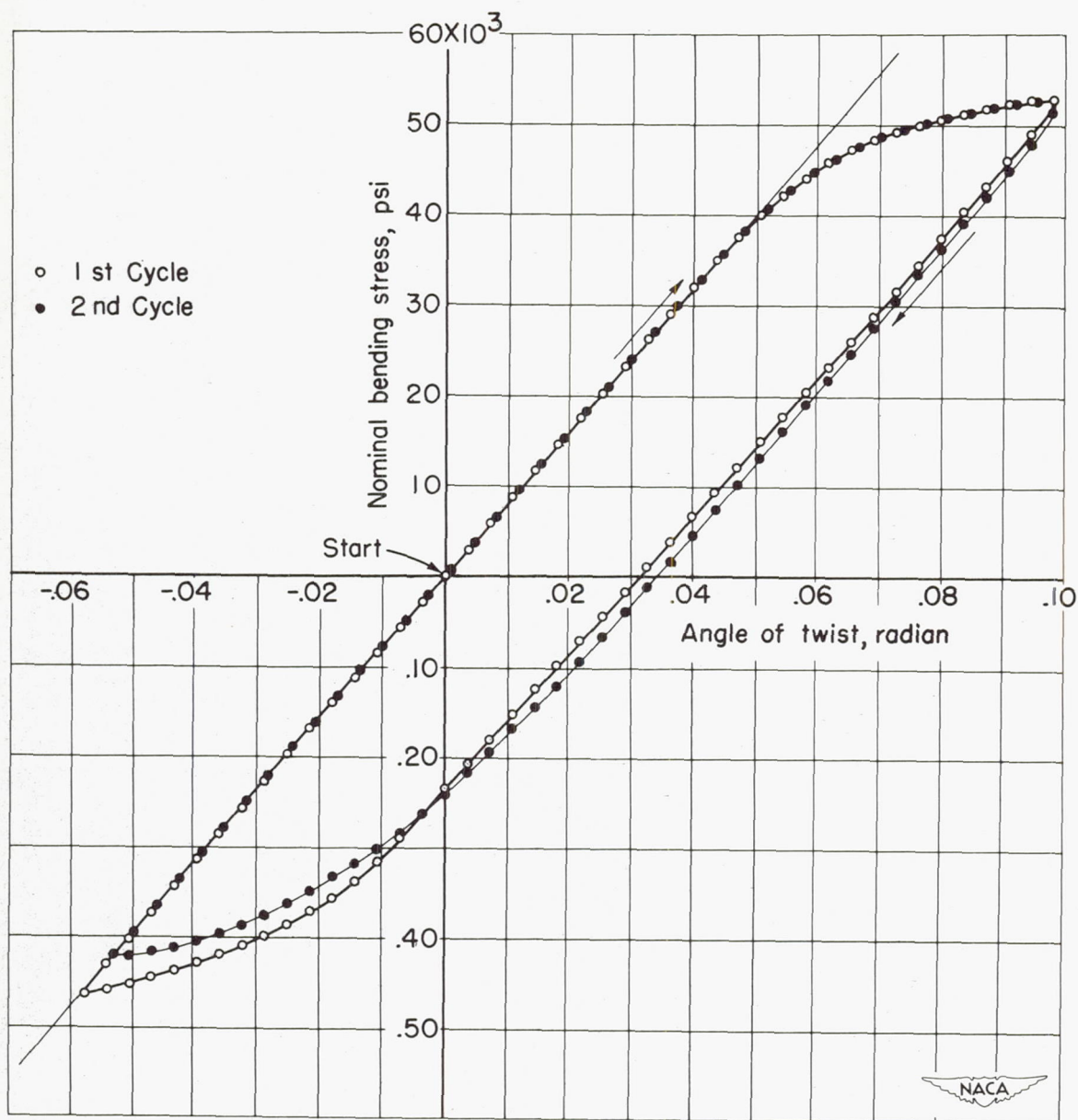


Figure 18.- Load-deflection test of fatigue specimen in torsion.

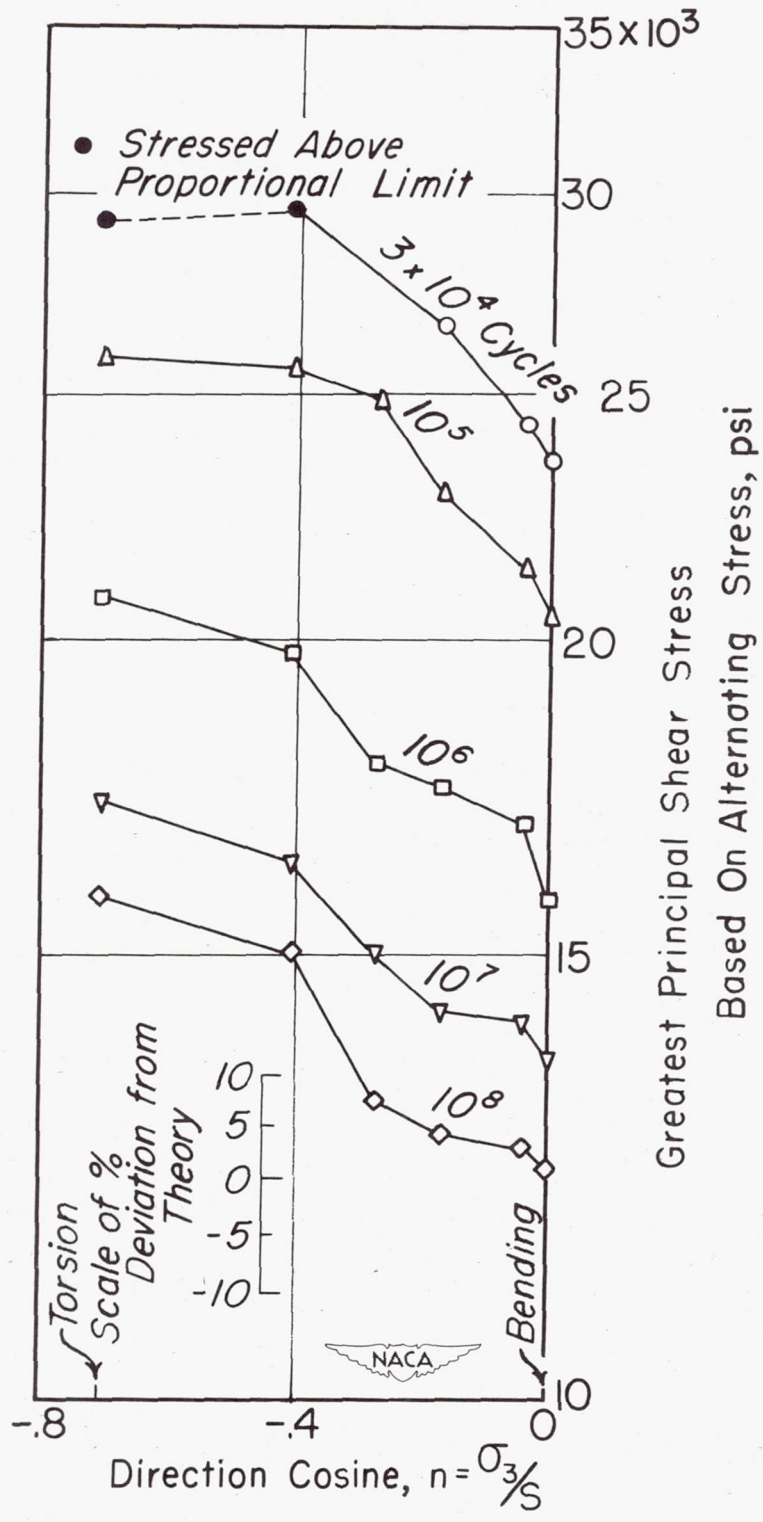


Figure 19.- Principal shear stress against state of stress; mean stress zero. See figure 5 for sketch of mean and alternating stresses.

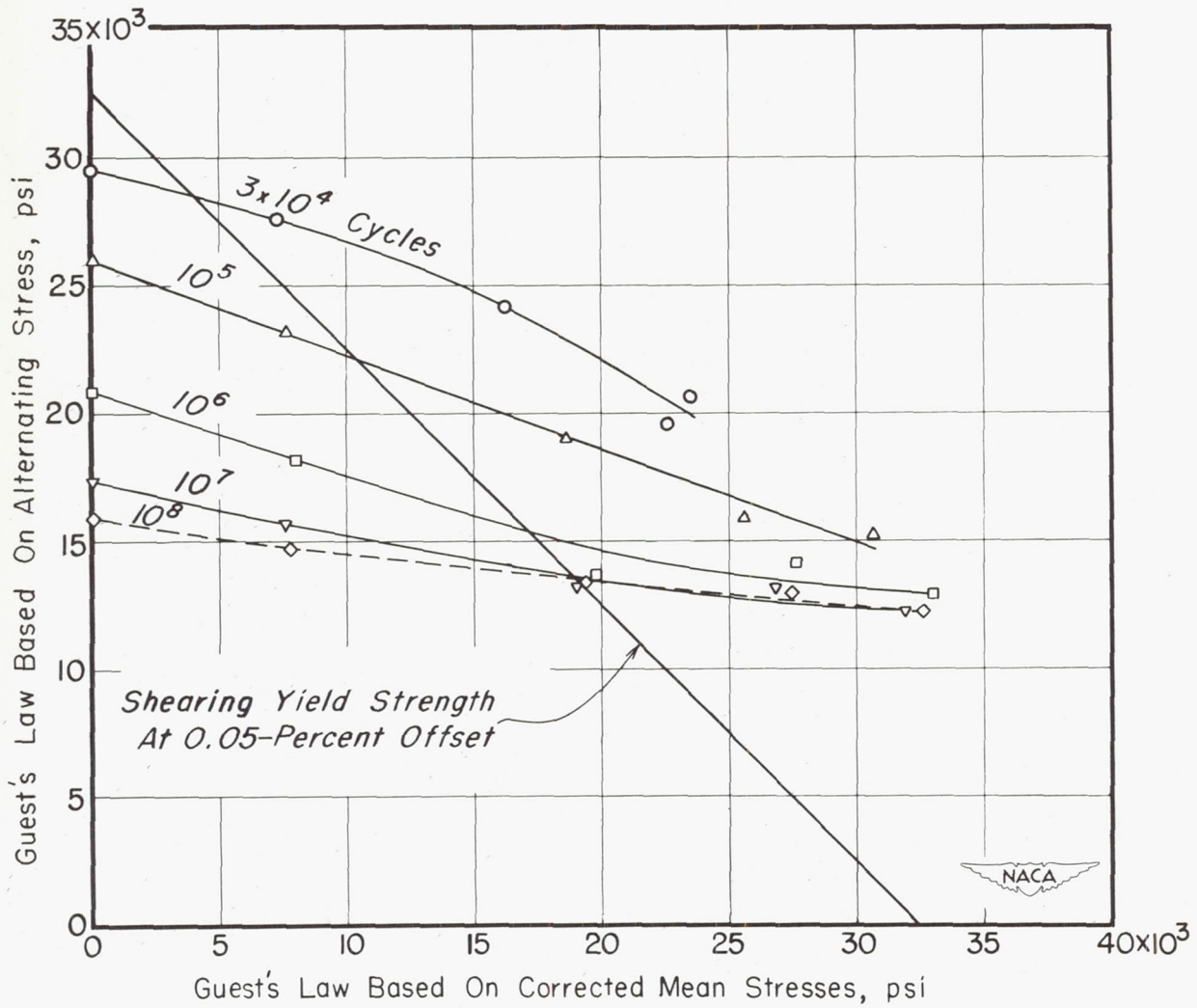


Figure 20.- Alternating against mean stress computed from Guest's law for tests in bending fatigue.

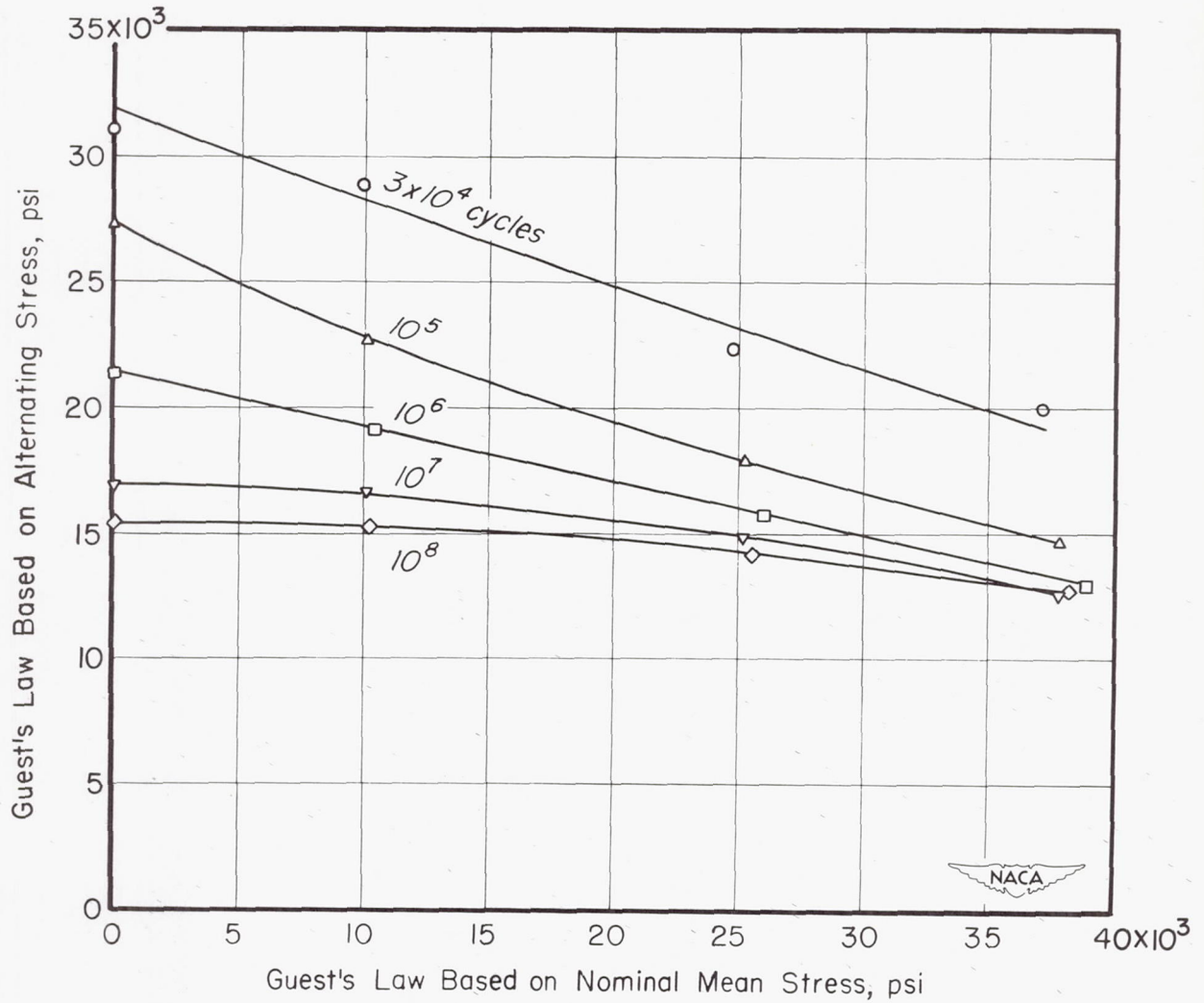


Figure 21.- Alternating against mean stress computed from Guest's law for tests in combined-bending-and-torsion fatigue.  $\tau = 0.5\sigma$ .

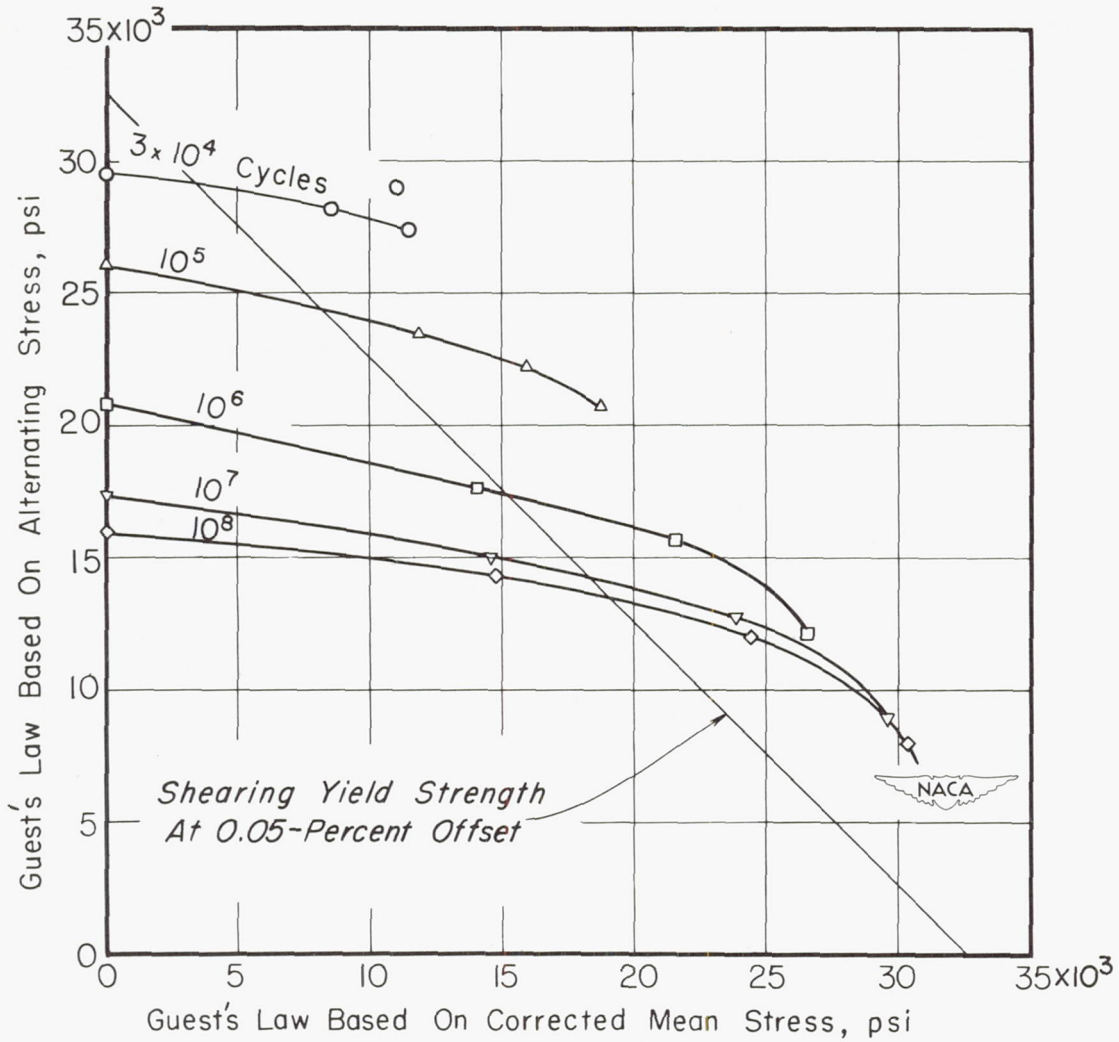


Figure 22.- Alternating against mean stress computed from Guest's law for tests in torsion fatigue.

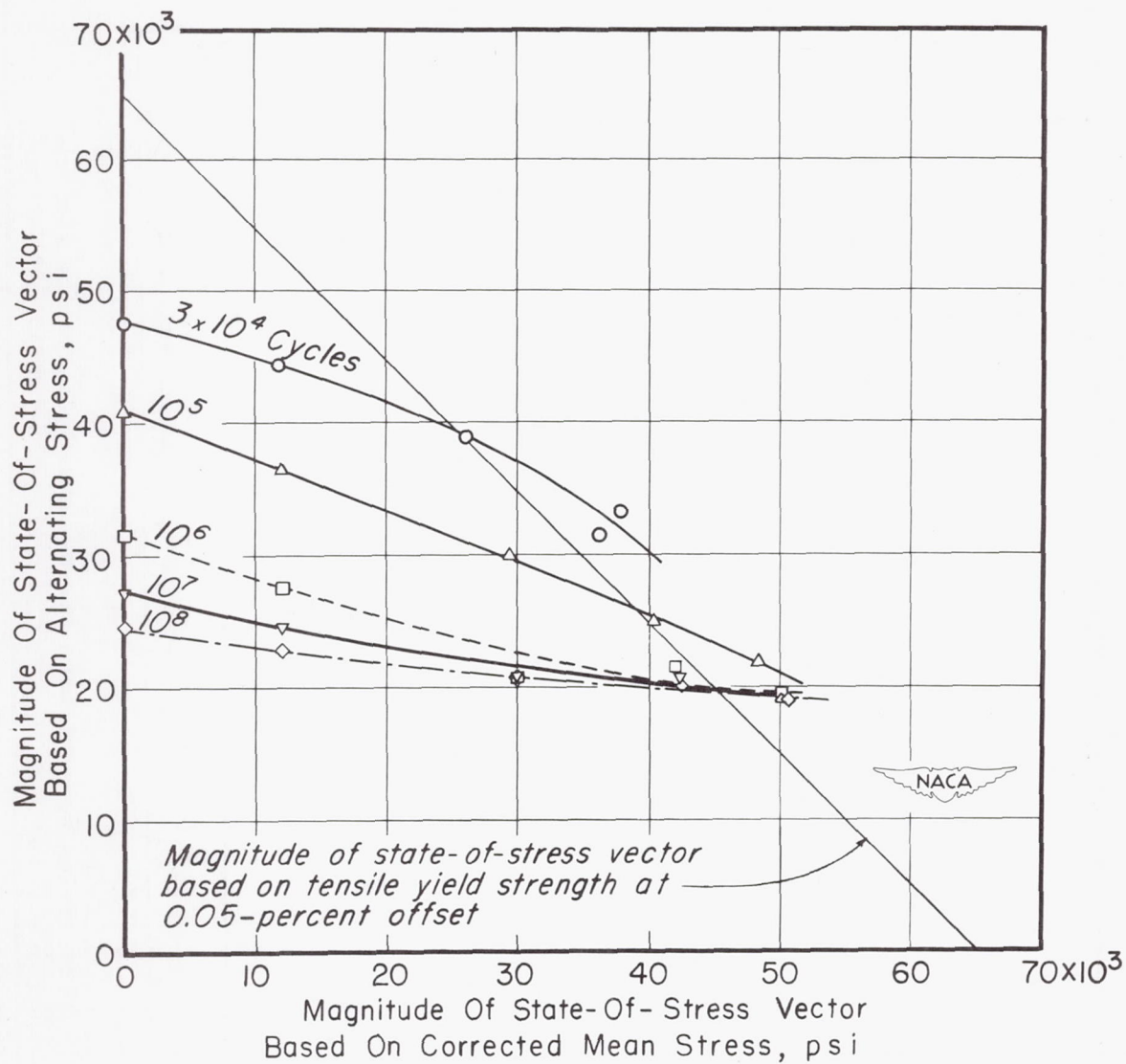


Figure 23.- Alternating against mean stress computed from the state-of-stress vector for tests in bending fatigue.

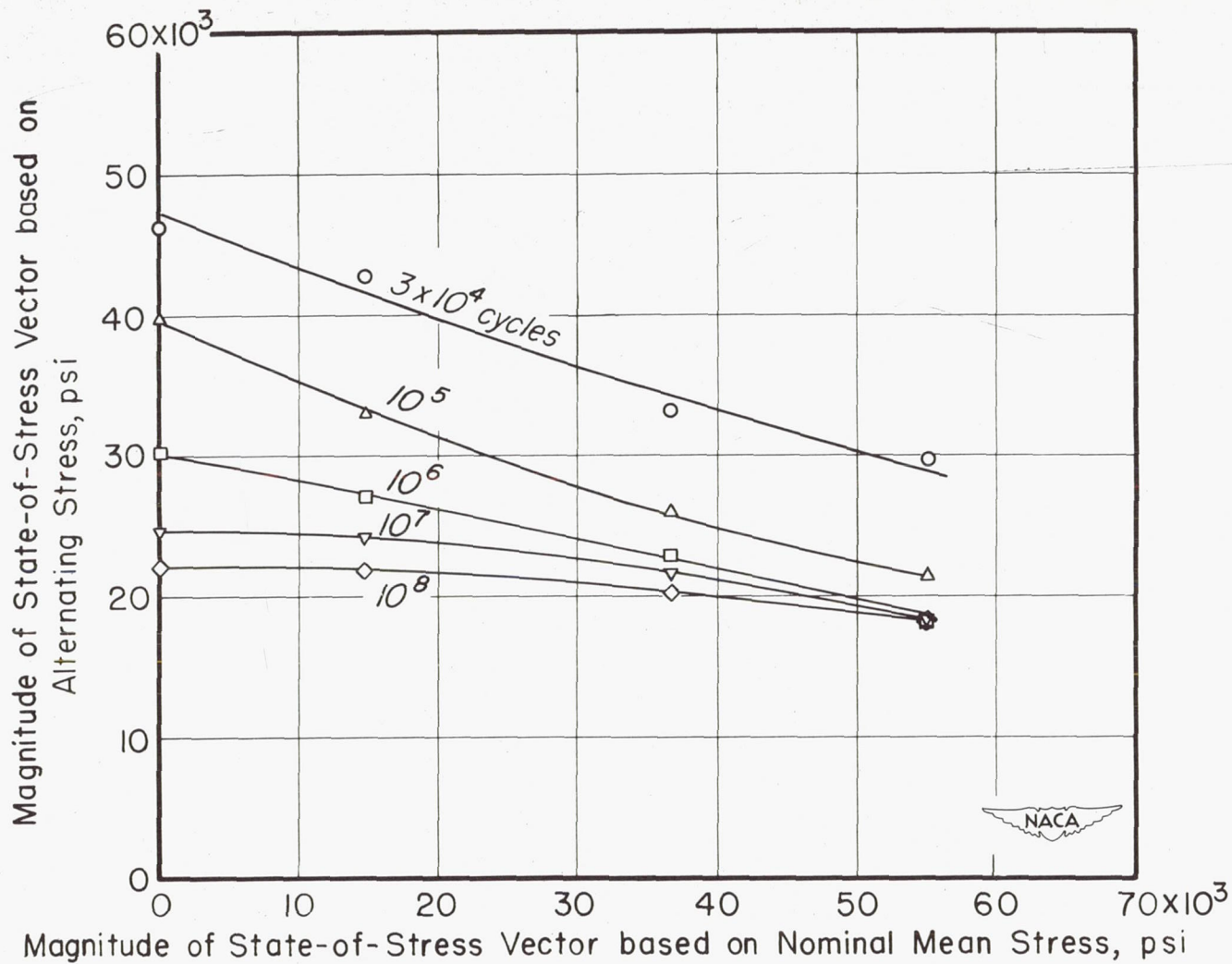


Figure 24.- Alternating against mean stress computed from the state-of-stress vector for tests in combined-bending-and-torsion fatigue.  
 $\tau = 0.5\sigma$ .

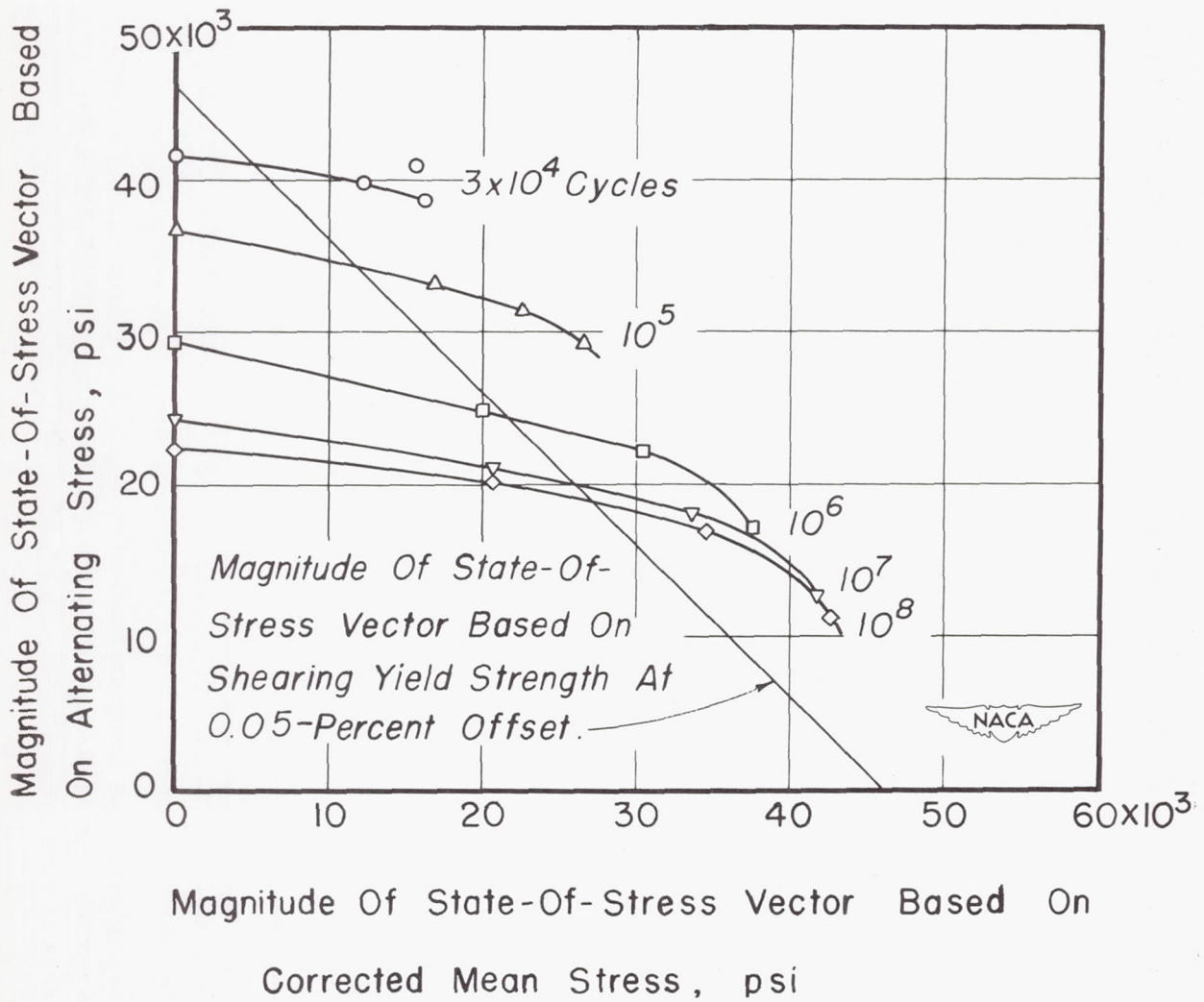


Figure 25.- Alternating against mean stress computed from the state-of-stress vector for tests in torsion fatigue.

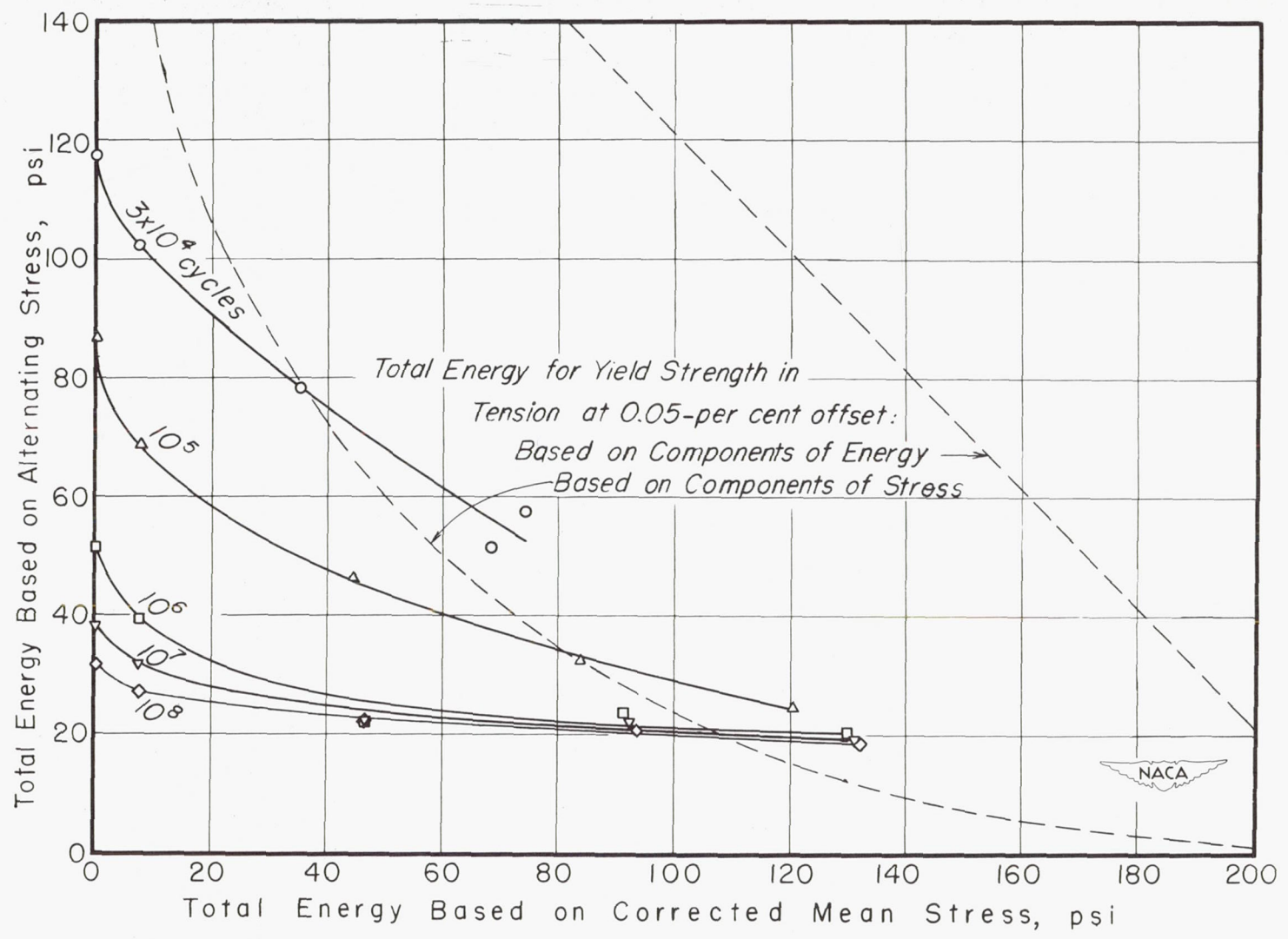


Figure 26.- Total energy based on alternating stress against total energy based on mean stress in bending fatigue.

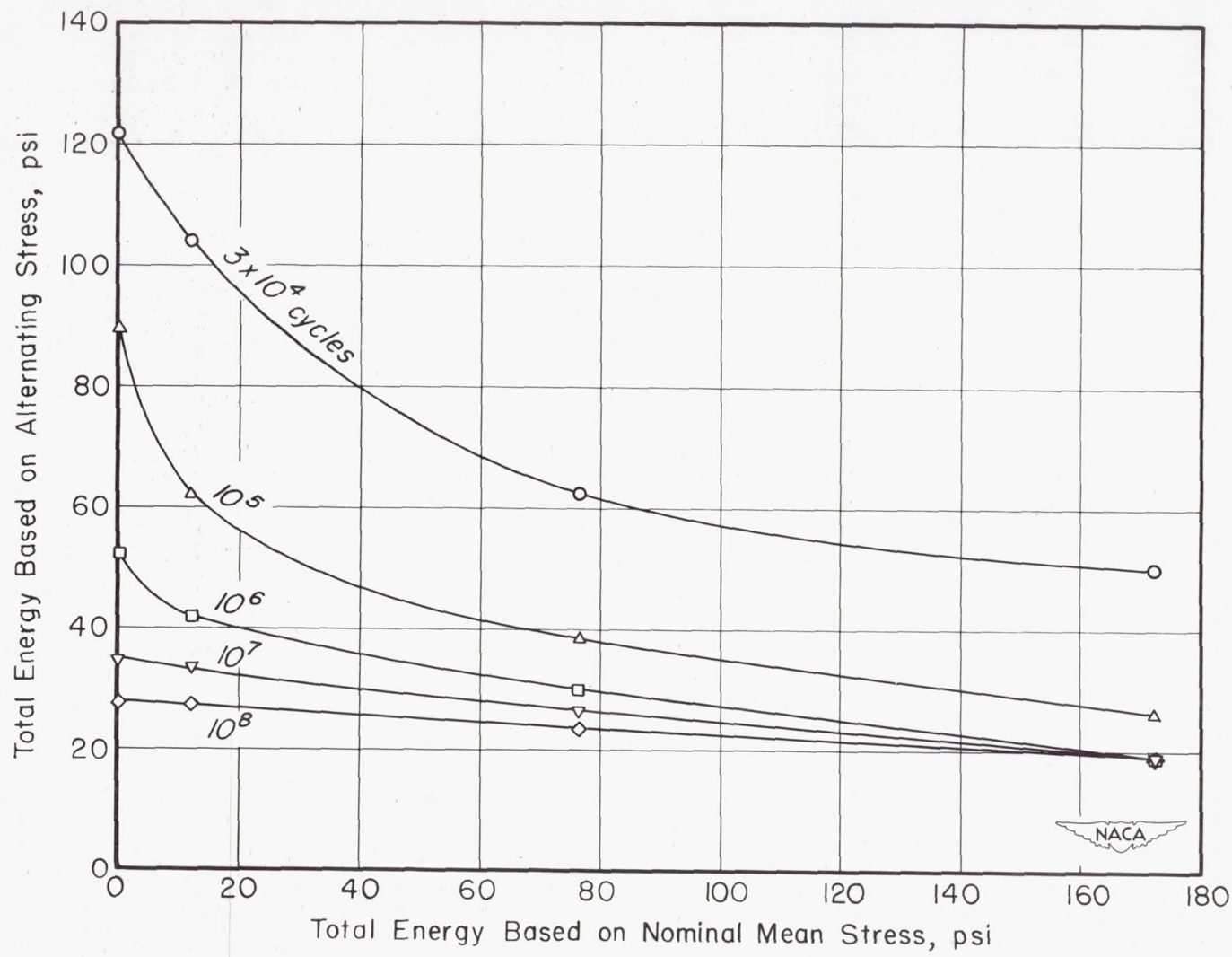


Figure 27.- Total energy based on alternating stress against total energy based on mean stress in combined-bending-and-torsion fatigue.  $\tau = 0.5\sigma$ .

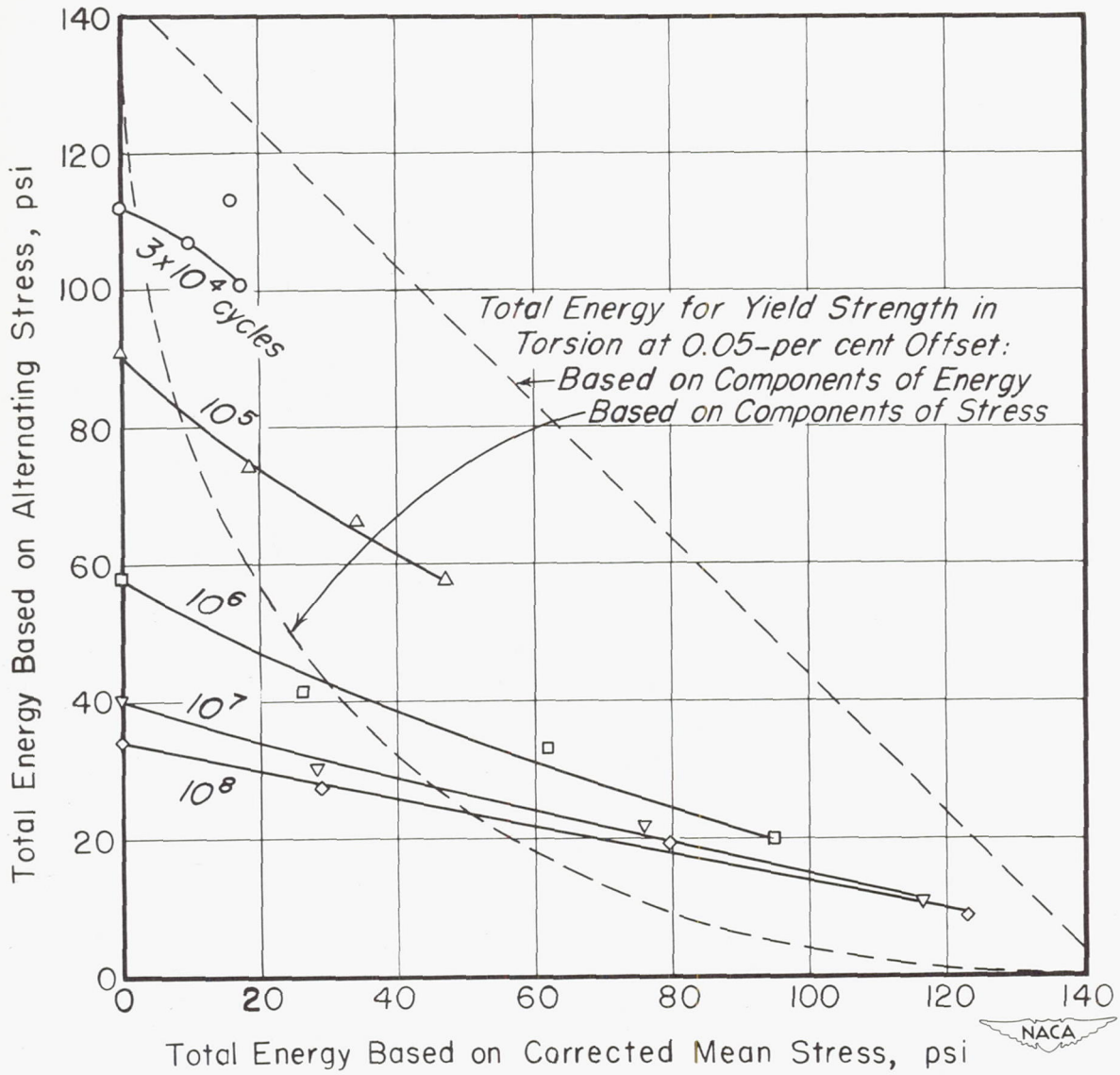


Figure 28.- Total energy based on alternating stress against total energy based on mean stress in torsion fatigue.

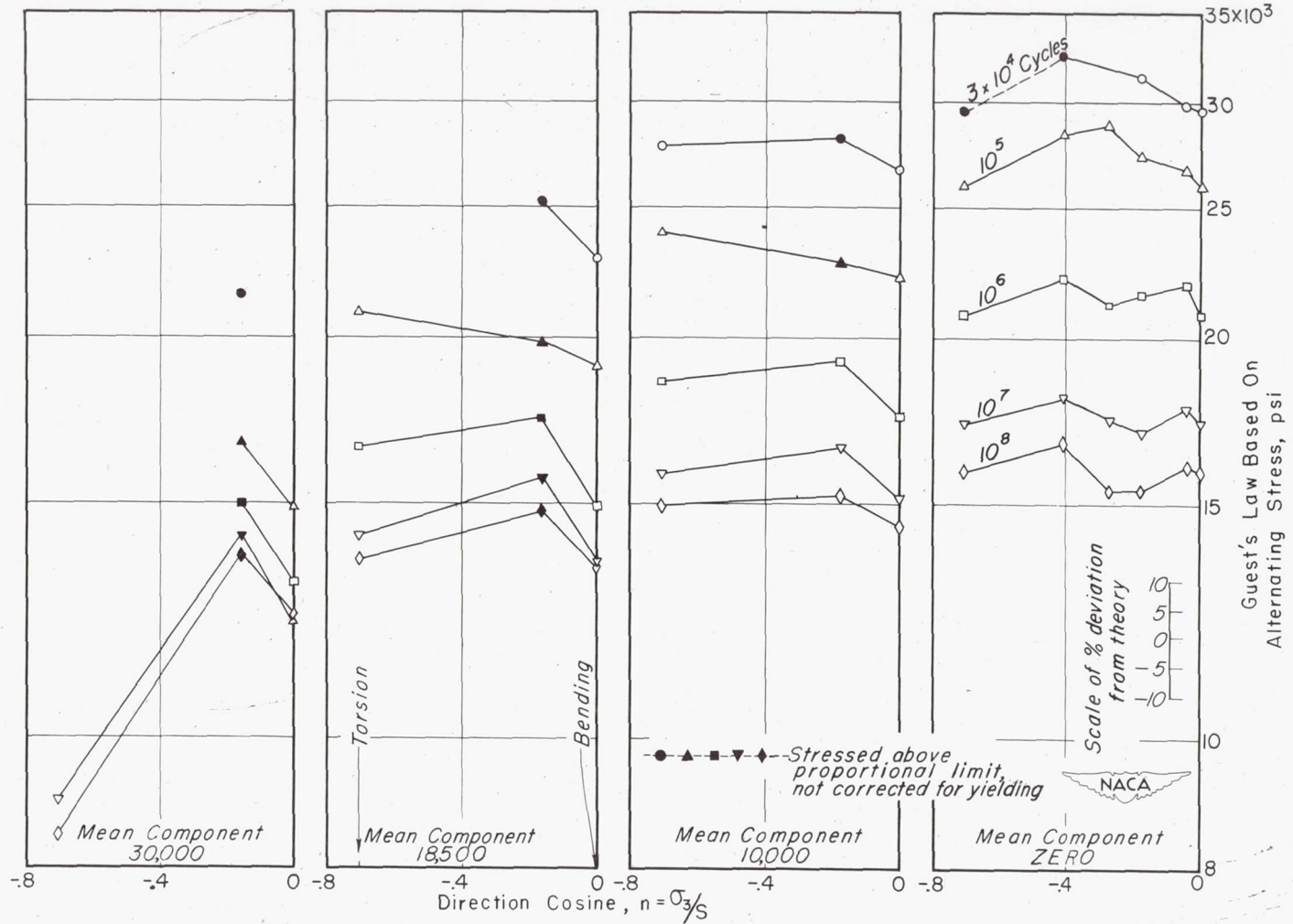


Figure 29.- Guest's law against state of stress. Mean component is Guest's law based on mean stresses. See figure 5 for sketch of mean and alternating stresses.

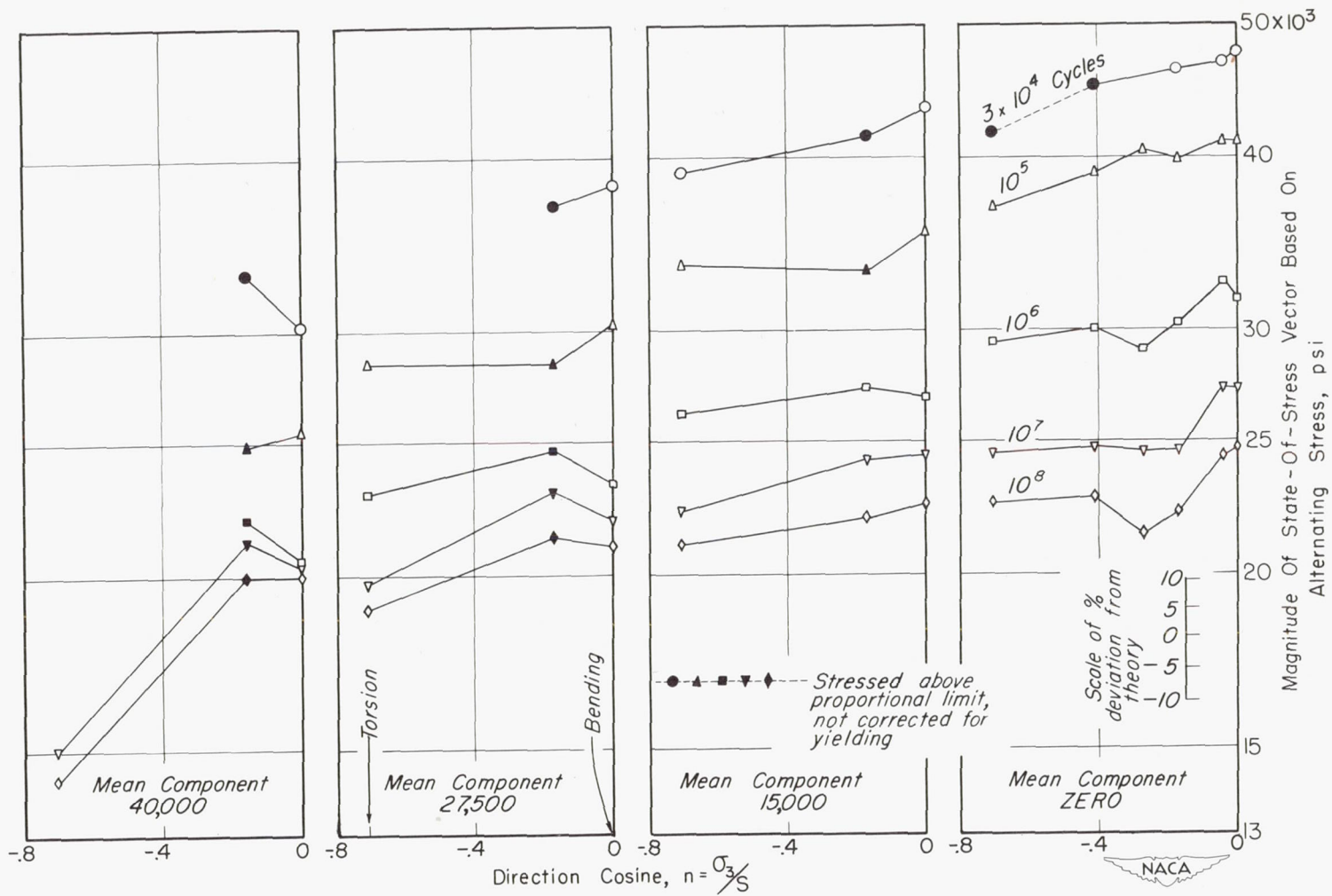


Figure 30.- Magnitude of state-of-stress vector against state of stress. Mean component is magnitude of state-of-stress vector based on mean stresses. See figure 5 for sketch of mean and alternating stresses.

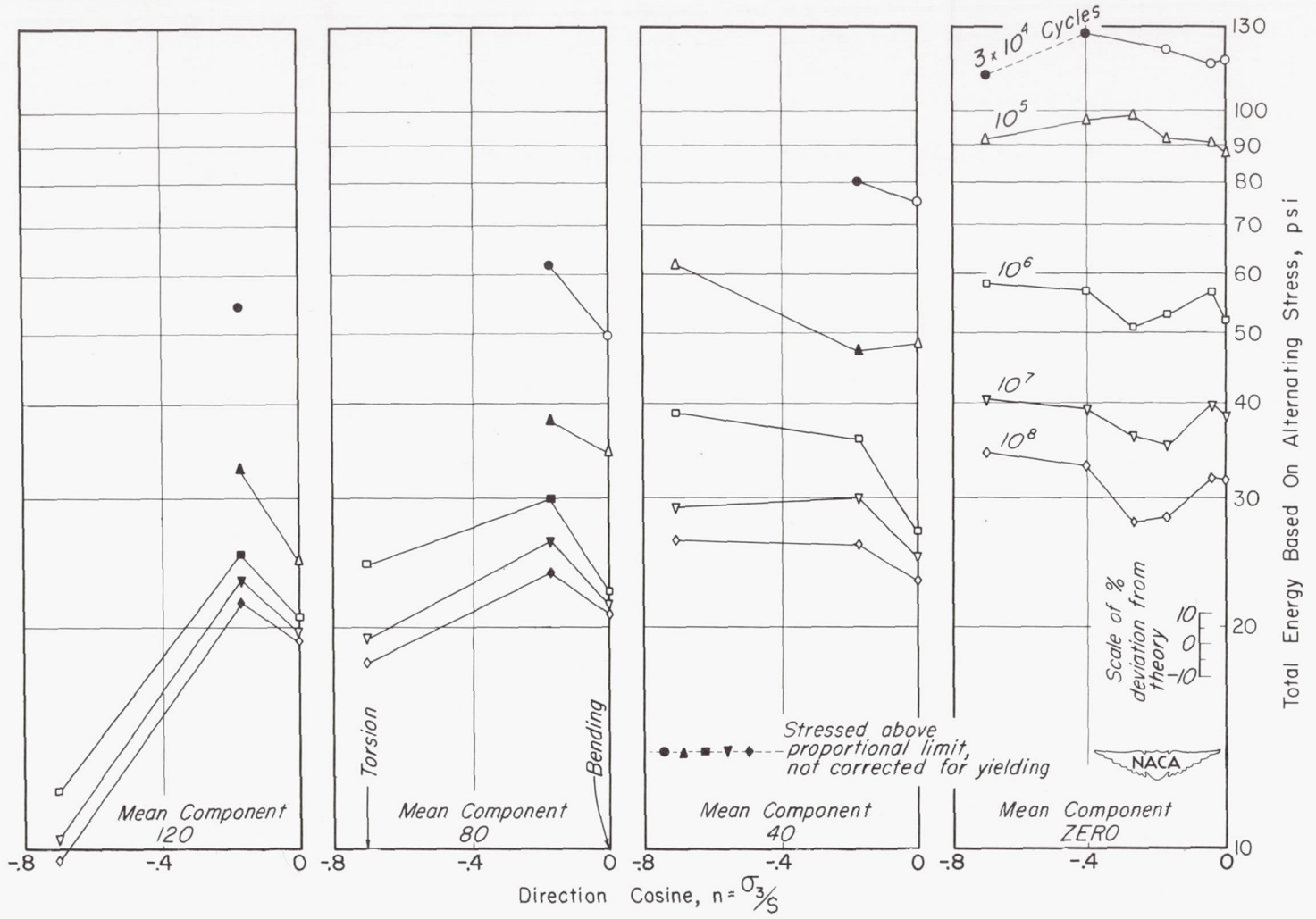


Figure 31.- Total energy against state of stress. Mean component is total energy based on mean stresses. See figure 5 for sketch of mean and alternating stresses.

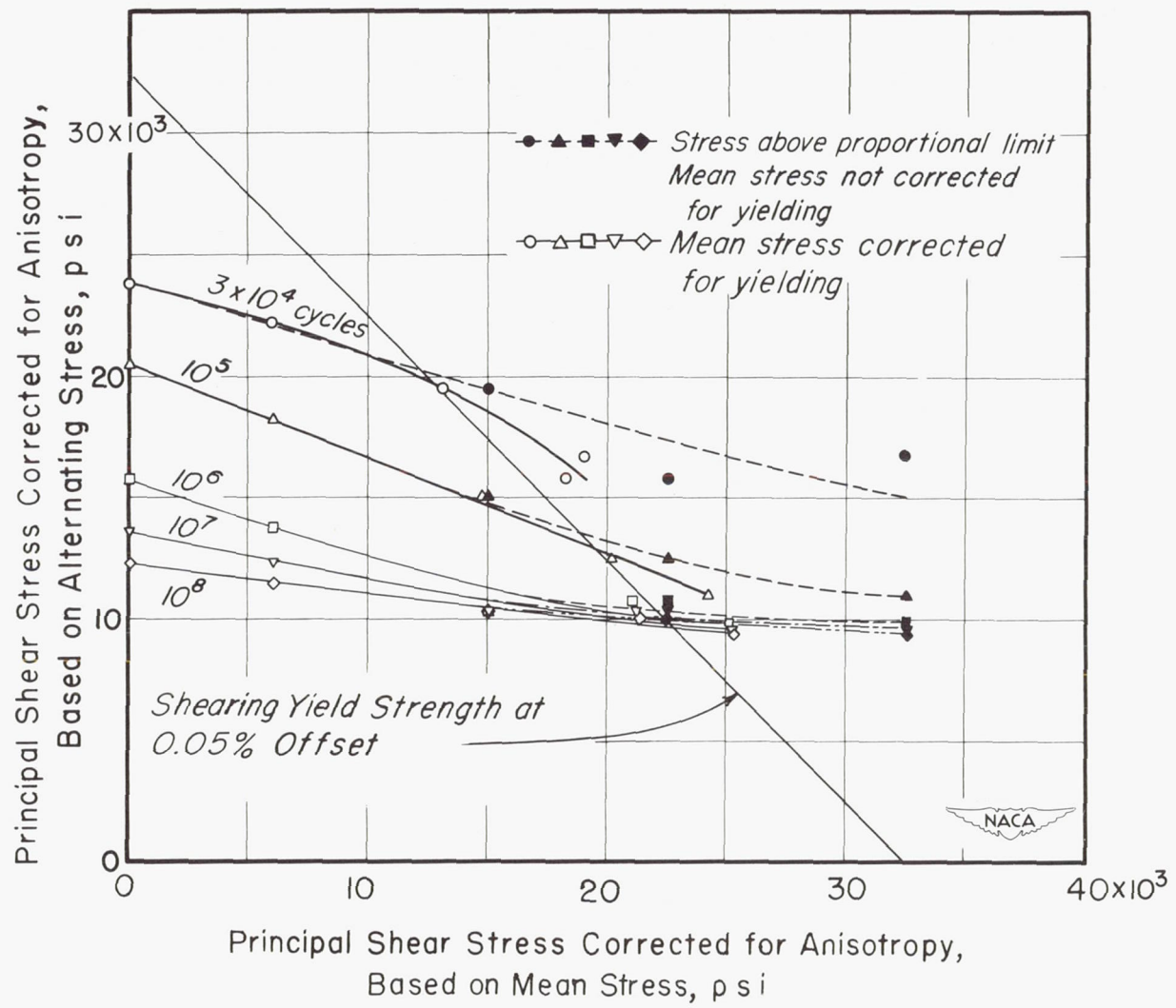


Figure 32.- Alternating against mean stress in bending fatigue for principal shear stress corrected for anisotropy.

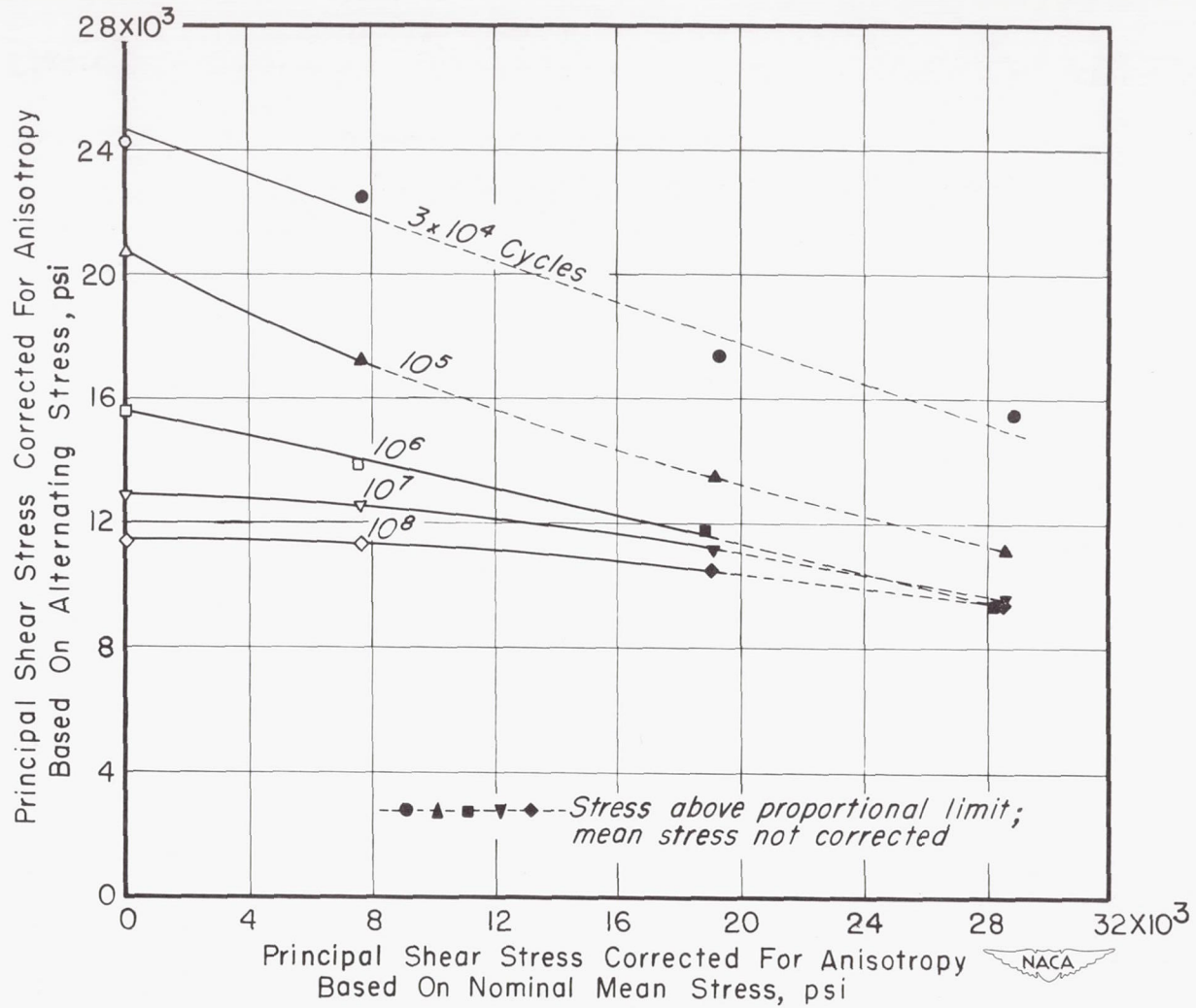


Figure 33.- Alternating against mean stress in combined-landing-and-torsion fatigue for principal shear stress corrected for anisotropy.  $\tau = 0.5\sigma$ .

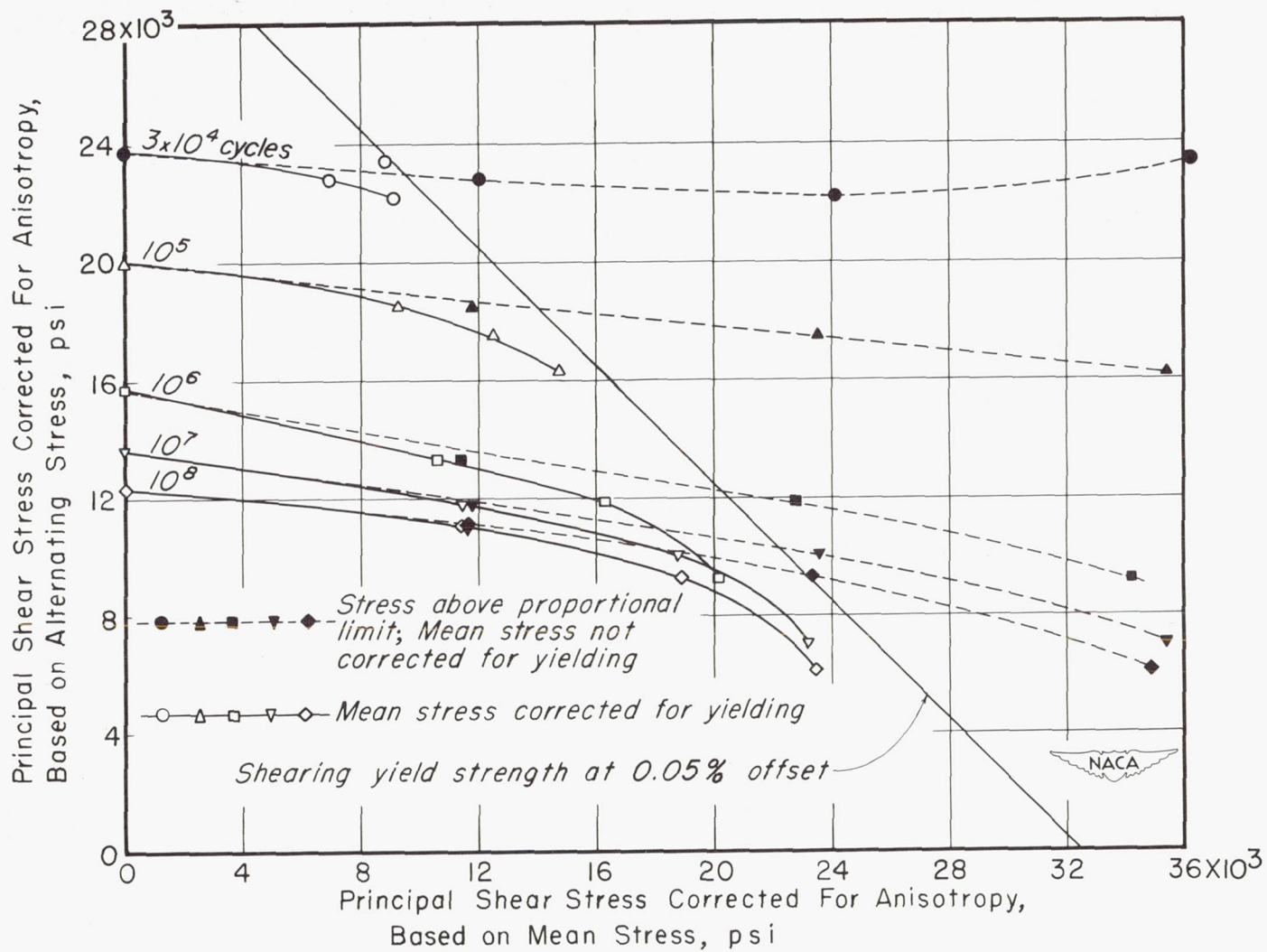


Figure 34.- Alternating against mean stress in torsion fatigue for principal shear stress corrected for anisotropy.

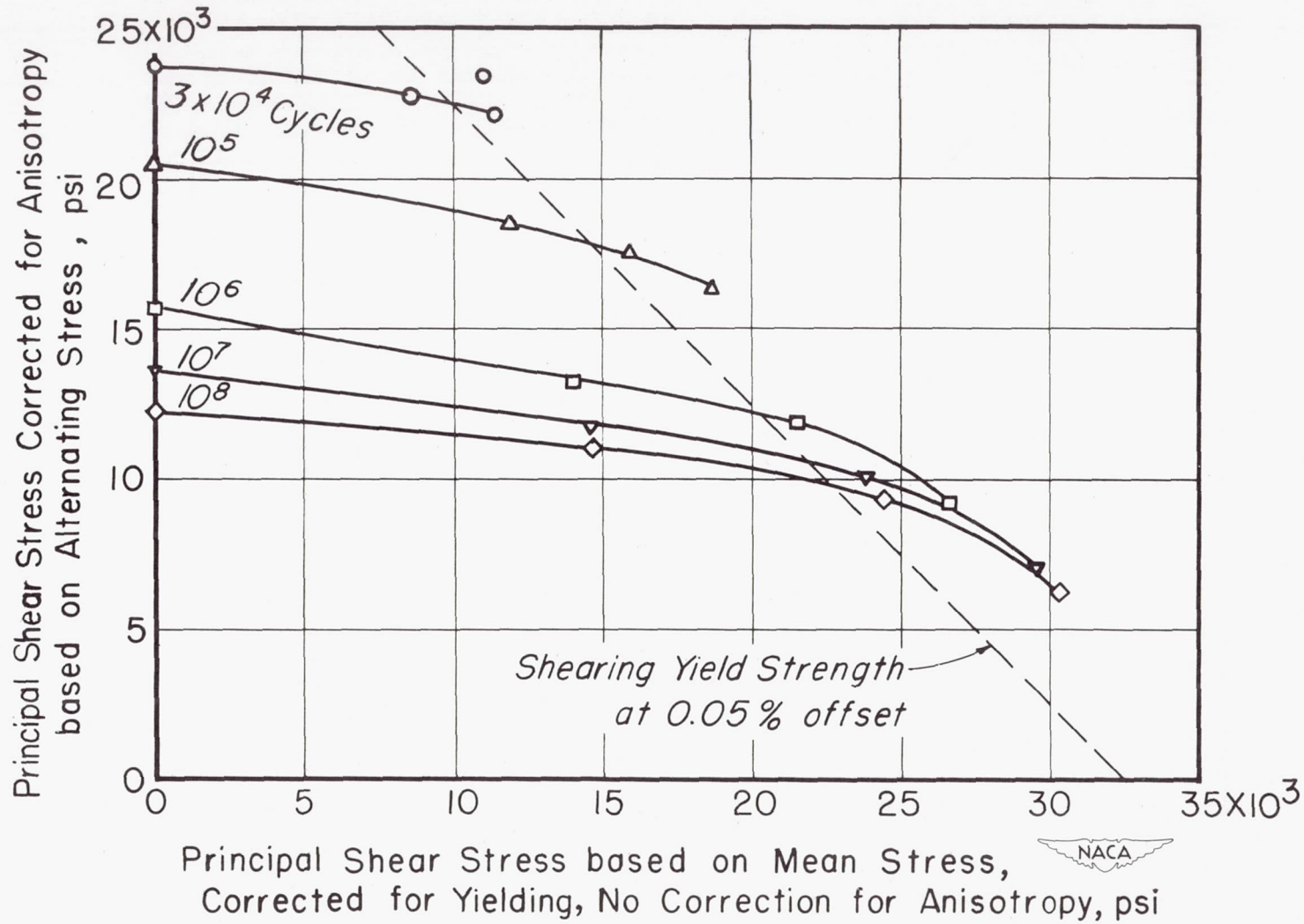


Figure 35.- Alternating shear stress (corrected for anisotropy) against mean shear stress (corrected for yielding) in torsion fatigue.

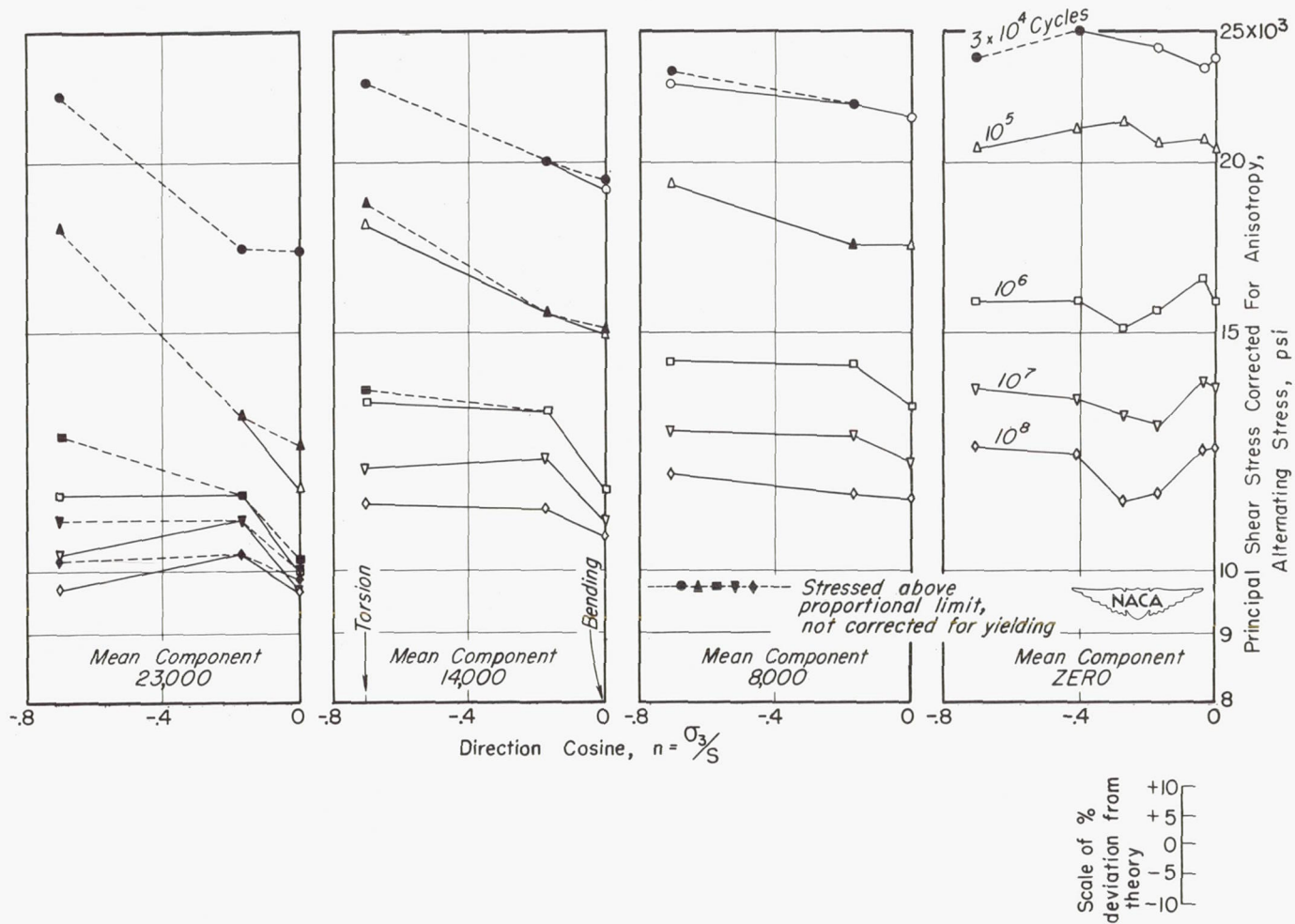


Figure 36.- Principal shear stress against state of stress. Alternating stresses corrected for anisotropy. Mean component is principal shear stress based on mean stresses. See figure 5 for sketch of mean and alternating stresses.

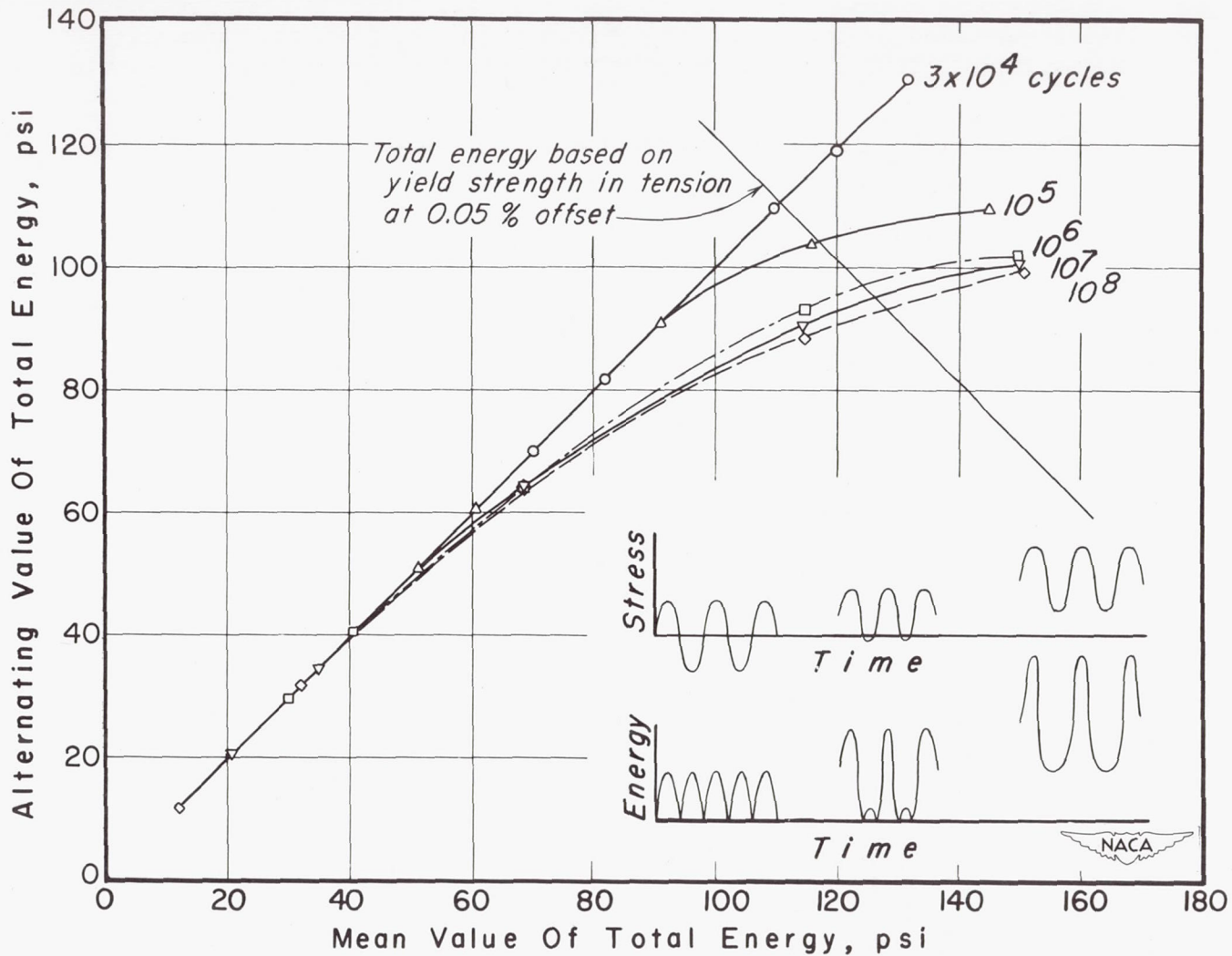


Figure 37.- Alternating against mean total energy in bending fatigue based on actual fluctuation in energy cycle.

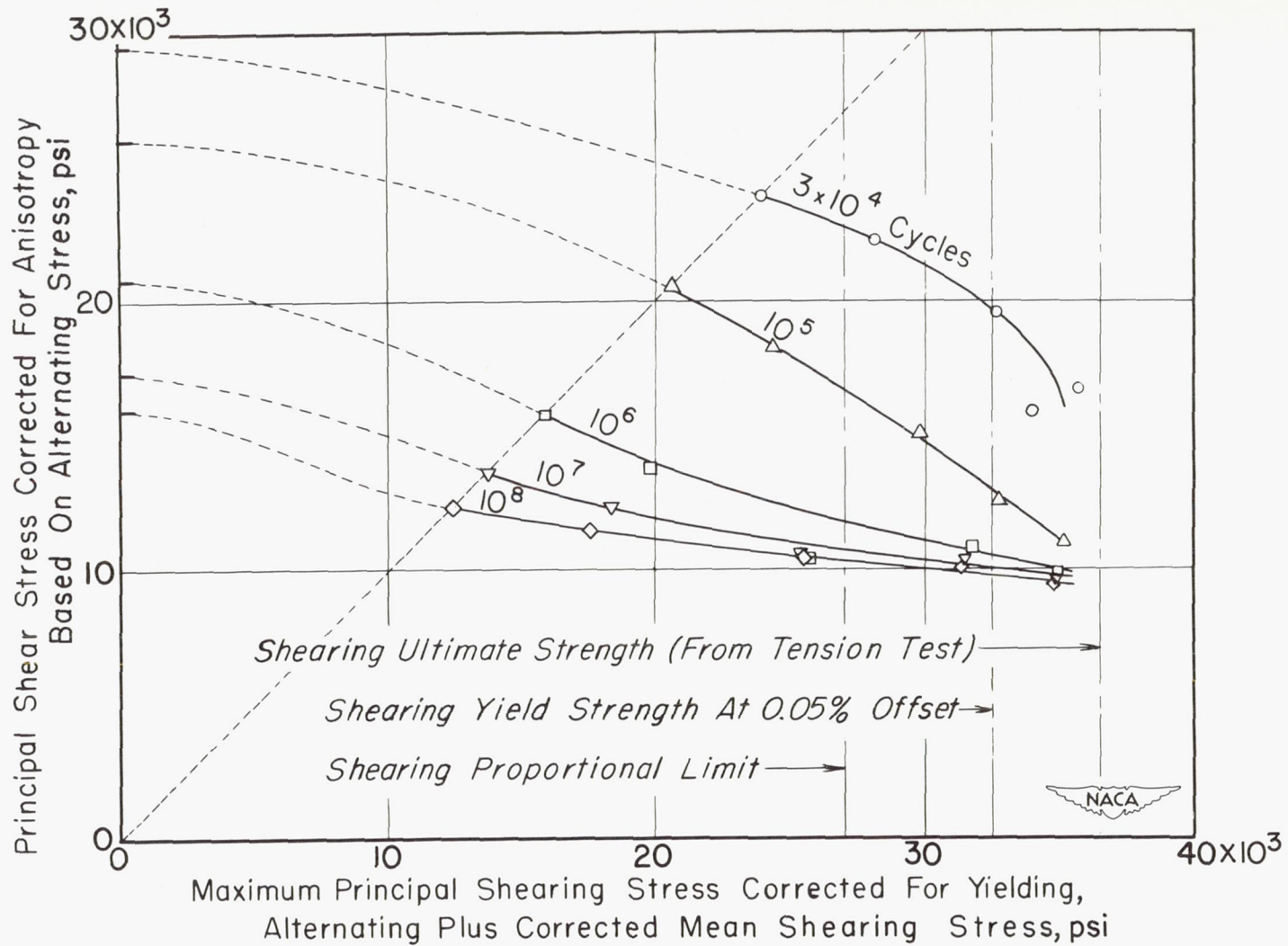


Figure 38.- Alternating shear stress against maximum shear stress in bending fatigue.

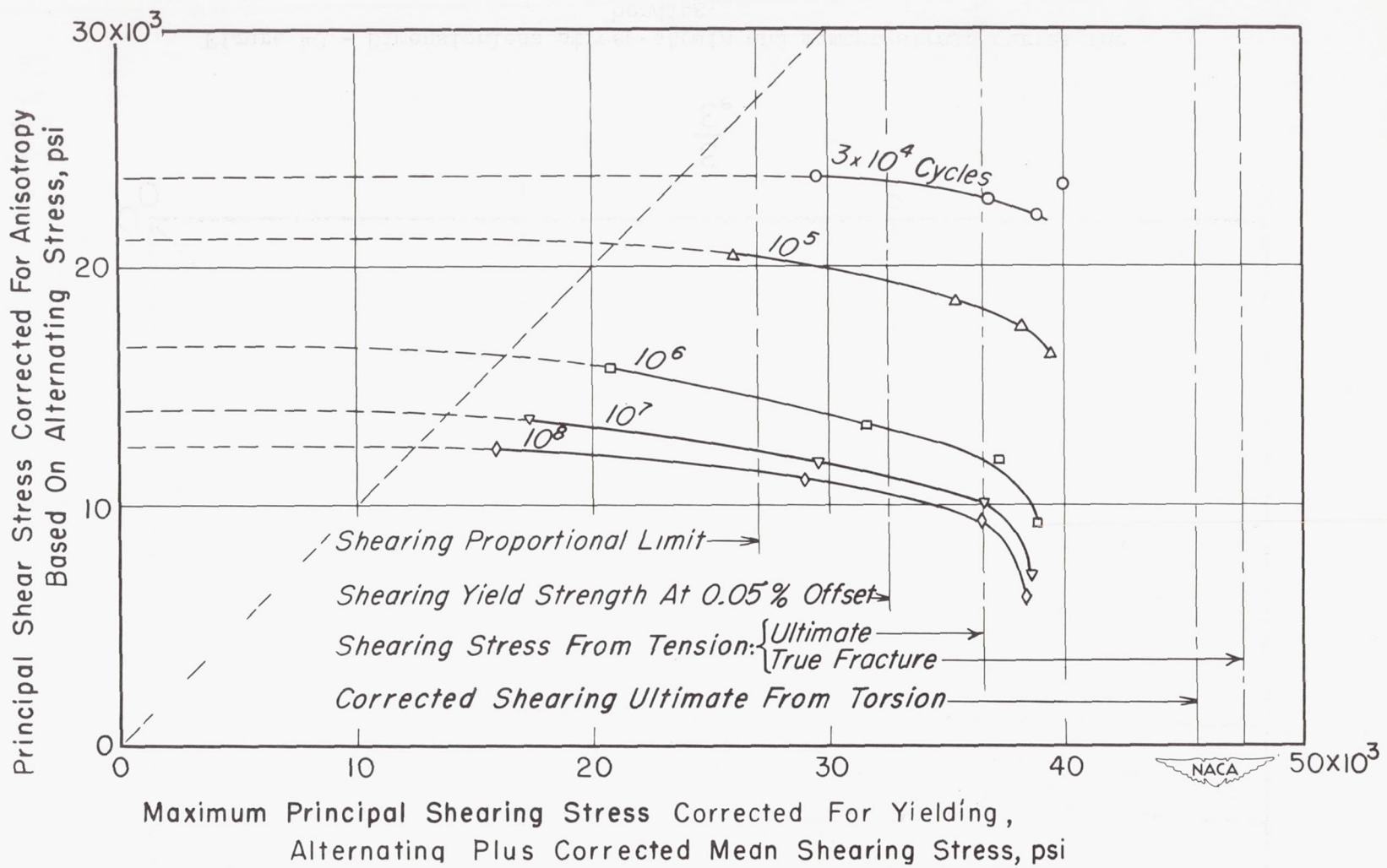


Figure 39.- Alternating shear stress against maximum shear stress in torsion fatigue.

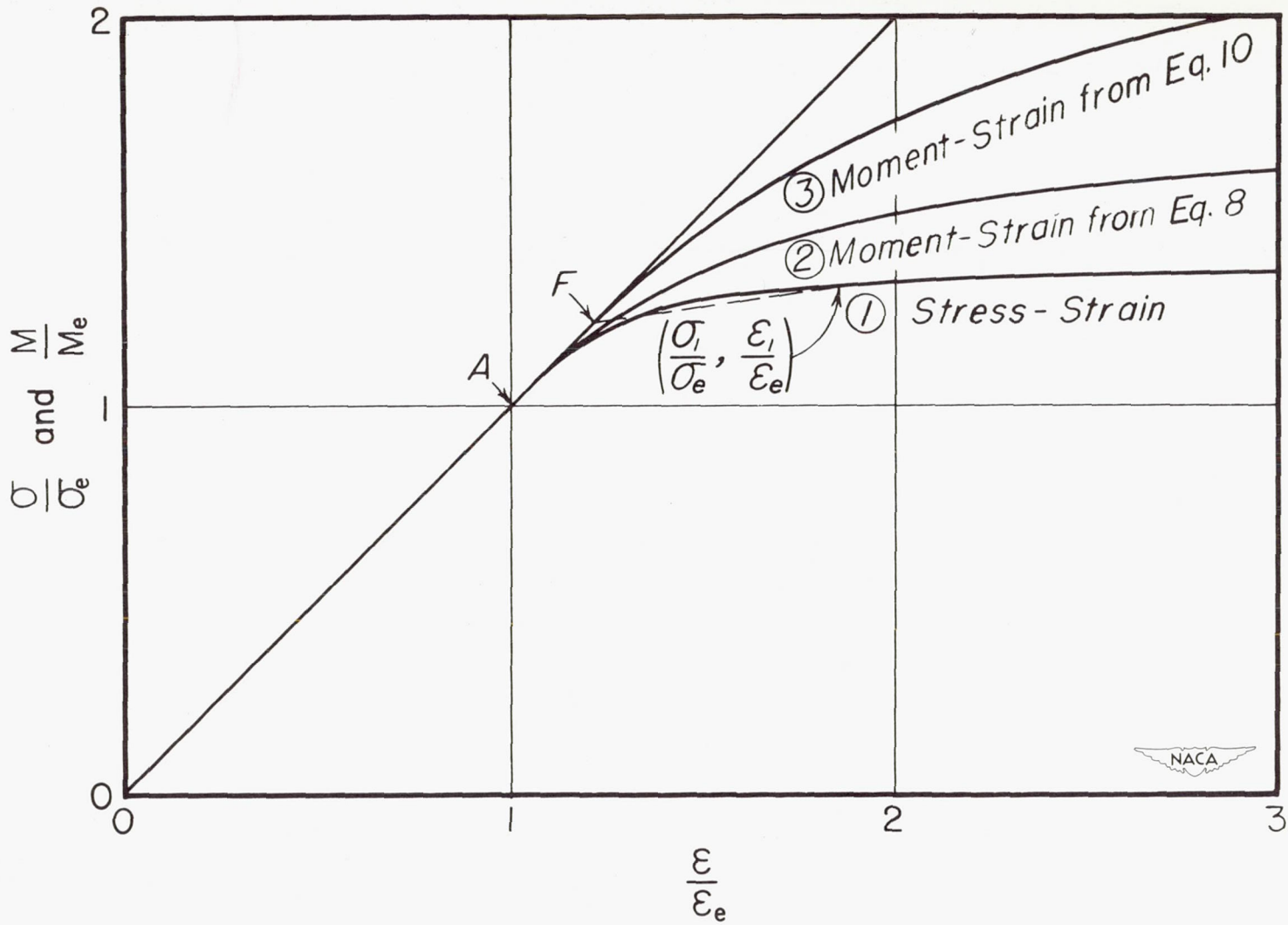


Figure 40.- Dimensionless stress-strain and moment-strain curves for bending.